ALMOST-PERIODIC, STOCHASTIC PROCESS OF LONG-TERM CLIMATIC CHANGES

by

WILLIAM Q. CHIN and VUJICA YEVJEVICH

HYDROLOGY PAPERS
COLORADO STATE UNIVERSITY
Fort Collins, Colorado

65

ALMOST-PERIODIC, STOCHASTIC PROCESS OF LONG-TERM CLIMATIC CHANGES

by

William Q. Chin*

and

Vujica Yevjevich**

HYDROLOGY PAPERS
COLORADO STATE UNIVERSITY
FORT COLLINS, COLORADO

March 1974 No. 65

*Former Ph.D. graduate student at Colorado State University, and at present Senior Hydrologist, Water Resources Branch, Inland Waters Directorate, Environment Canada.

**Professor-in-charge of Hydrology and Water Resources Program, Department of Civil Engineering, Colorado State University, Fort Collins, Colorado 80521.

TABLE OF CONTENTS

ABSTRACT

A mathematical procedure for quantitative evaluation of long-term climatic changes as an almost-periodic stochastic process is described. The procedure relies on two basic hypotheses: (1) that long-term climatic changes are reflected in the fluctuations of the Oxygen-18 content measured in carbonate shells from deep-sea sediment cores and in the ice core from the Greenland ice sheet, and (2) that long-term almost-periodic variation in the distribution of incoming solar radiation at the top of the earth's atmosphere, as derived from the Milankovich theory of orbital and axial motions of the earth, is the basic deterministic process affecting long-term climatic changes. The background information necessary for a general appreciation of the nature of the oxygen-isotope data and the probable cause and effect of the Milankovich mechanism are outlined.

The results of this study show that the problems of long-term climatic changes are amenable to analyses and syntheses by a deterministic-stochastic approach, with the deterministic component being almost-periodic. Deterministic-stochastic models of several Oxygen-18 time series are presented. Parameters of the models have been estimated from which the generation of new samples of the process can be made.

Models for estimating the deterministic component of the process are in the form of functional mathematical expressions which can be viewed as a gray box representing the response of the atmospheric-oceanic-terrestrial system. These models have the capability of converting deterministic solar radiation inputs derived from the Milankovich theory into an output which defines the deterministic pattern of changes in the long-term climate. When the deterministic component is removed, the time dependence of the stochastic components can be approximated by a first-order or second-order Markov model. The distribution of the independent stochastic component can be approximated by the normal distribution function in nearly all cases. On the basis of the models developed herein, it is shown that long-term climatic changes as reflected in the Oxygen-18 records have a high degree of stochasticity generated by the earth's environments.

The procedures, mathematical relationships and stochastic models presented in the paper appear to hold considerable promise as a technique not only for predictive purposes but also for reconstructing the history of climatic changes over the past two million years.

Although the deterministic component should not be used as a separate series for predicting the future outcome, it does provide a general indication of the pattern of events to come. A definite cooling pattern over the next 100,000 years is indicated with perhaps large advances in mountain glaciers. However, no ice sheet of continental dimensions is apparent for this period on the basis of the deterministic part of the model. The stochastic part of the model introduces some uncertainty into the prediction, because it can make the predicted, slow trend towards a cooler climate to depart more or less from the expected deterministic component. The stochastic component of the process during this predicted period can be added by using the Monte Carlo generation technique and the stochastic models and parameter estimates derived from this study.

ACKNOWLEDGMENTS

The sponsorship and the financial support of the Inland Waters Directorate, Canada Department of Environment, in the research leading to this hydrology paper are gratefully acknowledged. This paper is based on research performed by William Q. Chin during studies towards his Doctor of Philosophy degree at Colorado State University under the guidance of Dr. Vujica Yevjevich.

The authors would like also to acknowledge the financial support of the U.S. National Science Foundation, Grant GK-31521 X, in making available the time by the principal investigator (V. Yevjevich) and the staff members from the Statistics and Civil Engineering Departments and the Computer Center at Colorado State University.

CHAPTER I
INTRODUCTION

1.1 General

The hydrologic system is intimately related to the climate. Problems associated with paleohydrology, present day hydrology, and predictions of the hydrology of the future can be better resolved only through a fuller understanding of the variations, both in the pattern and magnitude of the long-term climate.

In the study of long-term climate, it is important to recognize that remarkable fluctuations of climate have occurred during the earth's history. The pattern and magnitude of climatic variations depend greatly on the length of the time span chosen for study. The major ice ages are measured in time intervals of hundreds of millions of years. The waves of continental glaciations during the most recent or Pleistocene ice age are measured in tens and hundreds of thousands of years. The lesser climatic fluctuations of post glacial and modern times are measured in decades, centuries, and millennia.

The theories and hypotheses of long-term changes of climate on a time scale of hundreds of thousands and millions of years open up a wide range of geotectonic, astrophysical, and astronomical considerations. On the other hand, long-term climatic changes on a time scale of decades, centuries, and millennia are mainly stochastic in nature with the atmosphere as the major source of stochasticity. The oceans, continental surfaces, and underground reservoirs combine to attenuate the high stochasticity produced by the atmosphere and add their share.

No matter what time scale is under consideration, the complex nature of climatic controls suggests a stochastic component, consisting of a large part of the entire process, which changes with time in accordance with the law of probability as well as with the sequential relationship between its occurrences. The concept of a deterministic-stochastic approach in the analyses of long-term climatic change has not been developed to any great extent as yet. The objective of this study is to formulate a mathematical model of the deterministic-stochastic climatic phenomenon which will have practical application in: (1) the evaluation of paleohydrology; (2) the study of the hydrology of modern times; and (3) the prediction of the hydrology of the future.

A general behavior may be discerned in natural sciences. A geophysical or hydrologic variable, as the integrated effect of many causative factors, is a stochastic process if the number of causative factors is very large and none of these factors dominates in such a way that it gives a significant deterministic impact on this integrated effect. The classical case of a Gaussian stochastic process is one in which the number of its causative factors is very large (theoretically it goes to infinity); each factor individually has a small effect (theoretically very close to zero); and these small individual effects are independent and additive. When only one or a small number of causative factors significantly dominate the total effect in comparison to all the other individual factors, the process can be conceived as deterministic-stochastic process. The part of the process related directly to the effects of a factor or a small number of dominating factors, is conceived as a deterministic component of the process; and the part which incorporates lower-order effects of a large number of factors is conceived as the stochastic component of the process. The basic conditions in applying this type of behavior to natural processes are: (1) the dominating natural factors are deterministic processes themselves, well predictable in time and/or space; (2) the multitude of other causative factors are mostly random processes, though some of them may have somewhat larger individual effects on the observed phenomenon than the others. This approach is used in deriving a deterministic-stochastic model of long-range climatic changes. The astronomical - deterministic processes produce the deterministic component; and a myriad of earth causative factors, none of them dominating the process, are responsible for the stochastic component.

Since geological evidence of continental glaciation was discovered more than two hundred years ago, some 60 major hypotheses have been advanced to explain the physical processes which cause long-term climatic fluctuations and their relation to continental glaciation (Eriksson, 1968). Many minor hypotheses with other causal factors, have been also suggested. Most of the researchers have concentrated on finding possible deterministic solutions to what must be a deterministic-stochastic process with a significant or non-negligible stochastic component. After a century or so of research, a universally acceptable theory of long-range climatic changes has yet to be found. The fact that so many hypotheses have been advanced to explain climatic changes is an indication not only of the complex nature of all factors of climatic control, but also indirectly infers a plausible structure of the long-range climatic process.

With the advent of the computer, numerical simulation models of general atmospheric circulation for deducing the climate are being developed, but the question of complete climatic determinism remains open (Alyea, 1972). For complete climatic determinism the problems of establishing the history of the earth environment and predicting its future would have to be resolved. Such phenomena as volcanic eruptions, variable ice and snow quantities with the resulting changes in ocean level, variable ocean currents, ocean salinity, trends in content of atmospheric and ocean carbon dioxide, and many other influences which are major sources in producing stochasticity in the climate, are difficult if not impossible to quantify at present.

The reconstruction of the climatic history of the earth has long been the subject of intensive research by scientists working in paleo-sciences of various disciplines, such as geology, climatology, oceanography, hydrology, geography, zoology, archaeology, geomorphology, glaciology, vulcanology, tectonics and solar physics. A large body of qualitative information on the paleoclimate of earth has been accumulated.

During the past decade and a half, new developments in deep-sea coring devices and oxygen isotope analyses of the carbonate shells contained in the deep-sea sediments are providing materials and techniques for producing some quantitative records of the paleo-

climate for the entire Pleistocene (Emiliani, 1955, 1966, 1972; Ericson et al. 1964, 1968). More recently, it has been found that the ice deposits on the two large ice sheets of Antarctica and Greenland contain paleoclimatic information in the form of varying oxygen isotopic composition of the ice. Furthermore, the ice cores offer the possibility of a continuous sedimentary sequence from which data for time intervals as short as a decade or less can be extracted, the only limitations being obliterations of isotopic gradients by diffusion in solid ice (Dansgaard et al. 1970). Quantitative evidences from the sea-sediment and ice-core data have all tended to reinforce the findings from the more diversified terrestrial records of Pleistocene climate.

The chronology of the Pleistocene climate as indicated by the sea-sediment data suggests strong agreement with the expectations of the astronomical theory commonly referred to as the Milankovich theory*. The Milankovich theory (Milankovich, 1941) assumes that perturbations in the orbital parameters (obliquity, eccentricity, and longitude of the perihelion) produce long-term changes in the amount of incoming solar radiation received at the various seasons and latitudes and consequently are responsible for long-range climatic changes.

The theory of Milankovich is now being given a hard second look by a number of paleoclimatologists and geologists (Mitchell, 1968; Hamilton, 1968; Zeuner, 1970). Broecker (1968) has stated that the Milankovich theory can no longer be considered just an interesting curiosity. It must be given serious attention. According to Emiliani (1955, 1966b) a significant correlation has existed for the past half million years between the paleotemperatures of the surface waters of the Caribbean sea and the variations in the astronomical parameters of the earth during the period as calculated by Milankovich and subsequently modified by van Woerkom. Conclusive proof of this correlation is not possible because a reliable method for absolute dating of the chronology of an entire sea-sediment core covering a period of several hundred thousand years is not yet available. The Pleistocene time scale is still a controversial subject. Nevertheless, the Milankovich mechanism appears to provide the general control of adequate magnitude to explain on a broad scale the advances and retreats of glaciations during the Pleistocene. According to Cornwall (1970), no other equally satisfactory theory has yet been advanced.

Although the Milankovich theory with the astronomical factors as a main cause of glaciation has been a subject of great controversy, this astronomical theory itself as quantified by Milankovich and its consequent effect on long-term seasonal and latitudinal distribution of solar radiation at the top of the earth's atmosphere have rarely been questioned (Kutzbach et al. 1968). The fact that the astronomical variations specified by Milankovich have had significant influence on terrestrial climate is undeniable (Mitchell, 1968). Nevertheless, long-term climatic changes are the result of the combined effects of many causative factors which are both deterministic and stochastic in nature. In this case, the astronomical causative factors included in the Milankovich theory, which have almost-periodic deterministic time variations, may be considered as the causes of the deterministic part; and all or majority of other causative factors may be considered as creating the stochastic part in long-range climatic changes. Since the interaction of these various factors has thus far defied a complete mathematical description, a good understanding and description of the process seems to be obtainable at this time only on an approach based on the outlined deterministic-stochastic process. The sea-sediment and ice-core data are now beginning to provide the quantitative records needed to carry out such an analysis.

1.2 Objective and Scope of the Study

The main objective of this study is to develop a feasible method for analyzing long-term climatic changes as a deterministic-stochastic process. In carrying out the study, the basic hypotheses is made that long-term climatic changes are reflected in the oxygen isotope values determined from sea-sediment core and ice core. Furthermore, it is assumed that the several oxygen isotope time series represent non-stationary processes consisting of an almost-periodic deterministic component which is attributed to the Milankovich astronomical theory of climatic effects, and a stochastic component which is attributed to various sources of randomness within the environment of the earth.

In the absence of quantitative information on paleometeorology, paleooceanography, paleogeology, paleohydrology, and paleoglaciology, this study will rely on published sea-sediment and ice-core data for analyses. Climatic changes occurring in different time scales at which different climatic control factors are operative will be analyzed. The sea-sediment data will be used to study long-term climatic changes on a time scale measured in 200-year intervals covering a time span of about two million years. Data from the Greenland ice core will be used to study long-term climatic changes on three time scales: 200-year intervals covering a time span of 126,000 years, 50-year intervals covering a time span of 10,000 years, and 10-year intervals covering a time span of 780 years. For convenience, the above series with different time intervals will be referred to hereafter as the Sea-Sediment series: Ice-200 series, Ice-50 series and Ice-10 series.

The several phases of the study consist of the following:

(1) To develop a mathematical model for estimating the sedimentation rate in each 10 cm interval of the sea core in order to obtain an absolute time scale for the sea-sediment series. The three ice-core series have already been time calibrated (Dansgaard, et al. 1970).

(2) To develop mathematical models which will account for the deterministic components in both the sea-core and ice-core time series.

(3) To study the structure of the stochastic component of each time series and approximate the time

*Milankovich is commonly spelled Milankovitch in the French and North American versions; but "Milankovich," an English transliteration of the Serbo-Croation version, Milankovic´, is used throughout this report.

dependence by an appropriate stochastic model.

(4) To remove the dependence structure of the time series and obtain a second-order stationary and independent stochastic component.

(5) To fit probability distribution functions to the independent stochastic component and select the function of best fit.

1.3 General Significance of the Study

The significance of this investigation is to demonstrate a methodology for analyzing the structure of the sea-sediment and ice-core time series from which valuable information can be obtained for reconstructing past and predicting more realistically future long-term climatic changes. This is a first approximation in developing a mathematical description of long-term climatic changes as a deterministic-stochastic process. The gross preliminary models and conceptual tools developed are based on the "best use" of limited data available at present. Further refinements and improvements in the methodology will surely come about both with a better anaylsis of presently available data and as more data are accumulated and the reliability of data are better understood and assessed.

The deterministic component can be explained by the astronomical theory which accounts for the long-term variations in seasonal solar energy over various areas of the earth's surface. Various influences within the earth's environment produce complex interactions and responses which serve to modify the effects of the long-term variations in insolation. Therefore, the stochastic component may be explained by various random processes inherent to processes in the atmosphere, oceans, and at the continental surfaces. These processes are so complex that it is beyond present capability to explain and analyze mathematically the entire process on a physical basis. An empirical, black-box approach is required at this time. Analysis of the structure of hydrologic time series and their decomposition into deterministic (signal) and stochastic (noise) components are considered here as the useful step toward a fuller understanding of the processes involved.

1.4 Hydrologic Significance of Studying Long-Term Climatic Changes.

Climatic changes have many significances for hydrology depending on the time scale and area of concern. Because hydrologic processes are very closely related to climate, all results of investigation and projections for expected climatic variations in the future affect the conclusions about hydrologic processes, water resources properties, and future behavior of natural and man-made water resources systems.

The major present-day continental hydrologic environments consist of river basins with specific geomorphologic patterns, stream density and river meanders, flood plains and terraces, lakes with their shapes and stages, groundwater aquifers (shallow and deep, including karstified limestone or dolomite, and lave-made aquifers), estuaries, deltas and other forms. Past geologic, climatic, and hydrologic processes have shaped the environments to their present states. To best understand the properties of these environments, a knowledge of their geneses is one way of contributing to this understanding. It is not surprising that petroleum engineers have long searched for physical models of the processes which led to the present oil and/or gas bearing porous media.

The science of paleo-hydrology is likely to become even more important as the pressures for better knowledge and description of the hydrologic environments increase with time. Paleo-hydrology cannot be separated from paleo-geology, paleo-climatology, and paleo-glaciology. Climatic changes of the past will be one of the major inputs for the study of paleo-hydrology and for examining the remanents of the long hydrologic processes responsible for shaping the present-day continental surfaces. On the other hand, the present-day problems of man-made water resources systems are likely to be less concerned with the long-range climatic changes as it concerns the potential changes in water inputs, or the available water resources. Statistical evidence on a multitude of observed hydrologic series shows that no basic change has occurred in natural water resource yields in the last 150 - 200 years if the man-made effects and some accidental natural disruptions at a limited number of places are neglected.

A hypothesis can be supported by significant evidence that the probability is very high for the average natural water availability as inputs to man-made water resources systems in the next 50-100 years to be very close to the average water supply experienced in the last 150 - 200 years. Since most systems have been built with the economic project life in the range 40-100 years, the chances are minimal that the expected natural water supply would be significantly different during these life spans than in the past 200 years. This statement must be qualified in the sense that the estimate of average water yields from the short observed time series may be highly in error in comparison with the true averages of the last 200 years, or of the expected values of the future 100 years. This confidence, to expect no significant climatic change which might impair the performance of any important water resource system, is at odds with present statements made in the literature and through the public media concerning imminent "cooling-off," "freezing-over," "warming-up," and similar pronouncements.

No important water resources system is built only for the assumed or prescribed economic life of 40-100 years. Some large dams, diversion canals and tunnels, and other basic structures may live without significant reconstruction for several centuries. The trend in long-range climatic changes -- when proven by good scientific facts -- may decide the future behavior of these systems. Even a small trend in climatic changes, taken over several hundred years, may show an impact on the future performance of present-day built systems. This question is, however, not crucial for the next several generations of contemporary earth population, but rather is more of an academic interest like many other human concerns with the long-term future.

CHAPTER II
BACKGROUND INFORMATION

2.1 Climatic Changes

In any discussions on long-term climatic changes, it is important to recognize that climatic variations on many time scales are going on continuously and simultaneously and probably with many different causes. Records from geological evidence indicate that the climate of earth for much the greater part of its life has been relatively warm everywhere with no permanent ice and relatively small differences between poles and equator. With the introduction of radioactive methods, it has been determined that deposits of undoubted glacial origin are recognized from only three intervals during the life of the earth (Fig. 1). The first major ice-age occurred some 600 million years ago in the Proterozoic period of the Pre-Cambrian era. The second major ice-age occurred some 250 to 300 million years ago in the Permo-Carboniferous periods of the Paleozoic era. The start of the third and last major ice-age, known as the Pleistocene epoch, has been placed variously at 400,000 to 2 million years ago extending from the Tertiary period to the present (Cox, 1968; Sutcliff, 1969; Bertin, 1972; Emiliani, 1966; Ericson et al. 1968).

The time intervals between major ice ages is longer than 200 million years whereas the time interval between successive glaciations within the Pleistocene ice age is only about 100,000 years or less. Accordingly, the processes which control the onset of a major ice age are probably quite different in scale from those which determine their oscillatory character within an ice age. Similarly, the processes which control the oscillatory character of glaciation within an ice age are different in scale from those which determine the short-period fluctuations of present day alpine glaciers. According to Fairbridge (1963), the ranges in the scales of climatic changes can be conveniently subdivided into three major orders of magnitude (also see Mitchell, 1968).

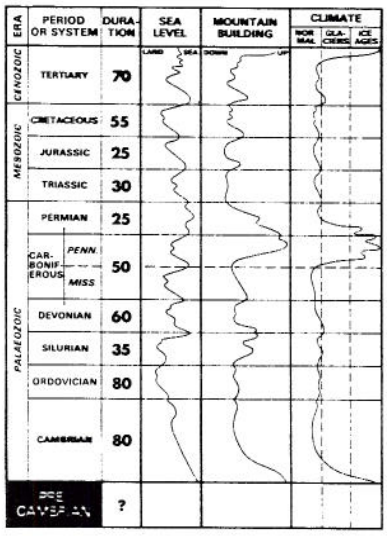

Pleistocene epoch of 2 million years duration

Fig. 1 Rhythms in the history of the earth showing the oscillations of sea level, mountain building and climate (from Bertin, 1972, after Umbgrove, 1947).

(1) Time Scale of 10 Million to 1 Billion Years

Climatic controls at this time scale are related to geotectonic and astrophysical causes. The geotectonic controls are mainly of endogenic origin including polar wandering, continental drift, orogenesis, and continental uplift. The astrophysical causes are related to exogenic forces such as stellar evolution (aging of the sun), solar variability (changes of solar constant), changes in density of interstellar matter (galactic dust clouds), and changes in gravitational waves in the universe. These are the forces that can create conditions favorable for the onset of a major ice age. Whether the great ice ages of the past have the same or different causal origin is, of course, unknown. Many theories based on the above suggestions or combinations of them have been advanced.

(2) Time Scale of 10,000 to 100,000 Years

Climatic controls at this time scale are related mainly to planetary movements which affect the orbital and axial motions of the earth. Their effects on the seasonal and latitudinal distribution of solar energy at the upper atmosphere have been determined by Milankovich in a rigorous mathematical treatment. Other factors such as meteorite interactions, variations in the amount of carbon dioxide, volcanic dust, water vapor, and ozone in the atmosphere as well as changes in ocean currents and salinity, rise and fall of sea level, increase and decrease in the sea ice, and the feedback interaction of all these elements likely influence climatic variations on this time scale. The influences of many of these factors are of a stochastic nature.

(3) Time Scale of 10 to 1000 Years

Climatic controls at this time scale are mainly stochastic in nature with mean solar radiation assumed to be a constant. The processes which affect the climate at this time scale embrace almost all aspects of the earth-atmosphere-ocean environment. These processes are outlined further in Chapter V. Feedback from interaction between atmosphere, ocean, and continental environments is such a complex process that qualitative cause-effect arguments are generally insufficient and often misleading. Much of the literature on climatic change seems to have suffered for that reason. At the current state of knowledge, a stochastic approach is mainly indicated in any analysis of climatic variations at this time scale.

The volume of literature on the subject of climatic change is over-whelming. The major theories on physical processes which cause long-term climatic fluctuations and their relation to continental glaciation are summarized by numerous authors. For details the reader may refer to Sellers (1965); Mitchell (1965, 1968); Shapely (1960); Brooks (1949); Nairn (1963); and Flint (1971).

Mountain building is a popular theory of climatic change, particularly among geologists, who have found excellent correlation between the general period of orogenesis and subsequent glaciation (Fig. 1). Both the Permo-Carboniferous and Pleistocene glacial epochs are known to have been preceded by periods of extensive

mountain building. That mountains are necessary for glaciations is now generally accepted. But it is also true that some major orogeneses have been accompanied by little or no glaciation (Sellers, 1965). Perhaps mountain building can be considered a necessary but sometimes not sufficient condition for glaciation. On the other hand, Cornwall (1970) suggests that most of the Precambrian glaciations did not follow orogenesis. Some other factors than mere pronounced relief of the land are at work. He believes that these factors are related to a fortuitous (or unfortuitous) combination in the distribution of land and water resulting from earth-movements that happens to restrict ocean and atmospheric circulation causing conditions favorable for glaciation.

Whatever the cause or causes may be, it is known that during the past million years or so, throughout the Pleistocene, the geography of the earth has remained essentially the same as it is today. The Pleistocene ice age which followed a period of major alpine orogenesis is known to have experienced several waves of advance and retreat of continental ice fields. Extensive records have been compiled from terrestrial observations. Data from the deep-sea sediment cores and ice cores from the Greenland and Antarctic ice caps are now providing supplementary information of a quantitative nature. The picture of the Pleistocene (Figs. 2 and 3) is continuously being revised as new data are accumulated and analyzed. Climatic change at a time scale measured in decades, centuries, and millennia within the Pleistocene epoch (which is considered to include the present) is the subject of interest in this investigation.

2.2 Ice Sheets

(1) Late Pleistocene Epoch

Long-term climatic changes on the scale of the Pleistocene epoch have a direct relationship to the growth and retreat of ice sheets. During the last glacial maximum (some 15,000 to 20,000 years ago) over 37.5 million square kilometers of the earth's surface were covered by glacier ice. This is equivalent to about 28 percent of the present land surface. Major ice sheets up to 3300 meters thick lay on North America and northern Europe. Smaller ice sheets occurred in Iceland, Spitzbergen, and Franz Josef Land. Extensive mountain glaciation existed in Siberia, the Himalayas, the Caucasus, the Alps and Pyrenees, the Andes, and in New Zealand. Alpine glaciers developed in the high mountains of Japan, Hawaii, East Africa, New Guinea, and Tasmania. The ice sheets of Antarctica and Greenland were more extensive than today (Mellor, 1964).

The Laurentide ice sheet in North America was the largest of the Pleistocene ice sheets excluding Antarctica. It extended from the eastern seaboard across the continent to join with the Cordilleran ice sheet west of the Rocky Mountains and ran from the Arctic Ocean in Canada as far south as New York City, Cincinnati and St. Louis in the United States. Large parts of Alaska and the Arctic Archipelago in Canada apparently remained unglaciated (Mellor, 1964; Moran and Bryson, 1969; Bryson et al. 1969).

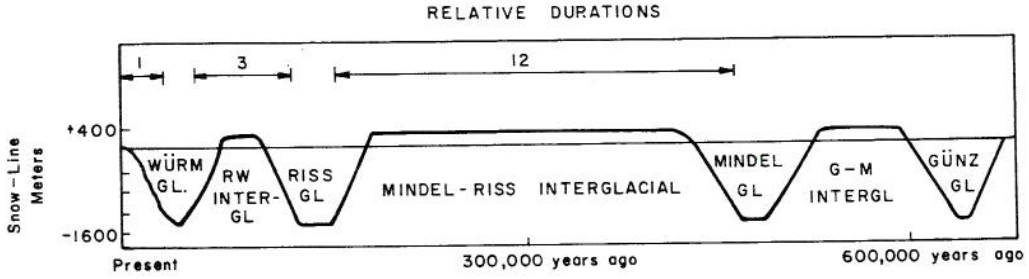

Fig. 2. Duration of Pleistocene interglacial and glacial stages in the Alps according to the scheme of Penck and Bruckner (from Daly, 1963).

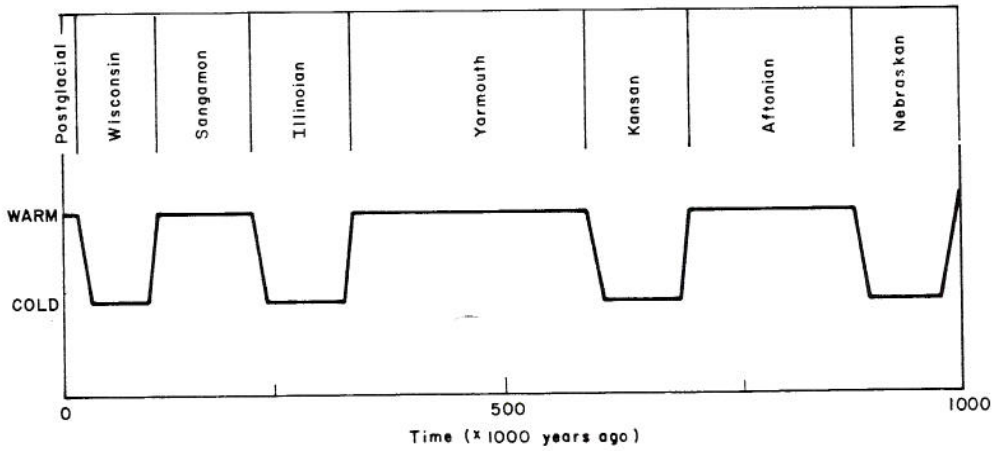

Fig. 3. Classical picture of Pleistocene interglacial and glacial stages (from Emiliani, 1972, based on terrestrial data after Flint, 1952).

(2) Glacier Flow Theory

A considerable amount of work has been carried out over the past 20 years to develop a proper understanding of glacier mechanics. Modern theory on glacier flow is based on application of ideas in solid state physics and metallurgy. Since ice is a crystalline solid it must deform like other crystalline solids such as metals at temperatures near their melting points. An excellent outline of the recent work in this field is given by Paterson (1969).

Early theories of glacier flow were based on the assumption that ice behaves as a Newtonian fluid, in which strain rate is proportional to the applied stress. However, viscous flow alone could not explain many features of glacier movement (Mellor, 1964). More recently, glacier movement was analyzed on the assumption that ice is perfectly plastic; that is, it has a sharply defined yield point. Although the plasticity theory permitted more realistic consideration, it was not fully acceptable because it has been shown that ice continously deforms under the smallest stresses (below the formerly assumed yield stress) and cannot, therefore, be ideally plastic (Nye, 1959, 1963; Weertman, 1964). Current theory evolved from the ideal plastic case to conform with a non-linear visco-plastic flow equation referred to as the Glen's Creep law. This law states that the final strain rate is proportional to the shear stress taken to the n-th power. The constant of proportionality depends on the temperature of the ice and "n" is obtained experimentally.

The field of study is undergoing rapid evolution. Much of the work to date has been directed towards temperate zone glaciers of the alpine type. Studies of polar glaciers in Greenland and Antarctica are now beginning to provide new data for a better understanding of the theory of development of continental ice sheets. For example, Dansgaard et al. (1969, 1971) utilized the theories of glacier flow in establishing a time scale for the Greenland Camp Century ice core from which to interpret climatic history for the past 126,000 years.

Although the internal processes of mountain glaciers and continental ice sheets are controlled by the same laws, they are sharply different in character. They are subjected to different types of climatic stresses created by length of daylight, diurnal temperature cycles, and diurnal differences in both solar and long-wave radiation. Mountain glacier shapes are varied and are controlled by topography. They seldom reach large extent and thickness because steep slopes of the underlying surface cause rapid ice flow even with small thickness. On the other hand, ice sheets are formed over continental regions where underlying slopes are small. Horizontal transfer over great distance is the result of glacier surface slopes provided by thick ice sheets with surface profiles approximating the shapes of a parabola or ellipse. The rather slight slopes of the ground topography underneath the ice sheet have little or no influence on the horizontal movements of ice sheets of continental size.

There is little direct evidence on the early history of a continental ice sheet (Flint, 1971). An idealized development of an ice sheet such as the Laurentide ice sheet is shown in Fig 4. It probably developed originally as a glacier complex on the plateau and mountains of the Arctic islands such as Baffin, Bylot, Devon, and Ellesmere with peaks exceeding 2400 meters. According to Barry (1966) and Tanner (1944), quoted in Flint (1971), the Labrador-Ungava region of Canada with its cold winters and short cool summers, is meteorologically ideal, when conditions are favorable, for the initiation of a glacier complex and ice sheet.

(3) A Model of Growth and Shrinkage of Non-equilibrium Ice Sheets

Weertman (1964) presents a simplified model based on the perfect-plasticity theory to analyze the rate of growth or shrinkage of non-equilibrium ice sheets of continental dimensions. Figure 5 illustrates the situation for this model. The idealized cross-section of the ice sheet is assumed to extend an infinite distance in an east-west direction. The snowline elevation is assumed to rise linearly with decreasing latitude and is equal to zero at the northern edge of the

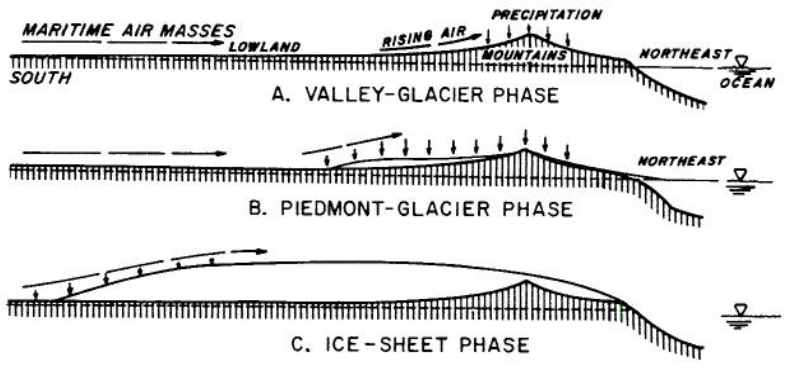

Fig. 4. Idealized development of an ice sheet such as the Laurentide ice sheet in Canada showing mountain effect (after Flint, 1971).

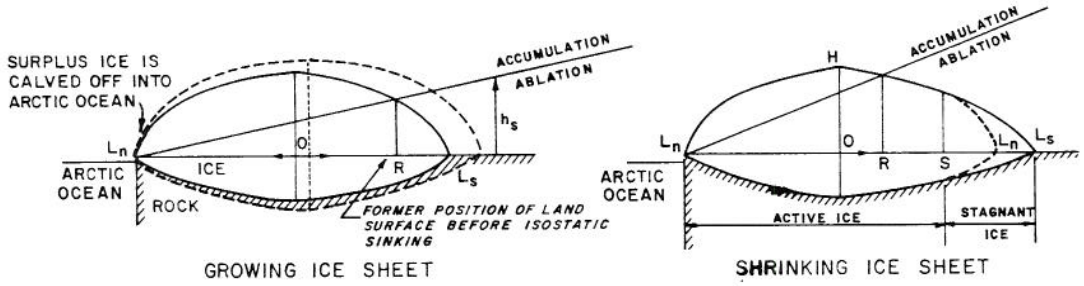

Fig. 5. The Weertman model of an idealized ice age ice sheet in the northern hemisphere (from Weertman, 1964).

ice sheet on the Arctic Coast. Accumulation occurs on any ice surface whose elevation is higher than the snowline and ablation occurs on any ice surface below the snowline. The land upon which the ice sheet is resting is assumed to be flat before the ice sheet started.

If total accumulation over the ice sheet exceeds total ablation, the ice sheet will start to grow in size. The rate of growth of the ice sheet will be determined by the rate of growth of the southern half of the ice sheet since the accumulation area of the southern half is smaller than that of the northern half. The accumulation on the northern half of the ice sheet which is in excess of the amount needed to keep pace with the growth rate of the southern half, would be eliminated by calving off into the Arctic Ocean. As long as the total accumulation is greater than total ablation, the ice sheet will continue to grow until it reaches a stable equilibrium condition as defined by an equation which is a function of the accumulation rate, ablation rate, and rate of rise of the snowline.

If for some reason the accumulation rate, the ablation rate, the rate of rise of the snowline or any combination of these quantities changes in such a direction that the equilibrium size of the ice sheet becomes smaller than the actual size of the ice sheet at the time, then the extremities of the ice sheet will become stagnant and a moderate decrease in accumulation or increase in ablation, if maintained, could cause a large ice sheet to shrink and, under certain conditions, to disappear completely.

Weertman's analysis shows that the growth time of a large ice sheet is of the order of 15,000 to 30,000 years on the assumption that the accumulation rate lies in the range of 0.2 to 0.6 meters per year. The shrinkage time of a large ice sheet is of the order of 2000 to 4000 years on the assumption that the ablation rate lies in the range of 1 to 2 meters per year and ablation occurs over an appreciable area of the ice sheet.

For the mathematical details of the model, the reader may refer to Weertman (1964). Weertman noted that perturbation-type theories have shown that the behavior of non-equilibrium glaciers and ice sheets is exceedingly complex. The perfect-plasticity theory used in his analysis would not be adequate for investigation of such detailed pheonomena as kinematic waves in non-equilibrium behavior of ice sheets. However, the theory offers considerable advantage by masking the detailed phenomena which are of no concern in the study of the gross behavior of ice sheets.

Weertman further contended that analyses with a more complex model would offer no better answers than that provided by his simplified model since there are virtually no data on paleo-accumulation and paleo-ablation rates to support more refined studies at this time.

(4) Contemporaneity of Glacial Fluctuation

Denton et al. (1971) quoting Hollin (1962) advanced a hypothesis which supports the contention that the Antarctic ice sheet fluctuated in phase with northern hemisphere glaciations.

Sea level is the dominant factor in determining the area and volume of the Antarctica ice sheet which is basically a huge accumulation area with most ablation occurring as icebergs calving from the periphery of the continent. The present size of the Antarctic is restricted mainly by the high sea level. However, during the Pleistocene glaciations eustatic sea level oscillations would permit the Antarctic ice sheet to expand and contract with lowering and rising sea levels (Fig 6).

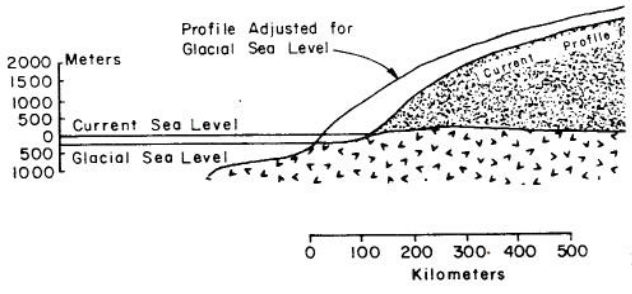

Fig. 6. Idealized profile changes in the Antarctica ice sheet showing effect of sea-level changes on a Pleistocene glacial stage (from Denton, 1971, after Hollin, 1962).

Sea-level fluctuations during the Pleistocene epoch were controlled mainly by the growth and retreat of northern hemisphere ice sheets, of which the Laurentide ice sheet in North America accounted for 60 percent of the variations. Thus, it is reasonable to

assume that the Antarctica ice sheet responded in phase with changes in major glaciations in the northern hemisphere due to the mechanical adjustments to sea-level changes, even though climatic events may not be in phase on the two hemispheres.

2.3 Methods of Dating and Evaluating Climatic History

Dendrochronology. The study of tree rings can provide absolute time scales extending over the past 3000 years. Tree-ring indices have been correlated in various studies with air temperatures, precipitation, runoff, frost and drought (Fritts, 1965; Zeuner, 1970).

Varves. This technique uses proglacial lake sediments. Alternate layers of summer and winter deposition of glacial sediments of clays and sands can provide a means of developing a time scale with yearly intervals up to 15,000 years. Since thickness of varves depends on the melting effects of summer heat, they have been used to estimate historical weather conditions (Zeuner, 1970).

Palynology. The study of pollen and diatom spectra has been widely used by geologists and botanists. Pollen analysis consists of estimating the frequency of occurrence of various species of plants in a given time period by counting the pollen contained at the various depths in the deposits of peats, organic muds, and peaty soils. Various flora species are associated with warm, cool, dry, or wet climates.

Paleontology. The study of both continental and marine fossils and their classification into warm or cold fauna provide a means of estimating climatic changes. Recent developments in oxygen isotopic measurements and radiometric dating have enhanced the usefulness of this technique.

Geological Methods. These methods are based on estimated time series of sedimentation, denudation, erosion, weathering, chemical changes in minerals, glacial deposits, and many other geological processes. Some have been used to estimate climatic changes for the entire life span of the earth (Zeuner, 1970). Radioactive techniques are now providing absolute time scales for many of the processes.

Sea-level Fluctuation. Considerable work has been done in recent years on documenting sea-level variations for many parts of the world (Andrews, 1970). The standard method is by radiometric dating of submerged organic material that can be related to former sea levels with some confidence, such as salt marsh peats and intertidal fauna. Such data can be used to establish dates of high sea levels during the late Pleistocene epoch from which to deduce occurrence of interglacial periods. Attempts have been made to relate eustatic sea-level changes to glacial volume from which to infer periods of advance and retreat of the late Pleistocene ice sheet.

Oxygen Isotope Curves. Measurement of the Oxygen-18 content in the carbonate shells from deep-sea sediment cores and in ice cores from the Greenland ice sheet and from Antarctica are providing data for inferring general changes of climate in the late Pleistocene epoch. Further details are given in Chapter III.

Isotope Geochemistry. Rapid progress has been made in recent years in the development of isotope geochemistry for measuring both time and paleotemperature. Before the introduction of radioactive methods to the measurements of geologic time, the ages of the geologic eras, periods and epochs were expressed only in relative terms based on assumed rates of weathering, biologic evolution, marine invasion, loss of heat by sun or earth, sedimentation in geosynclines, accumulation of salt in sea, the rise of mountains and so on (Bertin, 1972). Since 1948, radiocarbon dating based on the disintegration of carbon-14 in dead organic matter has added considerably to the knowledge of the chronology of the late Pleistocene. Its usefulness is limited to about 20,000 years for carbonate materials and 40,000 years for organic materials. By pre-enrichment of the C-14 in the sample carbon, measurement sensitivity to 70,000 years can be obtained in some cases. Various uranium disequilibrium-series methods have now extended isotope dating to samples ranging in age from tens of thousands to several hundreds of thousands of years and more. The potassium-argon dating method is the widest ranging of all isotopic dating methods. Under ideal circumstances it can overlap the radiocarbon method and extend to samples billions of years old. In practice, accuracy decreases sharply for samples less than several hundred thousand years old.

Morrison (1968) cautioned that many isotopic dates have large standard errors (particularly beyond the range of carbon dating). Such dates indicate merely a time-probability zone in which the true age lies. The time-probability zone of a given isotopic-age determination can be so wide (varying from thousands to tens of thousands of years) that the determination would be of little value for precise correlation. A detailed review of the isotope dating methods in current use is given by Broecker (1965).

Paleomagnetic Correlation. Paleomagnetic studies of extrusive igneous rock have established epochs or intervals in which the polarity of the earth's magnetic field have been reversed. According to Ericson and Wollin (1968), it has been shown that the remanent magnetism of deep-sea sediments is sufficiently strong and stable that these polarity reversals can be detected and used to date and correlate geological events throughout the world that are recorded in the deep-sea sediments over the past 5 million years. The major limitations of the paleomagnetic technique for use in the study of the details of climatic oscillations during the Pleistocene is its dependence at present on calibration by potassium-argon dating. The time required for a complete transition from one polarity to another is difficult to measure directly because potassium-argon dating possess a statistical uncertainty longer than the transition time. Transition times from one polarity to another vary from 5,000 to 20,000 years (Cox and Doell, 1968).

CHAPTER III
REVIEW OF PREVIOUS WORK ON CLIMATIC CHANGES

This chapter outlines the history and the recent advances made in the extraction of information on paleoclimate from the deep-sea sediment cores and ice cores from the Greenland ice sheet.

3.1 Deep-Sea Sediment Cores

(1) Core Acquisition

Since the early 1930's oceanographers have tested many devices for probing the sedimentary layers of mud and dead marine organisms on the ocean bottom. It was not until 1945 that the Swedish oceanographer Borje Kullenberg was successful in developing a piston corer which can recover cores more than 20 meters long from the ocean floor and without compaction due to coring. The Kullenberg device consists of a steel tube with a sharp cutting edge, which can be driven deep into the deposits on the ocean floor to bring back long cylinders of sediment about 5 cm in diameter. The Kullenberg piston corer with subsequent modification by Ewing to prevent loss of sediments in the upper 40-50 cm of the core remains the most efficient method today (Ericson et al. 1964).

The sediment cores must be located in regions where the water depth is less than 5 km, otherwise the carbonate fossils needed for analyses will have been dissolved. Also, the site must be above the abyssal plain to avoid sampling of reworked sediments carried down from the continental slopes by turbidity current action. The best places to obtain sediment cores which have not been disturbed after deposition are the tops and flanks of gentle rises or ridges on the deep-ocean floor. Most of the sediments settling on such areas may remain in place, but a certain amount of slumping can occur on the steeper slopes. Slumping can be useful in removing sediment of late Pleistocene age to bring older sediment within reach of the coring tube (Emiliani, 1958; Ericson et al. 1964).

(2) Climatic Indicators

Among the countless number of organisms that comprise the plankton floating in the sunlit surface water of the oceans is a group of one-celled animals known as foraminifera or forams for short. These temperature-sensitive micro-organisms secrete some of the most delicate calcareous shells known in nature. For millions of years, these animals have lived near the surface of the oceans and their secretions of dead shells have collected layer upon layer at the bottom of the sea. The foram shells mixed with shells of other sea-dwelling animals and fine mineral particles washed down from the continental surfaces together form a sedimentary layer referred to as "globigerina ooze" facies.

It should be noted that there are two types of foraminifera: the planktonic type which lives mainly within the upper 100 to 300 meters of the ocean surface and can serve as indicator of ocean surface temperature; and the benthonic type which is a rarer bottom dwelling species that can serve as indicator of ocean bottom temperature.

Since the pioneer work of Schott in 1935, micropaleontologists have attempted to use fossil planktons in the deep-sea sediments of globigerina ooze facies to infer Pleistocene marine climates. In the past two decades, considerable progress has been made in constructing curves of near-surface ocean temperatures for the entire Pleistocene on the basis of data obtained from deep-sea cores from the Atlantic and Pacific Oceans and the Caribbean and Mediterranean Seas.

Climatic records of the past are obtained from sea-sediment cores in two ways. The first and widely used approach is based on paleontologic evidence of changes in fossil species at the different strata of the sea core as a result of environmental and climatic changes. The second approach is based on isotopic measurements of the ratio of Oxygen-18 to Oxygen-16 content in the calcareous shells of the foram fossils.

(3) Paleontologic Evidence

All paleoecological work on Pleistocene plankton is based on the fundamental assumption that the pelagic ecosystem being sampled today has remained essentially unchanged during the Pleistocene (Imbrie and Kipp, 1971). A study of the geographical distribution of most species of living foraminifera has been made. It has been found that the boundaries of the geographical ranges of the species trend east and west, which suggests that temperature is the most important factor limiting their ranges (Ericson et al. 1964).

The general approach in paleontologic studies of sea cores which can represent hundreds of thousands of years of undisturbed history, has been to measure the relative abundance of cold and warm water species of pelagic foraminifera found in the different strata of the core to make semi-quantitative interpretations in terms of climatic changes. The assumption is made that such variations record shifts in the geographical ranges of the species and that these shifts were consequences of the climatic changes of the late Pleistocene.

Many investigators (Wollin et al. 1971) have found that the Globorotalia menardii group of planktonic foraminifera is the most reliable of the climatic indicators. High abundance of the Globorotalia menardii group indicates warm climate. Other reliable climatic indicators found in the Atlantic and Caribbean cores are based on coiling ratios of Globigerina pachyderma and coiling ratios of Globorotalia truncatulinoides. In warm water, the dextral or right coiling form of Globigerina pachyderma dominates. In cold water, the left coiling or sinistral form dominates. For the Globorotalia truncatulinoides, the reverse is true; that is, in warm water left coiling dominates, and in cold water right coiling dominates.

Since 1947, the Lamont Geological Observatory, Columbia University has raised more than 5000 deep-sea cores from oceans all over the world. A series of studies has been carried out by Ericson et al. (1964, 1968) in which composite climatic records of the Pleistocene were obtained by piecing together overlapping

sections from selected cores of deep-sea sediments taken from the Lamont Geological Observatory collection. The paleontologic studies consisted of analyses of the relative numbers of warm-water and cold-water species of planktonic foraminifera occurring in each of the selected cores. The composite results were then correlated with the glacial and inter-glacial ages of the Pleistocene.

In general, the results of these paleontologic studies are presented in the form of semi-quantitative paleoclimatic curves with ordinates ranging from "warm" to "cold" and abscissas in terms of core depth or converted to a time scale by some appropriate dating technique (Fig 7).

In the Ericson studies, absolute time scale for the sea cores from the present back to about 175,000 years ago were determined by the radiocarbon, the protactinium-ionium and the protactinium dating methods. A time scale of about 1.5 million years for the entire Pleistocene epoch was estimated by extrapolation beyond 175,000 years ago. This was increased to about 2 million years on the basis of paleomagnetic studies. The beginning of the Pleistocene is defined to be at a particular stratigraphic level of a core mainly by the first appearance of Globorotalia truncatulinoides in abundance and by the near extinction of Discoasteridae.

Recently, Imbrie and Kipp (1972) have devised a new micropaleontological method to make fully quantitative estimates of past marine climates. Their method is based on a mathematical procedure known as Q-mode factor analysis to produce a set of equations relating ocean surface temperatures and salinity to the various species of fossils found at the core tops. These equations can then be used on samples taken from different strata of the cores to make fully quantitative climatic estimates. The model is still in the testing stage. Attempts were made to relate the results of their model to the Milankovich theory which would permit quantitative predictions of long-term fluctuations in the global temperature pattern. The test was made on deep-sea sediment cores taken from the Caribbean sea. For the test, Imbrie and Kipp adopted an average sedimentation rate of 2.35 cm per 1000 years to produce a time scale for the core. This average rate was determined radiometrically by Broecker and van Donk (1970) using the protactinium-ionium method. The expected eccentricity frequency was found to match the observed spectrum in the paleontological curve developed from the Imbrie-Kipp model; but the expected tilt and precessional frequencies were not apparent. They concluded that final evaluation of their method and conclusion regarding the Milankovich theory must await the study of a suite of cores by the same method.

(4) Oxygen-Isotope Method

Concentration Index. The method of determining paleotemperatures by measuring the relative abundance of two isotopes of oxygen in fossil sea shells was originally devised by Urey. Urey found that the ratio of Oxygen-18 and Oxygen-16 in the calcium carbonate of a shell indicated the temperature of the water at the time the shell was growing. The greater the proportion of Oxygen-18 to Oxygen-16 the higher the temperature of the water. The technique has been used extensively by Emiliani (1955, 1958, 1966a, 1966b, 1970, 1972) and others in the analyses of pelagic foraminifera components of deep-sea sediment cores.

Essentially, a concentration index value $\delta(O^{18})$ is measured which gives the per mil difference between the Oxygen-18 to Oxygen-16 ratio in the fossil sample and in a fixed standard. The concentration index is given by the equation

$$\delta(O^{18}) = 1000 \left[\frac{(O^{18}/O^{16})_{sample} - (O^{18}/O^{16})_{standard}}{(O^{18}/O^{16})_{standard}} \right] . \qquad 3.1$$

The concentration index $\delta(O^{18})$ is measured by alternately passing the sample and the standard through a mass spectrometer. The standard used in Urey's laboratory at the University of Chicago is based on a pulverized specimen of Belemnitella americana from the Upper Cretaceous Peedee formation of South Carolina. This standard is commonly referred to as the Chicago Standard PDB-1. The mass spectrometric analysis is performed by balancing the currents developed by the two ions beams in the dual ion collector when the standard is run, and then by measuring the current excess

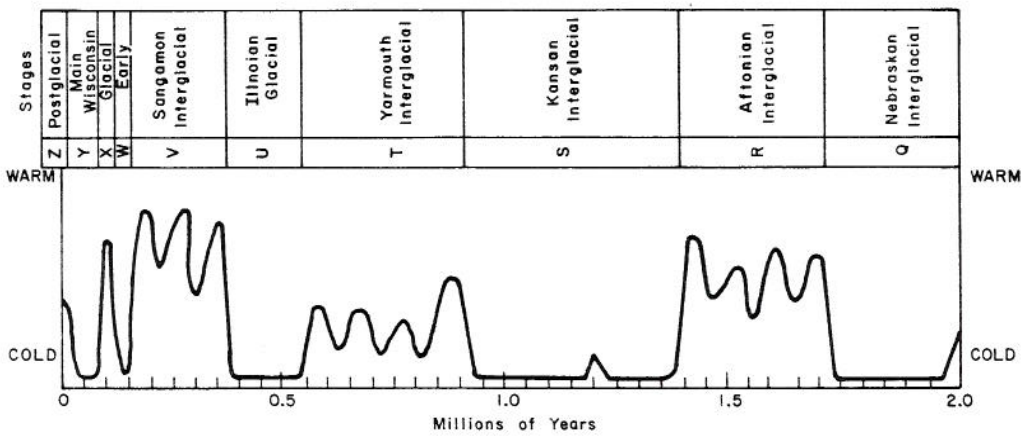

Fig. 7. Pleistocene curve based on paleontological studies of deep-sea cores from equatorial Atlantic, the Caribbean and the Gulf of Mexico (from Ericson et al. 1968).

or deficiency from the null point when the sample is run. The difference is proportional to the per mil difference in the O-18 to O-16 ratios.

An error analysis for the isotope technique was made by taking 102 measurements of the same calcium carbonate sample of a pulverized specimen of Glycimeris violacea obtained from a beach deposit in Spanish Morocco. The error analysis gave a standard deviation of 0.10 per mil which corresponds to 0.4°C according to Emiliani (1955).

Temperature Relationship. The relationship between the concentration index and the environmental temperature of the water in which the fossil shells were formed was established empirically (Epstein et al. 1951, 1953). The relationship is given as

$$T = 16.5 - 4.3\,(\delta - A) + 0.14\,(\delta - A)^2 , \qquad 3.2$$

where T is degree centigrade of environmental temperature of the water, δ is the concentration index $\delta(O^{18})$, and

$$A = \frac{(O^{18}/O^{16})_{w'} - (O^{18}/O^{16})_{w}}{(O^{18}/O^{16})_{w}} , \qquad 3.3$$

with A a correction factor to be applied if the oxygen isotopic composition of the water (w') from which a given sample of calcareous shell was deposited is different from that of average ocean water (w). According to Emiliani (1961), estimates of A, the oxygen isotope composition for open oceanic waters of the past, can be made with reasonable confidence but the temperature values obtained using such estimates cannot be considered as unequivocally determined. The value of A used in computing the paleotemperature of the ocean surface waters has been a controversial subject which must still be resolved (Shackleton, 1967; Eriksson, 1968).

According to Emiliani (1955), oxygen isotopic analysis of marine carbonates gives at best the exact temperature at which the carbonate was deposited. At low latitudes where seasonal temperature variations are small, isotopic temperature obtained from pelagic foraminifera are probably close to the annual mean surface water temperature. At higher latitudes where seasonal variations are greater, the isotopic temperature is probably close to the summer mean surface water temperatures. Certain species of foraminifera such as Globigerinoides rubra and Globigerinoides sacculifera tend to register summer surface temperatures. Others such as Globigerina inflata may represent winter ocean surface temperatures for cores at mid-latitudes, and summer temperatures at a certain depth below the ocean surface for cores at low latitudes (Emiliani, 1957).

Foraminifera Species. In the extensive work by Emiliani most of the isotopic analysis on the Caribbean and equatorial Atlantic cores were made on the fossil species of Globigerinoides rubra and Globigerinoides sacculifera which live closest to the surface (30-40 m) and therefore provide the best record of ocean surface temperature variations. In cores from the Pacific and middle Atlantic, these two species are rare or absent so that the other species were used in analyses, namely Globorotalia tumide, Pulleniatina obliquiloculata and Globigerina inflata. These species generally occupy a deeper habitat (down to about 140 m) and as a result register temperature variations smaller than those species occurring at the surface.

Generalized Paleo-Temperature Curve. The numerous $\delta(O^{18})$ curves (Fig 8) produced by Emiliani for Pleistocene cores in the Caribbean and equatorial Atlantic show remarkably consistent fluctuation patterns (Emiliani, 1955, 1966a, 1972; Broecker and van Donk, 1970). By using all the isotopic curves obtained so far from Caribbean and Atlantic cores, Emiliani (1972) has reconstructed a generalized paleo-temperature curve by averaging stage by stage the information provided by each core. The latest curve (1972) is a revision of earlier curves produced in 1955 and 1966 (Fig 9).

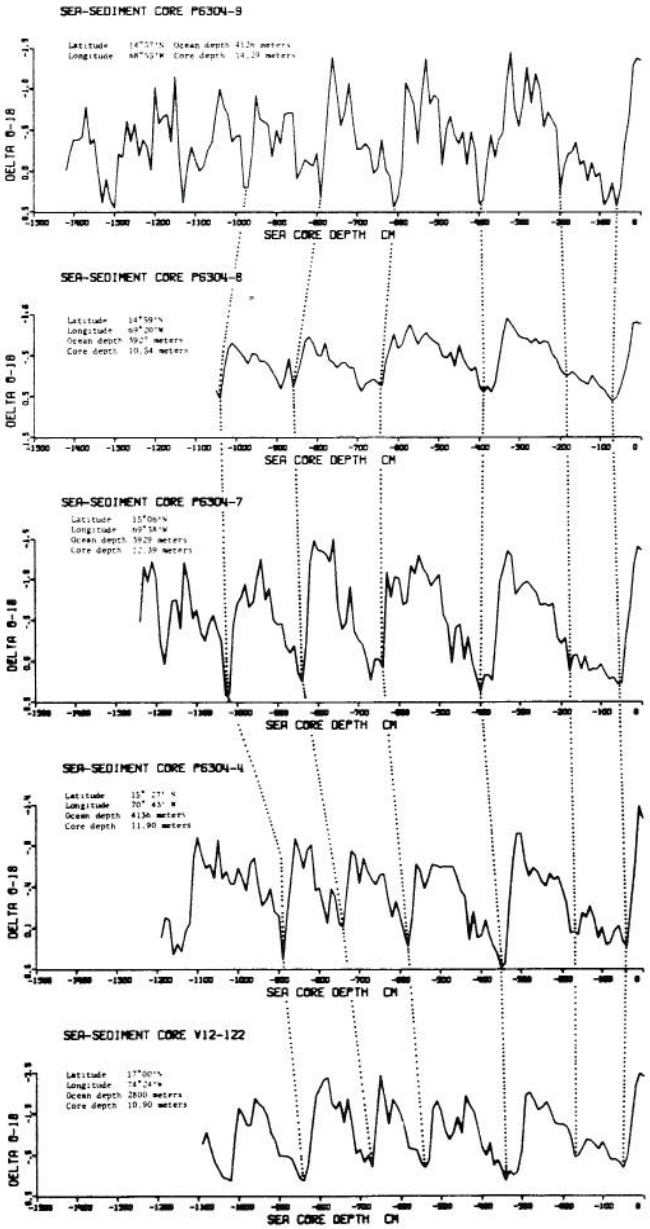

Fig. 8. Plots of Oxygen-18 curves for selected sea-sediment cores from the Caribbean Sea showing visual correlation between cores.

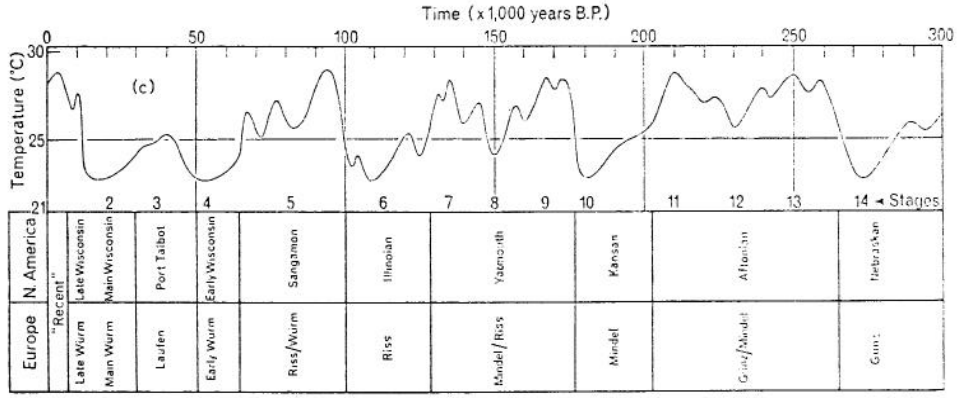

(a) 1961 version based on data from cores P6304-8 and P6304-9, showing Emiliani's correlations to the continental Pleistocene with European and North American terminology.

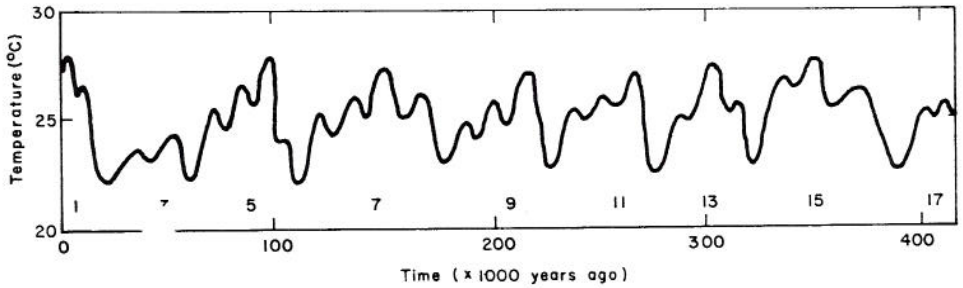

(b) 1972 version based on data from cores P6304-4, 7, 8 and 9.

Fig. 9. Generalized Pleistocene temperature curve for the surface water of the central Caribbean Sea based on oxygen isotope analysis of deep-sea sediment cores (from Emiliani, 1961, 1972).

The scale adopted by Emiliani (1972) is based on the Carbon-14 dating method and the Protactinium-ionium dating method for the time interval from present to 150,000 years ago. Beyond this interval, the chronology is based on the ages of northern summer insolation minimum according to the Milankovich cycle as calculated by Brouwer and van Woerkom (van Woerkom, 1960).

Problems of Interpretation. According to Broecker and van Donk (1970), it is still not clear whether the major factor causing the observed temporal variations in the O-18 to O-16 ratio in the shells of planktonic foraminifera found in deep-sea sediment cores is due to changes in the surface water temperatures, or in the isotopic composition of sea water in which the shells grew or on a combination of both factors. Imbrie and Kipp (1971) suggest that although the exact interpretation of the $\delta(O^{18})$ curves is uncertain, there can be no doubt that the fluctuations shown on the curves contain important paleo-oceanographic information resulting from changes in ice volume, water temperature or some combination of these factors.

Shackleton (1967) quoting Broecker (1965) indicated that the well-documented movements in marine planktonic provinces during the Upper Pleistocene could have been caused by changes in salinity rather than by changes in temperature. Shackleton suggested that the changes in salinity could be accounted for by changes in ocean water density resulting from the extraction of large quantities of water from the oceans and their storage in the form of continental ice and the subsequent release of the fresh water from the continental ice sheets to the oceans. If such were the case Shackleton (1967) proposed that every faunal or isotopic curve be re-read "cold" to mean "extensive continental glaciation" and "warm" to mean "glaciers reduced to their present level." Regardless of the cause of the isotopic changes, Broecker and van Donk (1970) stated that a first-order synchroneity between isotopic composition of the fossil shells and the extent of continental glaciation might be expected. Shackleton further suggested that the time sequence for the Pleistocene developed by Emiliani (1966) from oxygen isotope analysis and correlation of many deep sea cores is enhanced by the certainty that it is a time sequence for terrestrial glacial events, rather than oceanogrophic events.

(5) Time Resolution of Deep-Sea Cores

Deep-sea cores of globigerina ooze facies generally consist of a mixture of fine mineral particles brought by rivers or winds from continental surfaces and particles of calcium carbonate shells secreted by planktonic organisms. According to Wollin et al. (1971), the rate of sediment accumulation under normal conditions in the deep oceans varies from 1.5 to 3 cm in 1000 years. Within the upper few centimeters of the deep-sea floor exists a variety of benthonic macro-organisms which are mud dwellers and mud eaters. These deep-sea animals burrow into and mix together within the upper few centimeters of sediment as it accumulates. Consequently, records derived from deep-sea sediments can provide, in general, only a rather coarse time resolution of 2000 years or more. Temperature oscillations shorter than a few thousand years such as the Valders re-advance and other minor oscillations recorded in the geological records of glacial chronology are generally not resolvable by deep-sea cores.

According to Emiliani (1958), it is believed that levels in the sea core 10 cm apart contained little common material and sampling at stratigraphic intervals greater than 10 cm should represent truly gradual

changes. In the paleontological studies by Ericson et al. (1968), samples for analysis were taken at 10 cm intervals. In the oxygen isotope studies carried out by Emiliani (1955) half core samples 2 cm thick were taken at 10 cm intervals from each of the Atlantic and Caribbean cores.

Under ideal deposition conditions and in the absence of burrowing deep-sea animals, Emiliani (1955) suggested that a time resolution of about 10 years could be possible from sediments obtained with present coring devices; the time resolution being limited only by the largest practicable diameter of the coring device and the amount of material needed for the various analyses in the laboratory. Other than some studies on a few short pilot cores, however, no oxygen isotope studies have been made on any long cores in the detail required to assess these possibilities. On the other hand, Wollin et al. (1971) have studied a suite of seven cores selected from the Lamont Geological Observatory which they believe are suitable for detailed study of late Pleistocene climate. Using paleontological techniques, they were able to resolve minor climatic fluctuations as short as 550 years duration.

(6) Chronology of Sea Cores

The ages of the different strata in the deep-sea sediment cores is a subject of controversy. In practice, the chronology for the Pleistocene from deep-sea core data has been estimated on the basis of radioisotopic age determination of samples taken from the upper portion of the core. The average or constant rate of sedimentation thus obtained was applied to the entire core. A comprehensive summary of ten methods of radioisotopic dating that have been used for this purpose is given by Broecker (1965). These include the radiocarbon method, potassium-argon method and various uranium disequilibrium-series methods.

Although different investigators may use the same technique in their dating studies, results often differ. Age determination by radiometric methods is subject to many errors such as: analytical errors, error caused by contamination, errors due to loss or exchange of isotopes and possibly other reasons (Morrison, 1968). For example, Broecker and Ku (1969) found results that were substantially different from that of Emiliani and Rona (1969) with both teams of investigators using the protactinum-ionium method in dating the same or adjacent samples taken from the same cores. Broecker and Ku suggested that the Emiliani and Rona time scale should be increased by 25 percent.

Broecker et al. (1958) carried out an analysis of an Atlantic deep sea core which showed that sedimentation rate is not a constant but is related to temperature variations at the surface of the ocean as well as to the extent of continental glaciation. Thus, the assumption of constant sedimentation rate can introduce appreciable errors.

It also should be noted that the chronologies of the Pleistocene determined by Ericson and Wollin (1968) using paleontological methods and Emiliani (1966) using the oxygen isotope method differed widely. Emiliani (1966) placed the beginning of the Pleistocene about 425,000 years ago, whereas Ericson and Wollin (1968) placed this boundary at about 2 million years ago. The latter represents a revision from an earlier study by Ericson et al. (1964) as a result of subsequent paleomagnetic considerations. In the earlier study, the boundary was assumed to be at 1.5 million years ago.

3.2 Greenland Camp Century Ice Cores

(1) Core Acquisition

Core drilling in glaciers to obtain thickness measurements are reported to have begun in Switzerland as early as 1842. It was not until 1950 that limited success was achieved almost simultaneously by three major core-drilling projects conducted by groups from France, the Scandinavian countries, and the United States. In all cases core recovery was discontinuous and mainly of poor quality. At that time, core diameter was limited to 5 to 8 centimeters and depth of penetration did not reach much more than about 100 to 150 meters (Langway, Jr., 1967; Langway, Jr. and Hansen, 1970).

Stratigraphic studies of the Greenland ice sheet by the United States Army Cold Regions Research and Engineering Laboratory (CRREL) and its predecessor SIPRE began in the early 1950's. Studies were initially performed in hand-excavated pits and were followed by deep-drilling programs using rotary, thermal and electromechanical coring devices. In 1966, a combined thermal and electromechanical coring system was used to recover a 1390-meter core reaching from surface to bedrock at Camp Century on the North Greenland ice sheet. With the electromechanical system, chips remaining in the bore hole were dissolved in an aqueous solution of ethylene glycol and the sample recovered in a bailer. The hole was "dry bore" to a depth of 400 meters. At greater depths the bore hole was filled with fluids consisting of 88 percent trichloroethylene and 12 percent arctic diesel oil to prevent closure. Contamination from the fluids can present problems for certain ice-cores studies. Also, in using the thermal system, heat can alter the physical and chemical composition of the upper 70 meters of core (Langway, Jr. and Hanse, 1970).

The best place to drill for deep core in a polar glacier is in an area of simple environment. The better environmental conditions are found usually in areas of high elevation where wind motion is low and summer surface temperatures do not cause excessive melting. Wind can redistribute the year's accumulation so that estimates of accumulation based entirely on the occurrence of isotopic maxima and minima can be completely misleading (Gow, 1968). Excessive melting and percolation through the ice sheet can obscure stratigraphic structure on recrystallization. Camp Century on North Greenland was chosen for the drill site primarily because of its suitable environmental conditions (Langway, Jr., 1967).

(2) Climatic Indicator Based on the Concentration Index of O-18

The use of Oxygen-18 concentration in glacier ice as a climatic indicator of past conditions was first proposed by Dansgaard in 1954. The concentration of O-18 in precipitation, particularly at high latitudes, is determined mainly by its temperature of formation. Since the isotopic composition of precipitation in the form of snow remains unchanged as glacier ice for long periods of time, ice cores offer an important source of paleoclimatic information. Increasing content of O-18 in the ice-core profile indicates warming climate

and decreasing content of O-18 in the ice core indicates cooling climate. Unfortunately, it is not possible to use the O-18 concentration index to infer time variation in the rate of accumulation. The thicknesses of old annual layers depend on many unknown parameters which can influence their relation to the accumulation rate (Dansgaard et al. 1969, 1971).

The concentration index $\delta(O^{18})$ is defined as the relative deviation of the ratio of O-18 to O-16 in a sample of the ice core from that of Standard Mean Ocean Water or SMOW (Dansgaard, 1964), as

$$\delta(O^{18}) = 1000 \left[\frac{(O^{18}/O^{16})_{sample} - (O^{18}/O^{16})_{standard}}{(O^{18}/O^{16})_{standard}} \right] \quad 3.4 .$$

It should be noted that values of $\delta(O^{18})$ in the ice core are not in the same units as that for the sea-sediment core. They are referenced to different standards. For the sea sediment, the reference is the Chicago Standard PDB-1. For the ice core, the reference is the Standard Mean Ocean Water (SMOW). The units used for the two types of core data are in fact in the opposite sense; increasing values of $\delta(O^{18})$ in the sea-sediment core analysis indicate a cooling trend, whereas increasing values of $\delta(O^{18})$ in the ice core indicate a warming trend.

The ice-core measurements were made by a mass spectrometer with measurement accuracy given as ±0.2%. Details of the measurement techniques is given by Dansgaard (1961) and Craig (1961).

The 1390-meter long and 12-cm diameter ice core from Camp Century Greenland ice sheet was cut into some 7500 core segments and analyzed in a continuous sequence to obtain values of $\delta(O^{18})$. The upper 283 meters of the core were cut to represent 10 to 20 years per sample in the time range of 0 to about 800 years B.P. The next section of core from depths of 296 to 1150 meters was cut to represent 50 year increments between 1000 and 12,000 years B.P. The remaining section of the core down to a depth of 1373 meters was cut to represent 200 year increments (Fig 10). The lowest 17 meters of silty ice were not considered since its mode of creation is still open to question (Dansgaard et al. 1971).

The main advantage of ice-core data over the sea-core data as a climatic indicator is the fact that the ice-core data offers the possibility of a continuous sedimentary sequence from which data for time intervals as short as a decade or less can be extracted, the only limitations being obliteration of isotopic gradients by diffusion in solid ice (Dansgaard et al. 1971). For the purpose of studying the degree of stochasticity in climatic changes created by random processes in the earth's environment, a time series which can resolve climatic fluctuations of short duration is most important.

The disadvantage of the ice-core data in comparison to the sea-core data is basically in their relative lengths of record. Sea cores offer the possibility of deriving hundreds of thousands to millions of years of climatic history covering the entire Pleistocene epoch with all the glacial stages. Whereas, the total ice-core profile from the Camp Century site represents slightly more than a hundred thousand years which covers only the last main glacial or Wisconsin stage of the Pleistocene epoch. Data from the Byrd Station core in the Antarctic offer a longer record but studies show that the climate of the Byrd Station region is extremely complicated which makes climatic interpretation from the isotopic record very difficult (Langway, Jr. and Hansen, 1970).

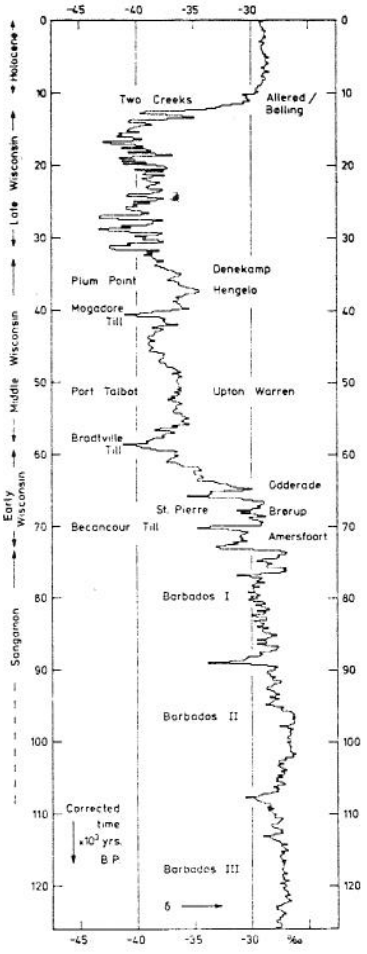

Fig. 10. Late Pleistocene Oxygen-18 curve for the ice core from Camp Century, Greenland. Oxygen-18 values are given in 200-year intervals. Labels show tentative interpretations in European and North American terminology for various glacial events of the late Pleistocene epoch (from Dansgaard et al. in Turekian, ed., 1971).

(3) Temperature Relationship

Dansgaard (1964) presents a graph which shows a strong correlation between the annual mean value of $\delta(O^{18})$ and the annual surface air temperature t_a. The $\delta(O^{18})$ values of precipitation were taken over a wide temperature range including values from North Atlantic coast and Greenland ice-cap stations. The graph is shown in Fig.11 and the equation is

$$\delta(O^{18}) = 0.695\ t_a - 13.6 \quad 3.5$$

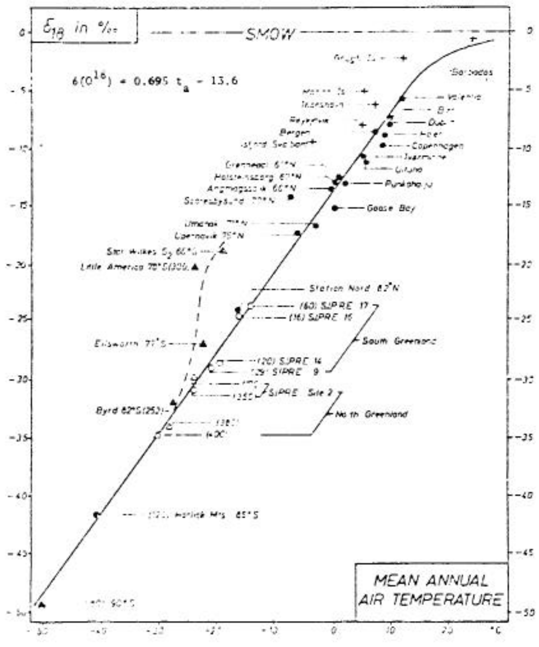

Fig. 11. The annual mean Oxygen-18 value of precipitation as a function of the annual mean air temperature at surface. The figures in parenthesis indicate the total thickness (in cm) of the investigated snow layers (from Dansgaard, 1964), (SMOW, standard mean ocean water).

Despite the strong geographical correlation between $\delta(0^{18})$ and air temperature using present day data, Dansgaard et al. (1969, 1971) emphasized that the $\delta(0^{18})$ profile of the ice core should not be strictly interpreted as a paleo-temperature record since other parameters may influence the isotopic composition as well. Their reasons are enumerated as:

(a) the deeper strata originated further inland where perhaps slightly different climatic conditions existed;

(b) the isotopic composition of sea water, which provides the moisture for the precipitation changes;

(c) the ratio of summer to winter precipitation possibly changed;

(d) the mean meteorological wind pattern possibly changed;

(e) the flow pattern of the ice in the accumulation area possibly changed; and

(f) the thickness of the ice sheet possibly changed.

They suggested, however, that a given increase in $\delta(0^{18})$ may be properly interpreted as a consequence of warming and a decrease as a consequence of cooling. In any case, they conclude that the $\delta(0^{18})$ curve, while valid primarily for the North Greenland area, shows a general trend for the past 75,000 years that agrees quite well with other parts of the world.

(4) Chronology of Ice Cores

The value of the isotopic curves for the ice cores depends upon a knowledge of the age of the ice in question. For shallow cores, it is possible to establish an absolute time scale by measuring seasonal oscillations in the isotopic composition of the ice and count the summer isotopic maxima continuously from the surface to determine annual layers. For deep cores, however, molecular diffusion in the solid ice will gradually obliterate the short-term oscillations so that the counting technique becomes impractical as the depth increases beyond a certain limit corresponding to not more than a few thousand years (Dansgaard et al. 1969).

Radioactive isotope dating techniques have not yet been developed to the degree that they can now be applied to calibrate ice cores from deep-bore holes. For example, it was found in recent tests of a technique for sampling C-14 from ice "in situ" that 1 ton of glacier ice was required to perform the measurement (Dansgaard et al. 1969).

As a consequence, Dansgaard et al. (1969, 1971) resorted to a theoretical ice flow model to develop a preliminary time scale for the Camp Century ice core. The model is based on a generally accepted glacier flow theory with reasonable assumptions concerning the parameters that influence it. The preliminary time scale obtained from the theoretical model was further adjusted by calculating the Fourier power spectra for the 200 year samples in sliding 10,000 year intervals to detect persistent oscillations. This provided the data for a step-wise correction of the preliminary time scale. For details of their dating technique, readers should refer to Dansgaard et al. (1971). A brief discussion of the technique is presented in Chapter VII.

CHAPTER IV
THE MILANKOVICH ASTRONOMICAL THEORY OF LONG-TERM GLOBAL VARIATIONS OF INCOMING SOLAR RADIATION

4.1 General

This chapter outlines the basic concepts of the Milankovich astronomical theory. The outline is descriptive in nature and is intended to be a concise and convenient background reference for the presentations given in this study. For detailed and complete mathematical treatment of the subject, the reader is referred to the work of Vernekar (1972) and the original work of Milankovich (1941) which has been translated into English from German by the Israel Program for Scientific Translation, Jerusalem (1969). Since the basic hypothesis in this investigation of deterministic-stochastic models of long-term climatic changes is based on the concept that its deterministic component is produced by a transformation of the almost-periodic astronomical process, review of the Milankovich theory is given special attention.

The astronomical theory is commonly referred to as the Milankovich theory in recognition of the fact that his rigorous mathematical treatment of the problem gave it a firm theoretical ground. In addition to the astronomical calculations, Milankovich developed a physical model to describe the effect of changes in incoming radiation on surface air temperatures and related the calculated air temperature fluctuations to the glacial and interglacial periods of the Pleistocene epoch. His work on the astronomical theory is seldom questioned but his quantitative estimates of the astronomical effects on atmospheric temperature and glaciation have been a subject of wide controversy. Much of his meteorological analyses seems to have been superceded (Mitchell, 1958). This chapter is concerned only with the Milankovich astronomical theory and not with the Milankovich physical model of atmospheric temperature and glaciation.

4.2 The Basic Motions of the Earth

(1) Short Period Variations

Once each 24 hours the earth rotates on its axis, spinning from west to east on its path around the sun causing diurnal variations in many geophysical and hydrologic phenomena and producing the daily cycle. Once each month the moon makes a complete revolution around the earth causing almost-periodic oscillations in tides and related hydrologic phenomena and producing the lunar cycle. Once each year the earth moves in an elliptic orbit around the sun causing the annual periodic variation of incoming solar radiation received over the whole planet and producing the annual cycle.

(2) Long Period Variations

As determined from celestial mechanics the long-term variations in the elements of the earth's orbit are due to the interaction between the earth and eight other principal planets, namely, Mercury, Venus, Mars, Jupiter, Saturn, Uranus, Neptune and Pluto. Changes in the gravitational field accompanying motions of the planets result in perturbation of the earth's orbit and its axis of rotation. Three parameters are used to describe changes in the earth's motion as a function of time. These parameters are: eccentricity of the orbit, tilt or obliquity of the ecliptic, and precession. Vernekar (1972) has recomputed Milankovich's results following essentially the mathematical and theoretical treatment developed by Milankovich but with corrections, modifications and more accurate equations derived by subsequent researchers including Brouwer and van Woerkom, Sharaf and Budnikova, and Vernekar. Figure 12 shows diagramatically the various motions of the earth. Variations of the three parameters, eccentricity, tilt, and precession, are shown as a function of time in Fig. 12.

Eccentricity. The earth and moon trace an elliptical path in their annual orbit around the sun with the sun at one focus. The sun's gravity acts on the earth and moon as if they were coupled into a giant dumbbell. It is the center of the dumbbell mass, rather than the center of the earth which moves in a smooth elliptical orbit (Fig. 12, dashed line). The center of the earth follows a serpentine path (Fig. 12, dotted line). The earth-moon system does not quite retrace its orbit in successive years. With each revolution, it begins a path in a position slightly counterclockwise from the previous. Over the past 4 million years, Vernekar has calculated the eccentricity of the orbit to vary from a minimum value close to zero which was reached 534,000 year B.P.* to a maximum value of 0.061 which was obtained 2,775,000 years B.P. It can be seen on Fig. 13, upper graph, that variations in eccentricity exhibit an almost-periodic movement with maxima and minima changing in amplitude and spacing with time. The average time for one complete oscillation has been 93,000 years over the past 4 million years.

Tilt or Obliquity of the Eclipitic. The interactions between the earth and other bodies in the planetary system leads to an oscillatory change in the tilt of the earth's axis with respect to the orbital plane. The tilt has varied from 24.51 degrees to 22.10 degrees in the past 4 million years with an almost-periodic movement averaging 41,000 years per one complete oscillation. The present value of the tilt or obliquity is 23.44579 degrees.

Precession of the Equinoxes. Because the earth has an oblate shape which is flattened at the poles and bulging at the equator, the sun's gravitational attraction of the equatorial belt tends to pull the earth's axis of rotation towards the vertical in relation to the plane of the orbit. The external force applied to a rotating body causes the tilted axis of the earth to swing ponderously around in a tight circle to trace a double conical figure much like the wobbling of a spinning top. The movement is called precession and has an almost-periodic movement averaging

*B.P. means before present.

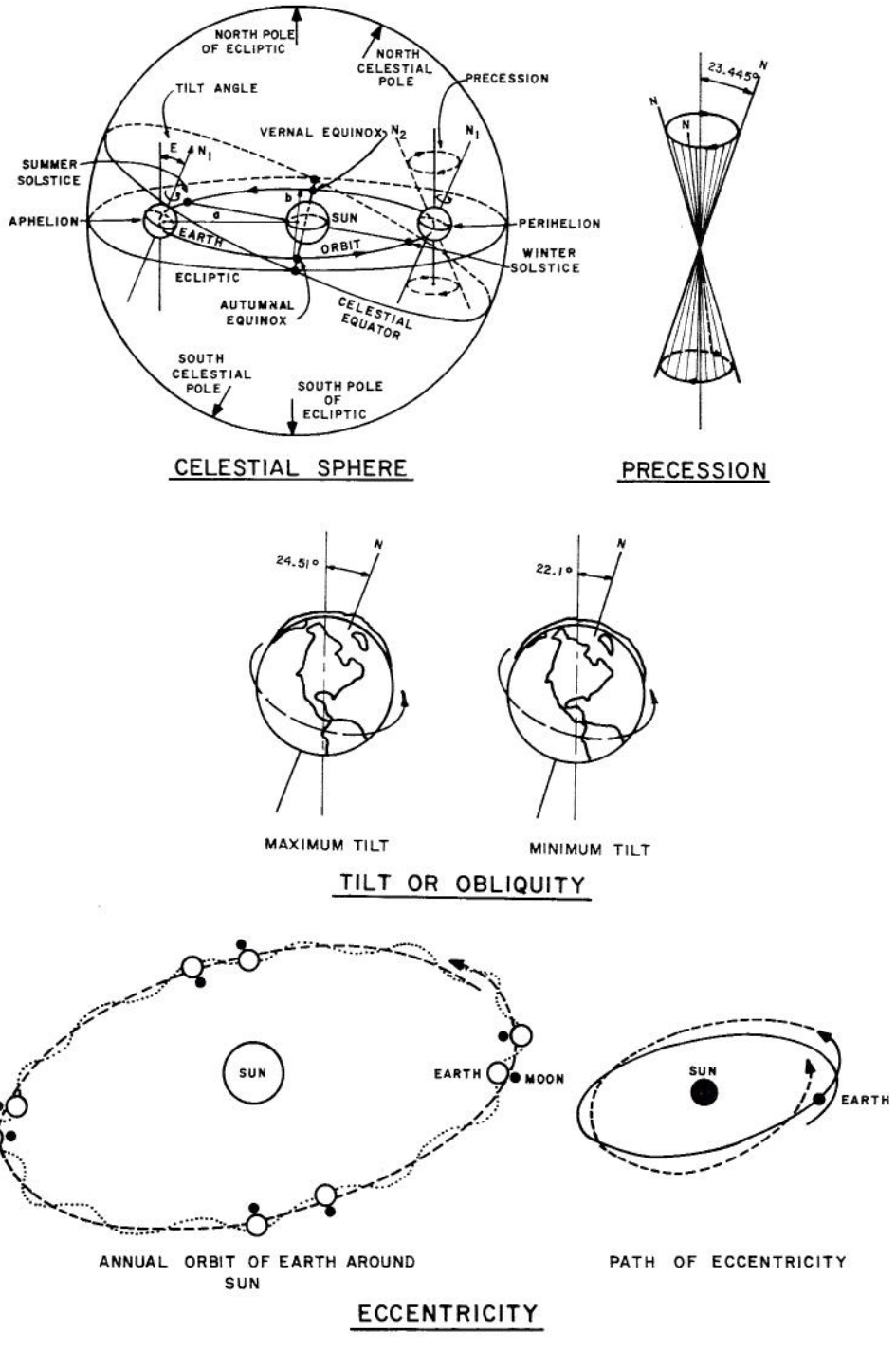

Fig. 12. The motions of the earth (from Imbrie and Kipp, 1971, after Yernekar, 1968).

21,000 years per one complete oscillation. This means that the line joining the equinoxes of the earth's orbit will make one complete revolution of the orbit in this time, on the average.

The cycles attributed to the various astronomical causes are shown graphically on Fig. 14. The daily, monthly, annual, and 11.3 years sunspot cycles are undisputed periodic movements with known physical explanations. The 21,000, 41,000 and 93,000 year, the average periodicities are the result of the Milankovich mechanism, and almost-periodic astronomic processes of eccentricity, tilt, and precession. These almost-periodic movements represent average frequencies and not exact cycles as in the case of truly periodic process with comensurate frequencies.

4.3 Milankovich Theory for Long-Term Variations in Incoming Radiation

The three above described concurrent motions of the earth do not have commensurate frequencies. At

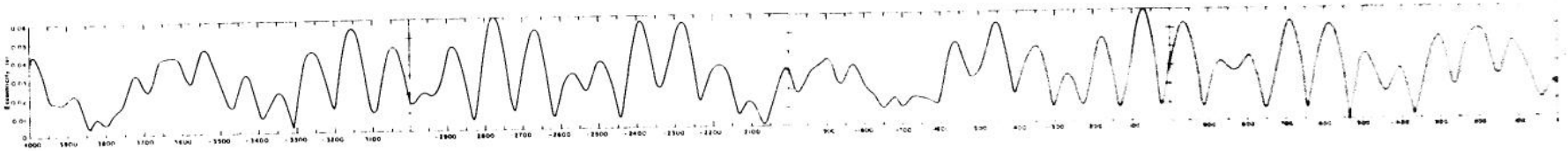

Time before 1950 A.D. in 1000 year intervals

(a) Eccentricity of earth's orbit

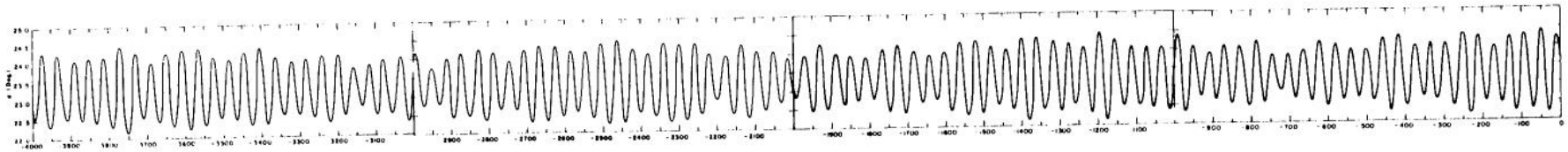

Time before 1950 A.D. in 1000 year intervals

(b) Obliquity or tilt of earth axis

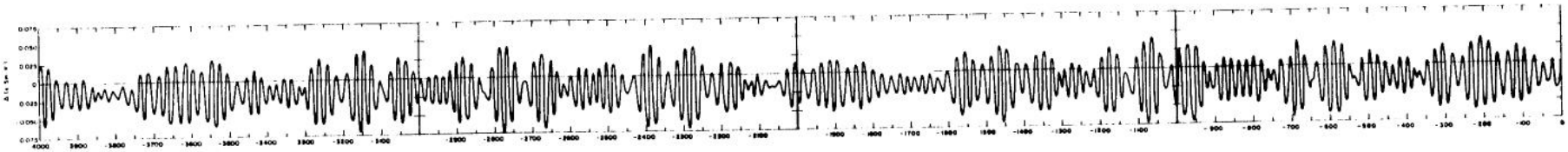

Time before 1950 A.D. in 1000 year intervals

(c) Precession or longitude of perihelion

Fig. 13. Variations of eccentricity, tilt, and precession as a function of time for the period from 4,000,000 B.P. to the present time (from Vernekar, 1972).

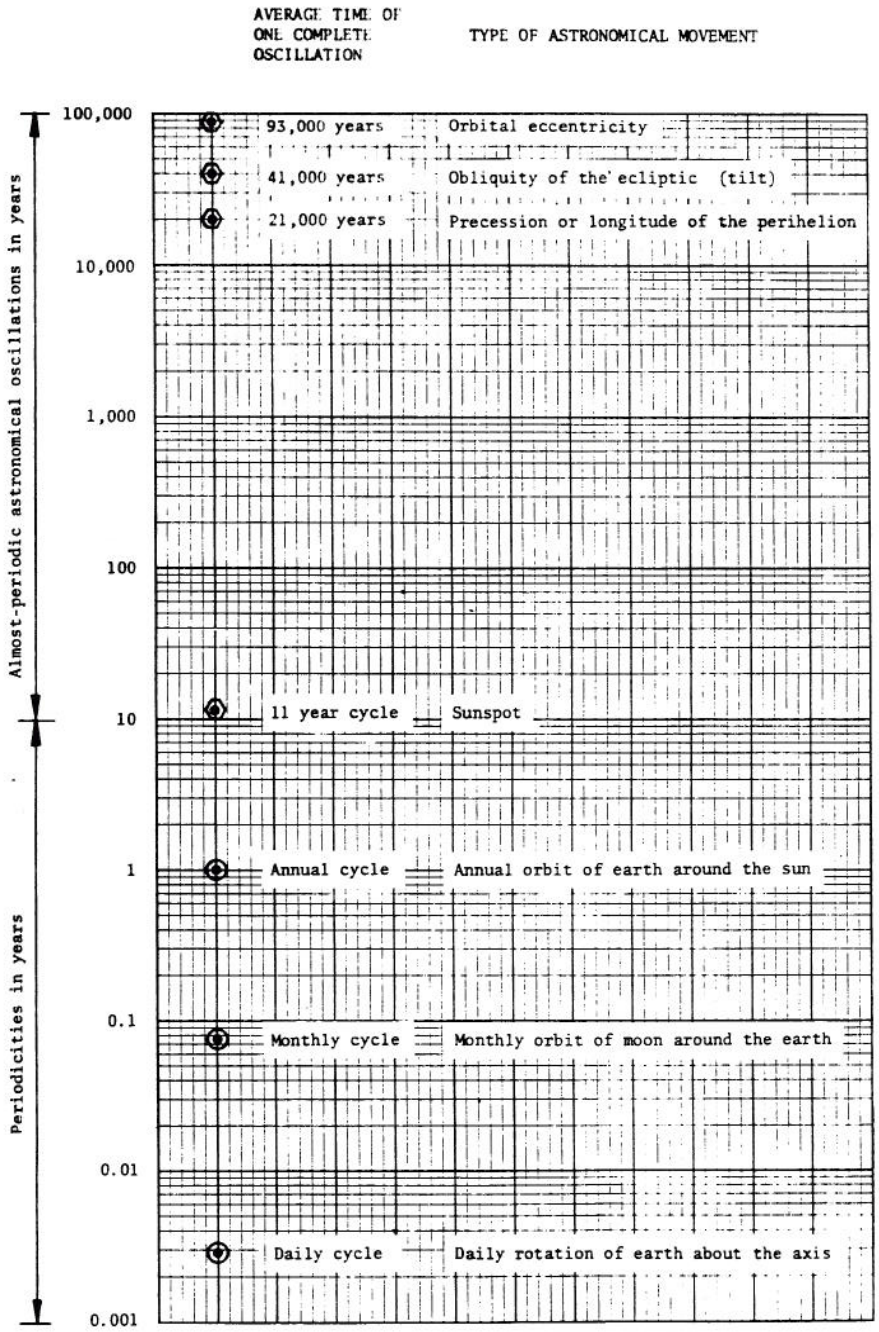

Fig. 14. Periodicities and almost-periodic movements due to astromical causes.

one time, they will reinforce each other, and at another time will oppose each other in their effect on the radiation received at a given point on the earth's surface. Vernekar (1972) following Milankovich's model has recomputed their integrated effect on the influx of solar energy received by the upper atmosphere as a function of latitude, and seasonal time. The results are expressed in langleys per day. It is important to emphasize that the total influx of heat received at the top of the earth's atmosphere over a year is a constant in the Milankovich model. The changes are in the seasonal and latitudinal distribution pattern. It should be noted that because of the unequal duration of the astronomical summer and winter half-years, the comparison of the average intensity of insolation during summer or winter half-years from one geological time to another yields only an approximate result. Milankovich, therefore, defined "caloric" half-years of equal duration such that the contrast in the insolation between the two halves is maximum. Three dimensional plots of the results are given by Vernekar are presented in Appendix of this paper.

The complex mathematical formulae developed to compute the long-term variations in seasonal contrast of solar radiation at the different latitudes are detailed by Vernekar (1972). An excellent non-mathematical description of the effects of the earth's motion on long-term changes in the seasonal and latitudinal distribution pattern is given by Broecker and van Donk (1970). Essentially, the radiation received by the earth as a whole on any given day depends on the position of the earth in its orbit. If the earth happens to be at the long end (aphelion) of the orbit, less than average radiation will be received, and if it is at the short end (perihelion) of the orbit, more than average radiation will be received. Thus during periods of high eccentricity, the seasonal contrasts will be enhanced and during periods of low eccentricity the seasonal contrasts will be reduced.

The magnitude of the precessional effect on seasonal contrast in solar radiation is related to the eccentricity of the earth's orbit. If the orbit were perfectly circular, precession would have no effect on seasonal contrast. Since the orbit is elliptical, changes in eccentricity have a considerable modulating effect on the amplitude of the 21,000 year average precession cycle. As a result of precession, the summer season or the winter season can occur either at the short end of the ellipse or at the long end of the ellipse. During periods when summer occurs at the short end of the ellipse, the days will be warmer than during periods when summer occurs at the long end of the ellipse. It is clear that the two hemispheres are exactly out of phase with respect to this effect. When the northern hemisphere is having a reduced seasonal contrast, the southern hemisphere will be having an enhanced contrast. Effects due to precession do not show a marked latitude dependence.

The tilt effect on seasonal changes in solar radiation is strongly latitude dependent, being almost absent at low latitudes and greatest at the pole. For example, at 45°N, the mean summer radiation increases by 1.2 percent for each 1 degree increase in tilt, while at 65°N, the corresponding change is 2.5 percent (Broecker and van Donk,1970).During periods of greater tilt the seasonal contrast is enhanced and during periods of smaller tilt the contrast is reduced. The two hemispheres respond synchronously to the tilt effect.

Since tilt effect is in phase for the two hemispheres and the precessional effect is not the resultant changes in seasonal contrast for the northern hemisphere will be different from that for the southern hemisphere. Because of the latitudinal dependence of the tilt effect, curves of long-term insolation values for different latitudes will differ in details.

Analyses of the power spectrum of insolation variations over the past 2 million years for every 10 degrees of latitude in the northern hemisphere starting at 5°N latitude have been carried out for both the summer and winter half-years. Plots of their power spectrum densities are shown in Figs. 15 and 16.

It is important to stress that variations in the intensity of solar radiation computed from the Milankovich model are the result of three variables which do not have commensurate frequencies. It is therefore reasonable to expect almost-periodic movements in the long-term variations of incoming solar radiation. If we assume the three variables to be independent with average periodicities of 93,000, 41,000 and 21,000 years, respectively, then it can be expected that the amplitudes and periodicities of the long-term insolation variations will not begin to repeat itself until a time span of 78 trillion years have elapsed. The time span is the product of the three periodicities. Thus, such repetition has not occurred during the life span of the earth.

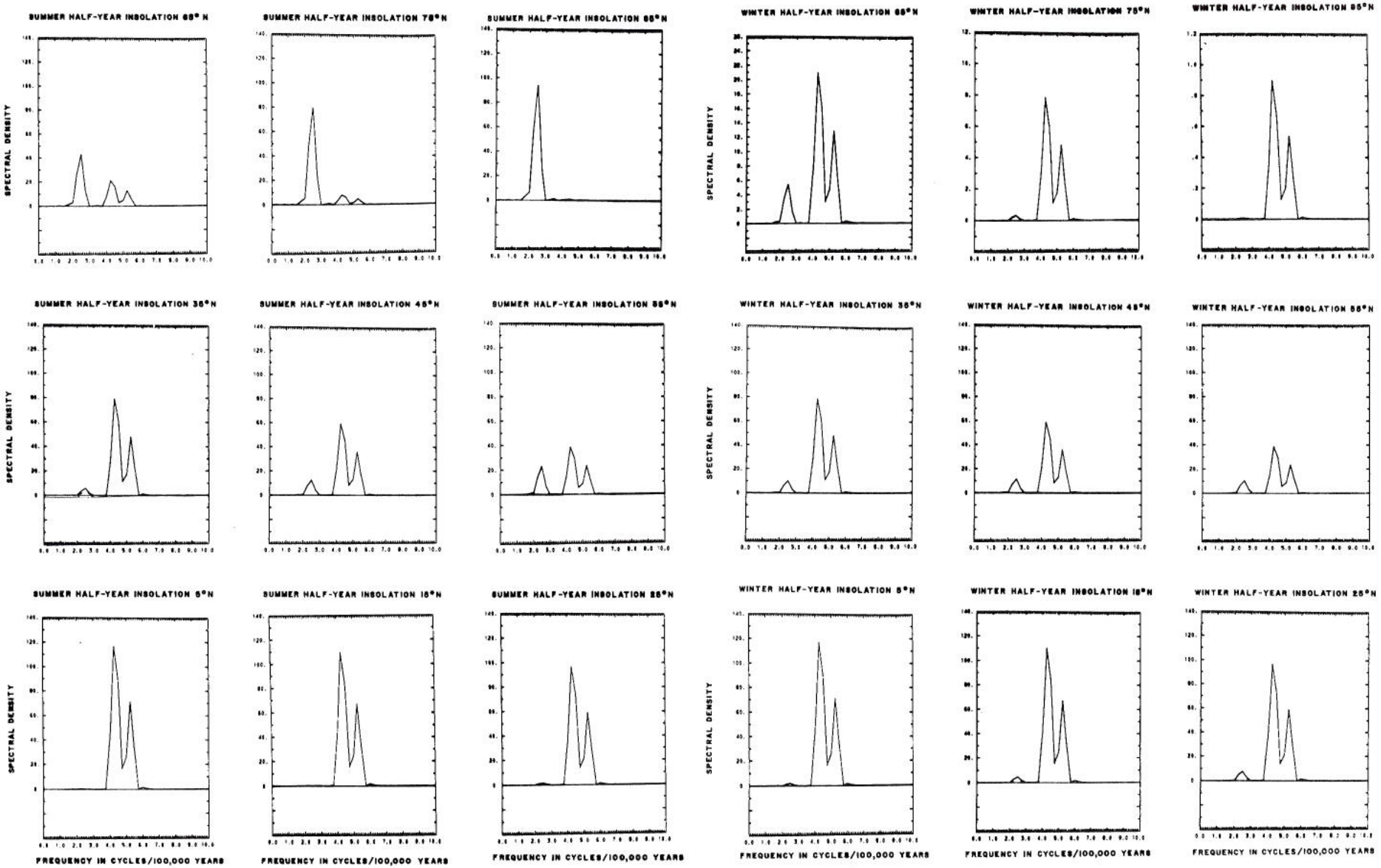

Fig. 15. Spectral density graphs of incoming solar radiation for the caloric summer-half year at selected latitudes in the northern hemisphere.

Fig. 16. Spectral density graphs of incoming solar radiation for the caloric winter-half year at selected latitudes in the northern hemisphere.

The insolation data used in the spectral analysis are expressed as deviations in langleys per day from their 1950 A.D. values at 1000-year intervals from 2,000,000 years before the present (BP) to 119,000 years after the present (AP).

CHAPTER V
MODEL FORMULATION

5.1 General

The existing models of long-term climatic changes can be divided into three broad categories. In the first categories are the models which attempt to explain the causes for the onset of a major ice age. These models are generally descriptive in nature and cannot provide the explanations for the waves of glaciations that are known to have occurred within the Pleistocene epoch.

In the second category are the models which attempt to explain climate oscillations within the Pleistocene epoch. Most of these models are concerned with the problems of providing an absolute chronology of Pleistocene events rather than the development of a tool for use in the prediction of future events. Typical of these models are the ones which attempt to correlate glacial phases determined from geological, paleontological, and other evidences with the minima of summer radiation as defined by the Milankovich theory. The curve of summer radiation for 65°N has been most widely used for this purpose. Other models such as the Emiliani and Geiss model (1957) provide a comprehensive theory for glaciations and their causes; however, they are mainly descriptive or conceptual without support of a mathematical model for the purpose of quantitative prediction.

In the third category are the physically-based mathematical models which try to take into account all essential components of the heat balance of the earth-atmosphere system and all important feed-back mechanisms (Matthews et al., eds., 1971).

These models are mainly in the early stages of development and are constantly improving as larger and faster computers become available. Eventually these models will provide a better insight into the impact of changes in the atmospheric, oceanic, and terrestrial environments on the long-term climate; but at present their applications are still restricted to relatively short-term predictions.

The investigation of this paper is based entirely on the available core data with the objective of analyzing long-term climatic changes as a deterministic-stochastic process. Deterministic component of the process is in the form of an almost-periodic movement. Mathematical models will be developed to permit quantitative projections considering both the deterministic and stochastic components. The following two assumptions are basic to the study: (1) the Milankovich astronomic theory of the orbital and axial motions of the earth is valid and the mathematical representations of the long-term variations in the insolation are correct; and (2) for the purpose of this study, it is not necessary to resolve questions concerning the exact interpretation of the $\delta(O^{18})$ curves derived from sea-sediment and ice-sheet cores, because the assumption is made that these curves are related to terrestrial glacial events and consequently reflect effects of long-term climatic changes.

5.2 A Process-Response Model

The study of long-term climatic changes on a paleo-time scale can be conveniently expressed as a system of processes and responses. Figure 17* illustrates a process-response model developed for this purpose, with the basic process controlled by the Milankovich theory. The long-term changes in latitudinal radiant energy supply can be considered as the basic input process. Changes in general climate reflected by changes of the indices of Oxygen-18 concentration in the sea sediment and ice core are considered the integrated response of interest in this study. Other factors in the model can be viewed as either intermediate processes or intermediate responses depending on the research interest and objective of any particular study. In this study, all the intermediate factors are lumped together in a black-box or gray-box approach.

This model illustrates the complexity of the interrelationships between the various factors. As stated in several places of the previous text, the physical basis of the deterministic component is derived from perturbations exerted on the orbital and axial motion of the earth by planetary forces which produce changes in the seasonal and latitudinal distribution of solar energy at the upper atmosphere. The physical basis of stochasticity in long-term climatic changes embraces many aspects of the earth-atmosphere-ocean environments. The most important of these are: the periodic-stochastic flitering of incoming solar radiation by the atmosphere; the energy flux exchange between the ocean and atmosphere which is mainly controlled by periodic-stochastic processes of atmosphere, but also by the ocean's own circulation, sea level, heat content and albedo changes due to sea-ice formation; the physical characteristics of the land masses including the presence of continental ice sheet, albedo, thermal capacity, surface water, relief, aerodynamic roughness, and the many other geophysical, chemical and biological random processes that are going on continually at the earth's surface and in the earth's crust; and the highly stochastic environment of the atmosphere including its circulation pattern, heat and moisture content, gaseous composition, turbidity and cloudiness. Because of the complexity of the system, a "lumped" or "black-box" approach in model formulation seems appropriate.

The "lumped" approach is particularly valid at the stage when quantitative data still are lacking on almost all aspects of the system. The use of various dating techniques related to the studies of flora and fauna fossils, sea-level fluctuations, and glacial deposits has provided vast amounts of qualitative information on many of the processes and responses. However, quantitative information for systems analysis is just about limited to data derived indirectly through the Milankovich theory and from sea sediments and ice cores.

5.3 General Hypotheses and Assumptions

* See page 25

(1) The models are to be applicable only within the past few million years on the assumption that the configuration of the earth's surface relative to the mountains, continents, and oceans have remained substantially the same during this period, except that the ocean level has fluctuated due to the ice-sheet build-up or disappearence. Thus the effects of geotectonic plate movements, such as continental drift, polar wandering and mountain building, and the astrophysical influences which are highly speculative, are not a consideration in this study. This assumption is particularly important since the physical causes of climatic changes are not one but many and the more important of these may not be the same in going from one period of geologic history to another or from one time scale of change to another (Mitchell, 1968).

(2) Solar constant is assumed to be unchanging over time, but the amount of incoming solar radiation received at the top of the earth's atmosphere is assumed to vary with time for the various seasons and latitudes in an almost-periodic manner according to the Milankovich theory, producing a deterministic component in long-term climatic changes.

(3) The deterministic component incorporates the feedback effect from the growth and retreat of continental ice sheets.

(4) Randomness or stochasticity is due primarily to the influences of the earth's atmosphere, ocean, and continental surfaces.

(5) Long-term climatic conditions are reflected in the $\delta(O^{18})$ values derived from sea sediments and ice cores.

(6) Changing values of $\delta(O^{18})$ reflect changing climatic conditions, namely: of air temperature, surface water temperature, ice-sheet volume or some combinations of these factors.

(7) The core data prescribe the upper and lower boundaries for values of the deterministic component corresponding to a non-glacial interval and to an interval of maximum glaciation, respectively.

(8) A non-glacial interval contains no continental ice sheet except for Greenland and Antarctica. According to a theory of Fairbridge (1961), the Greenland and Antarctica ice sheets did not melt during the radiation oscillation of the last one-half million years partly because of their bowl-shaped basins which prevented excessive calving at the margin of the ice sheets and partly because of the tremendous albedo of the high latitude ice. During a non-glacial interval, alpine glaciers can exist at high altitudes at all latitudes.

5.4 Basic Assumptions Relating Milankovich Insolation Variations to the Growth and Retreat of Ice Sheets

Initiation. Initiation of a continental ice sheet can occur only during long intervals, of say 5000 years or more, of mild winters with cool summers. This will occur when the poles are most nearly perpendicular to the ecliptic resulting in the suppression of seasonal contrasts. Mild winters produce high evaporation from the oceans at low latitudes and consequently lead to great snowfall and accumulation on the continents at both high latitudes and high altitudes. Cool summers result in low ablation rate of the snow and decrease the elevation of the snow-line thus permitting snow to accumulate through the summer. Over several millennia, the snow accumulation forms into an ice sheet starting at the high latitudes and on the high mountaineous regions of the midlatitudes.

Growth and Retreat. A continental ice sheet, once initiated can retreat and advance in response to the long-term increase or decrease in solar radiation following the almost-periodic fluctuations in the incoming solar radiation. However, it is affected by large random effects of earth's environment origin. While the ice sheet is still relatively small, increase in summer radiation and reduction in winter radiation over several millenia can cause substantial retreat of the ice sheet due to high ablation during the warm summers and low snow accumulation during the cold and dry winters.

As the ice sheet grows in size, the albedo of the ice will reflect as much as 70 percent of the incoming solar radiation back into space, thus nullifying the effect over a large area of any seasonal increase in solar radiation. This feedback effect further decreases the temperature and reduces the melting, even in summer. The general atmospheric circulation pattern is likely to become altered by the presence of the ice sheet in such a manner as to become favorable to the perpetuation of the ice (Mitchell, 1965). An ice sheet, once started, thus tends to provide its own impetus for growth. Nevertheless, during an interval of high summer solar radiation, small retreat of the ice sheet can occur due to melting at the southern edge of the ice sheet and calving of ice blocks into the sea as icebergs. With the onset of another interval of mild winter and cool summer, the ice sheet will once again advance. Alternate periods of retreat and growth will continue until the ice sheet has reached a latitude of about 40 degrees north which was about the southern limit of the Laurentide ice sheet in North America during the late Pleistocene epoch. Once the ice sheet attains this critical dimension, conditions become altered in such a way as to become favorable to the destruction of the ice sheet.

Deglaciation. Deglaciation of the ice sheet will occur once the ice sheet has grown to the maximum extent only during an interval when hot summers and cold winters are in phase at all northern latitudes. At maximum development, ablation by summer melting under greater solar energy input at the lower latitudes will begin to balance advance of the ice front. The volumes of cold glacial water returned to the neighboring oceans will enable parts of the North Atlantic to freeze over.

As a result, the glacial anticyclone will increase markedly in extent thus cutting off the supply of north-bound moisture to the ice sheet by diverting approaching westerly depressions in the northern temperate zone to a more southerly course. Supplies of new snow to the ice sheet may be virtually nil. It is obvious that even the most intense cold cannot produce snow when water vapor is absent in the air. The ice sheet becomes stagnant. Ablation at its edges soon surpass the rate of spread of the ice and retreat from the maximum begins. With the advent of an interval of hot summers and cold dry winters, the retreat is very rapid and the entire ice sheet can be dissipated within a short interval of a few thousand years. Thus the growth and decay of a continental ice sheet as indicated by the oxygen-isotope records of the sea cores has a dominant asymmetric sawtoothed-cycle. The sawtoothed cycle has been pointed out by Broecker and van Donk (1970) and ven den Heuvel (1966).

5.5 Support for the Basic Assumptions

Initiation. According to Milankovich (1941), one of the more important climatic effects of long-term variations in the seasonal and latitudinal distribution pattern of incoming solar radiation is in the displacement of the snowline. A low snowline during the summer season implies low snowmelt. A mathematical expression was developed by Milankovich relating the present-day elevation of the snowline at the different latitudes to the amounts of insolation received at the respective latitudes during the caloric summer-half year. Assuming interglacial periods within the Pleistocene to be similar to the present, the results from the snowline model in conjunction with the radiation curves for the various latitudes can be used to identify the position in time at which conditions may be suitable for initiation of glaciers and ice sheets.

For this study the mathematical expression developed by Milankovich is revised on the basis of the present-day insolation values given by Vernekar (1972). The present-day snowline elevations at the various latitudes are assumed to have the same values as that used by Milankovich following the work of Köppen. The data are fitted to a third-order polynomial rather than the linear function used by Milankovich. The equation is

$$H = -33{,}1259.88 + 1239.60\ Q_s - 1.557\ Q_s^2 + 0.00066\ Q_s^3, \qquad 5.1$$

in which H is the elevation of the snowline in meters and Q_s is the caloric summer half-year insolation in langleys per day. Curves of the basic data are presented in Fig 18 and the results are plotted in Fig 19.

Milankovich refers to "H" as the "solar altitude" of the snow limit because the value depends only on the summer insolation value. Other factors which affect the elevation of the snowline such as temperature, precipitation, and ocean currents are considered by Milankovich as secondary influences. These influences are excluded in the snowline model by assuming that they are uniformly active all over the earth's surface. For our purposes, the "solar altitude" may be termed the deterministic component and the effects of the other influences may be termed the stochastic component.

The application of the snowline model to the present study may be illustrated by the following hypothetical example. Consider an area at latitude 75°N near the Arctic Coast with an average elevation of 10 meters. The present-day snow limit at 75°N is 475 meters (from Fig. 18). According to the snowline model, a drop in summer insolation of 14 langleys per day from the present-day value is required to lower the snowline from 475 meters elevation to 10 meter elevation. Thus by inspecting the summer insolation curve for 75°N latitude, it is possible to identify those positions in time at which initiation of an ice sheet could occur in the area assuming interglacial conditions prevailed prior to those times.

Similarly, consider Mt. Synth at an elevation of 2000 meters at 50°N latitude. Once again, according to Koppen, the present snowline at 50°N latitude is 2600 meters. The snowline model requires a drop in summer insolation of 32 langleys per day from the present day values to lower the snowline from 2600 meters to 2000 meters (from Fig. 19). Thus by inspecting the summer insolation curve for 50°N latitude, it is possible to identify those positions in time at which initiation of an alpine glacier can occur at Mt. Synth assuming no glaciers were in existence prior to those times.

Furthermore, an examination of the winter insolation curves for the low latitudes will show whether the positions in time coincide with intervals of mild winters. Mild winters at the low latitudes coinciding with cool summers at the high latitudes should lead to greater precipitation in winter and reduce ablation of snow in summer, thus inducing the initiation and growth of ice caps.

The concept described above plays a vital role in the modeling procedure presented in Chapter IX. The model of the deterministic component is so structured that computations must start at a point in time corresponding to the end of an interglacial or the beginning of a glacial period. The wrong choice of a starting point will produce oscillations in the deterministic component that are completely at variance with that exhibited by the oxygen-isotope curves. From this phenomenon, it is possible, by repeated trials using different starting points in time for the model, to identify those positions in remote time within the Pleistocene epoch when interglacial periods probably occurred.

Growth and Retreat. Secondary oscillations averaging about 20,000 years in length are evident in the $\delta(O^{18})$-curves during general periods of glacial advance. The growth and retreat of the ice sheet suggested by these oscillations may be explained by Weertman's theoretical analysis (1964) of the rate of growth or shrinkage of non-equilibrium ice sheets.

According to Weertman, the growth or retreat of an ice sheet is a function of the accumulation rate, ablation rate, and the rate of change of the snowline. As long as the total accumulation is greater than the total ablation, the ice sheet will grow until it reaches an equilibrium size, as it concerns the deterministic component of the process. However, if for some reason the accumulation rate, the ablation rate, the rate of change of the snowline, or any combination of these quantities, vary in such a direction that the equilibrium size of the ice sheet becomes smaller than the actual size of the ice sheet at the time, then the periphery of the ice sheet will become stagnant and a moderate decrease in accumulation or increase in ablation can cause a large ice sheet to shrink. The half-length L_e of an equilibrium-size ice sheet is derived by Weertman as

$$L_e = \frac{1}{3} \cdot \frac{\tau_o}{\rho g s^2} \cdot \frac{\alpha}{(\alpha+\beta)}\ , \qquad 5.2$$

in which τ_o is considered as a constant representing the shear stress acting at the bottom of the ice sheet and parallel to its bed, ρ the density of ice, g the gravitational acceleration, s the gradient of the snowline, α the accumulation rate, and β the ablation rate.

Most of ice-sheet oscillations can be treated as a deterministic component resulting from the long-term changes in insolation at the northern latitudes. A period of high insolation during the winter-half year and low insolation during the summer-half will result in high accumulation and low ablation. Following the

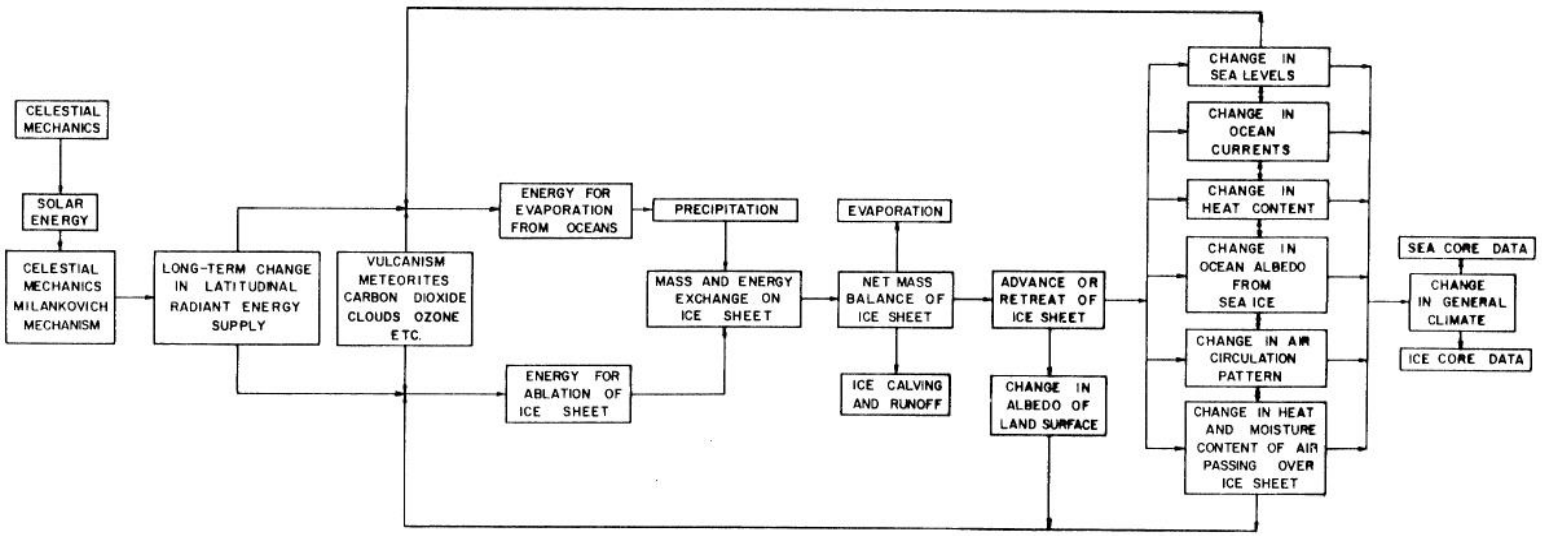

Fig. 17. A process-response model for the study of long-term change during the Pleistocene epoch.

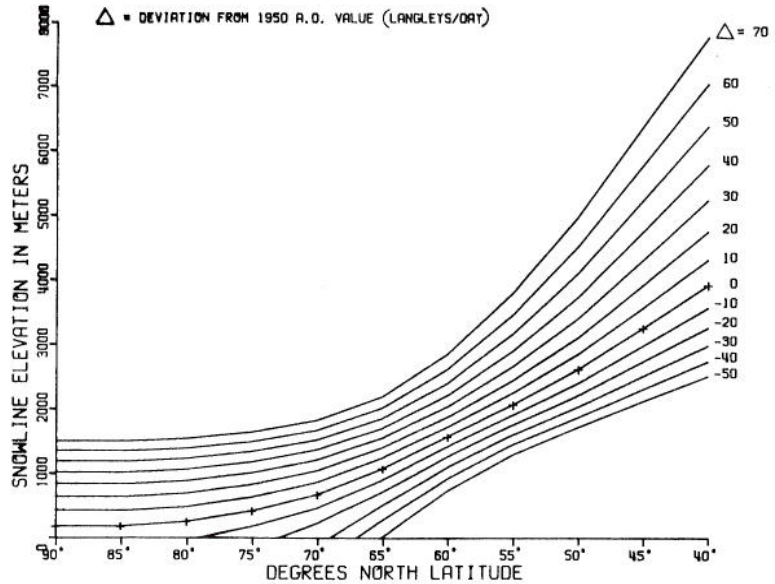

Fig. 19. Snowline elevation as a function of latitude and change in caloric summer-half year incoming solar radiation during any specified interval of time.

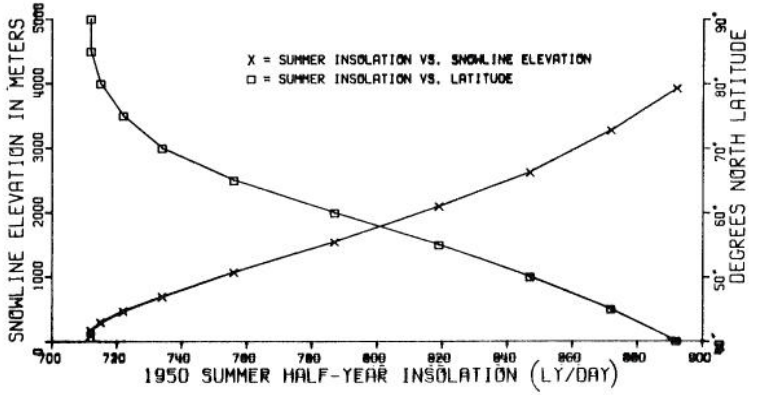

Fig. 18. Relationship between latitude, snowline elevation, and caloric summer-half year incoming solar radiation in 1950 A.D.

Weertman theory, this will produce a growing ice sheet. On the other hand, once the process enters a period of diminishing insolation during the winter-half year and increasing insolation during the summer half-year, changes in the accumulation rate, ablation rate, and snowline elevation over the ice sheet can reduce the equilibrium size to a critical level causing shrinkage to occur. Thus, the Weertman theory in conjunction with the Milankovich mechanism offers an acceptable explanation for the long-range deterministic oscillations in ice-sheet extension.

Secondary influences such as volcanic and meteorite activities, changes in CO_2 content of the atmosphere, and many other factors perturb the deterministic, almost-periodic oscillations by introducing stochasticity into the process. The mathematical model developed in Chapter IX treats the process in a systems approach to the available data rather than on a physical basis since there is no information on paleo-accumulation and ablation rates at the present time.

Deglaciation. Weertman (1964) has shown how a large continental ice sheet can be completely dissipated within a short span of a few thousand years. The mechanism is the same as that described in the preceeding section. The difference between minor retreats during a period of general glacial advance, and complete deglaciation is due mainly to the degree of reduction in the accumulation rate, the degree of increase in the ablation rate, and the increase in the snowline elevation. The reader may refer to the paper by Emiliani and Geiss (1957) in which a lengthy and detailed discussion is presented of the probable environmental conditions and interactions between ice and ocean which led to the rapid deglaciation of the last ice sheet.

In constructing the deterministic component of the model in this investigation it is assumed that deglaciation of a continental-size ice sheet can occur only during an interval in which summer half-year insolation variations at all northern latitudes are essentially in phase. Such intervals are conducive to high ablation rates and large increases in the snowline elevation. And, as stated in the basic assumptions, once the ice sheet has reached continental proportions, the atmospheric circulation pattern and oceanic conditions become altered so that the supply of moisture to the ice sheet is greatly reduced. Thus, the conditions of the Weertman theory for rapid deglaciation are staisfied.

The position in time at which conditions may be suitable for deglaciation of a continental-size ice sheet can be identified from the radiation curves. This feature is incorporated into the model of the deterministic component presented in Chapter IX. However, the deglaciation process is subject to high degree of stochasticity created by atmosphere, ocean, and terrestrial factors.

Synchroneity. The Milankovich mechanism produces climatic changes which are out of phase in the two hemispheres. This contradicts the evidences that all major glaciation have been world wide (Sellers, 1965). This contradication can be countered with the sea-level mechanism (Chapter II) by which glaciation in the southern hemisphere is largely controlled by glaciation in the northern hemisphere even though climatic events may not be in phase. In any case, climatic changes would be out of phase by only about 10,000 years which is too small to resolve conclusively by existing dating techniques (Sellers, 1965). The question of synchroneity is explored further in the paper by Emiliani and Geiss (1957).

CHAPTER VI

METHOD OF MATHEMATICAL ANALYSIS

6.1 General Model

The oxygen-isotope data obtained from the sea sediments and ice cores can be considered as time series representing realizations of non-stationary geophysical processes that are governed in part by laws of chance. The approach used in this study is built on the underlying hypothesis that the original non-stationary process, X_i, can be decomposed into one or more deterministic components and a stochastic component which can be reduced to a second-order stationary and independent process, ξ_i. A further assumption is made that the two basic types of components of time series, deterministic and stochastic are independent of each other and therefore can be superimposed on each other by simple algebraic equations of time series composition. This technique has been used in analysis of the structure of hydrologic time series by many investigators (Thomas and Fiering, 1962; Yevjevich, 1964; Beard, 1965; Roesner and Yevjevich, 1966; Quimpo, 1967; Beard, 1967; Salas La-Cruz and Yevjevich, 1972a and b).

A general heuristic model used to describe such processes is given by

$$X_i = D_i + Y_i \,, \qquad 6.1$$

in which X_i is a time dependent non-stationary hydrologic process sampled at equal intervals of time, D_i the deterministic component which may be periodic, almost-periodic, trend or jump movements, or some combination of these movements, and Y_i the stochastic component either time dependent or time independent.

6.2 Diagnostic Tools

Autocorrelation analysis and spectral analysis are the two main diagnostic tools used in this study to ascertain the structure of climatic processes reflected in the $\delta(O^{18})$ time series. The correlogram and variance density spectrum offer visual aids for distinguishing between different types of oscillatory time series. The shapes and properties of correlograms and power spectra of sample data are compared with those of known deterministic and stochastic processes or their combinations, for advancing hypotheses as to the appropriate mathematical models for use in representing the time series structure. Parameters of the hypothesized model are estimated by the best available techniques after which a suitable statistical inference test is made to accept or reject the hypothesized model.

Correlograms and power spectra provide equivalent descriptions of stationary processes because they are mutual transformations, with the autocorrelation analysis carried out in the time domain and spectral analysis in the frequency domain.

(1) Autocorrelation Analysis and the Correlogram

Correlogram. The autocorrelation coefficient is a measure of the interdependence between successive values of a time series at a specified lag. The correlogram is a graph of the autocorrelation coefficient ρ_k as a function of the lag k, with ρ_k plotted as ordinates and k as abscissas. The plotted points are generally connected by straight lines to set out the distinguishing features of the correlogram.

For a deterministic process represented by a periodic model, the correlogram is also periodic depending on the harmonic components of the periodic model. For the usual stochastic processes in geophysical phenomena represented by autoregressive models, the correlograms will show dampening oscillations. For the first-order autoregressive Markov model with ρ_1 positive, the theoretical correlogram decreases monotonically as ρ_1^k, $k = 1,2, \ldots$. For an independent stochastic process, the sample correlogram oscillates randomly about zero. For a time series consisting of only a small number of observations, sampling variations may cause the computed correlogram to deviate substantially from the expected population correlogram.

For the discrete time series used in this study, the population autocorrelation coefficient ρ_k is defined as

$$\rho_k = \frac{\operatorname{cov}(X_i, X_{i+k})}{[\operatorname{var}(X_i)\ \operatorname{var}(X_{i+k})]^{1/2}} \,,$$

$$= \frac{E(X_i\, X_{i+k}) - E(X_i)\, E(X_{i+k})}{E(X_i)^2 - [E(X_i)]^2} \,, \qquad 6.2$$

in which X_i and X_{i+k} are the observations at times i and i+k respectively, $\operatorname{cov}(X_i, X_{i+k})$ is the autocovariance function, and $\operatorname{var}(X_i)$ and $\operatorname{var}(X_{i+k})$ are the variances at lag 0 and lag k, respectively. For the open series approach, the ρ_k is estimated by the sample value r_k, computed by

$$r_k = \frac{\frac{1}{N-k}\sum_{i=1}^{N-k} X_i\, X_{i+k} - \frac{1}{(N-k)^2}\left(\sum_{i=1}^{N-k} X_i\right)\left(\sum_{i=1}^{N-k} X_{i+k}\right)}{\sigma_1\, \sigma_2} \qquad 6.3$$

with

$$\sigma_1 = \left[\frac{1}{N-k}\sum_{i=1}^{N-k} X_i^2 - \frac{1}{(N-k)^2}\left(\sum_{i=1}^{N-k} X_i\right)^2\right]^{1/2}$$

and

$$\sigma_2 = \left[\frac{1}{N-k}\sum_{i=1}^{N-k} X_{i+k}^2 \frac{1}{(N-k)^2}\left(\sum_{i=1}^{N-k} X_{i+k}\right)^2\right]^{1/2} \,,$$

with N the total number of sample observations.

Significance Test. Statistical inference for the open-series approach used in this study is based on the equation developed by M.M. Siddiqui quoted in Yevjevich (1972b). For normal independent variables

$$f(r_1) = \frac{(1 - r_1)^{(N-1)/2}}{2^{(N-1)}} \frac{(1 + r_1)^{(N-3)/2}}{B\left[\frac{N+1}{2}, \frac{N-1}{2}\right]} + O\left[\frac{1}{N^2}\right] , \qquad 6.4$$

in which $B\left[\frac{N+1}{2}, \frac{N-1}{2}\right]$ is the Beta function.

The above equation is applicable for relatively large N and small k. For sufficiently large N (say N > 30) the last term $O\left[\frac{1}{N^2}\right]$ may be neglected. To make the above equation generally applicable for any size N and k, it is only necessary to replace N by the term N+k-1. Equation 6.4 has been used to set the 95 percent tolerance limits in the correlogram analyses made in this study. If the computed value of r_k lies outside the tolerance limits, r_k is examined on the assumption that it may be significantly different from zero. A time series is always considered random if all r_k for $k \geq 1$ lie within the tolerance limits. However, because the sampling errors, a few values of r_k, corresponding to the probability level of the limits, may lie outside the tolerance limits even if the sample is taken from an independent random process.

(2) Spectral Analysis

Harmonic Analysis. Spectral analysis is applied to both deterministic and stochastic processes. Classical Fourier or harmonic analysis techniques are used in decomposing oscillatory, periodic, almost-periodic and transient phenomena to seek out deterministic regularities. Since the present study does not lend itself to harmonic analysis for reasons which will be discussed later, the mathematical equations and associated tests of significance of harmonics will not be repeated here. The equations and their derivations can be found in many references (Yevjevich, 1972a).

Aspects of Spectral Theory. Spectral estimation techniques in the analysis of stochastic processes are used in searching for average frequencies rather than for exact frequencies as in the case of analysis of deterministic periodic processes. Spectral estimation may be used also in examining average periodicities present in deterministic almost-periodic processes.

Spectral analysis decomposes a stationary time series into a set of frequency bands and measures the relative importance of each of these bands in terms of its contribution to the overall variance or power of the series. The power spectrum using standardized values of the time series is essencially a density function with the variance density of the process plotted as ordinates against their respective values of frequency as abscissas. The plotted points are connected by straight lines to define the variance density curve. If a band of frequencies is important, the spectrum will exhibit a high sharp peak in this frequency band. The spectral method will give an inventory of all frequencies (up to the Nyquist frequency) which go into making up the series.

It should be noted that a spectral estimation technique is based on the assumption of stationarity and does not require the specification of a model. This technique, therefore, is mainly an empirical tool. It does not chronicle the progress of any cycles but merely denies or confirms their existence in specific time series. Nonetheless, when knowledge is lacking on either the physical phenomena generating the observations or on the theory of stochastic processes necessary to model these phenomena, spectral analysis can provide clues as to major sources of variations in a process and detect trends, periodicities, and persistence linkages within a time series.

Variance Density Spectrum. For the descrete time series used in this study, the population variance density spectrum, $\gamma(f)$, is defined as

$$\gamma(f) = 2\left[1 + 2 \sum_{k=1}^{\infty} \rho(k) \cos 2\pi fk\right] , \qquad 6.5$$

in which f is the frequency, $\rho(k)$ the autocorrelation function, and k the lag. The range of f in practice is 0 to 0.5. The lower limit of the frequency is zero because $f_{min} = 1/N$; and for $N \to \infty$, $f_{min} \to 0$. The upper limit of the frequency is the Nyquist frequency for which $f_{max} = 1/(2\Delta t)$; hence if Δt is expressed as a unit time period of one, then $f_{max} = 0.5$.

In practice, the sample variance density spectrum is obtained from an equation containing a smoothing function D(k) applied to the limited number of the first m values r(k) of the sample autocorrelation function. The equation for the "smoothed" variance density spectrum is then

$$g(f) = 2\left[1 + 2 \sum_{k=1}^{m} D(k)\, r(k) \cos 2\pi fk\right] , \qquad 6.6$$

in which m is the maximum lag used for r(k). The smoothing function is often referred to as a weighting, filter, or kernel function and is also called the lag window or spectral window depending on whether its use is in the time or frequency domain.

With a finite amount of data it is possible to estimate only the average variance densities for a set of frequency bands. The spectral window is designed to give more weight to the power contributed by frequencies near the center of the band and suppresses the contribution of those frequencies distant from the center. Thus, the smoothed power spectrum may be thought of as a weighted average of the true spectrum taken over some frequencies. Many mathematical forms have been proposed for the spectral windows. The design or selection of window shapes is termed window carpentry. The rectangular, Bartlett, Tukey, and Parzen windows are common forms used in window carpentry (Jenkins and Watts, 1969). All four forms were examined in this study with the Parzen window selected for final computations.

The Parzen window in the spectral domain has the form

$$D(k) = \begin{cases} 1 - 6\left(\frac{k}{m}\right)^2 + 6\left(\frac{k}{m}\right)^3 & , k \leq \frac{m}{2} \\ 2\left(1 - \frac{k}{m}\right)^3 & , \frac{m}{2} \leq k \leq m \\ 0 & , k > m \end{cases} \qquad 6.7$$

with its transform in the correlogram domain

$$D(k) = \frac{3}{4} m \left[\frac{\sin \pi f\, m/2}{\pi f\, m/2}\right]^4 , \qquad 6.8$$

where m is the maximum lag parameter.

The maximum lag controls the band-width of the spectral window. In practice, smoothing of the spectral estimate is carried out empirically. The procedure is to compute the smoothed spectral estimates with a wide band-width and then use progressively smaller band-widths to explore details of the spectrum. This technique is called window closing. With wide band-widths, the estimates have a small variance but large bias or distortion. With small band-widths, the bias is small but the variance becomes large and unstable creating problems of interpretation. In practice, the desire is to achieve a compromise between bias variance using the smallest band-widths consistent with accuracy and stability of the power spectrum estimates.

Shapes of some smoothed power spectrum for first and second-order autoregressive processes are given in Jenkins and Watts (1969) and Yevjevich (1972a). If the generating process contains periodic terms, the frequencies of harmonic terms of the periodic and almost-periodic processes will appear as high sharp peaks in the power spectra.

Significance Test. Jenkins as quoted in Yevjevich (1972a) has shown that the distribution of g(f) may be approximated by a chi-square distribution with the equivalent number of degrees of freedom depending on the spectral window use. For the Parzen window, the equivalent degrees of freedom EDF is

$$EDF = \frac{4N}{m} , \qquad 6.9$$

The upper and lower tolerance limits used for testing significance are given by

$$T_1 = \frac{2[1 - X^2_{\alpha/2}\,(EDF)]}{EDF} , \quad T_2 = \frac{2X^2_{\alpha/2}\,(EDF)}{EDF} , \qquad 6.10$$

where T_1 is the upper tolerance limit, T_2 is the lower tolerance limit, and a is equal to 0.05 for 95 percent tolerance limit.

For practical application, Yevjevich (1972a) suggests that the values of T_1 and T_2 should be increased at the two extremes by 41 percent because variances of spectral estimates at f=0 and f=0.5 are twice as large as at other frequencies.

6.3 Deterministic Components

The usual approach in studying the deterministic components in hydrologic time series is to find and remove the trends in parameters by an appropriate exponential or polynomial model, and then find and describe the periodicities in the parameters by a set of trigonometric functions using classical Fourier analysis techniques. The approach for seeking out and describing periodicities in parameters of hydrologic time series is useful when periods can be substantiated by physical considerations. This approach has been used extensively in hydrologic analyses for describing the oscillations within the day and/or the year which are unmistakenly periodic in nature.

On the other hand, long-period oscillations such as those observed in tree-ring data showing such periods as 80, 405, 2400 years may be the result of a stochastic sampling origin rather than of a deterministic nature. Classifying such oscillations as deterministic periodic is a questionable approach.

The time resolutions of 10, 50, and 200 years provided by the $\delta(O^{18})$ ice-core data, and about 2000 years by the sea-sediment core data are far too coarse to detect any eventual deterministic short-period oscillations. Thus, for the purpose of this study, the oscillations in the $\delta(O^{18})$ curves with apparent periods varying from a few decades to about 20,000 years are considered sampling stochastic and not deterministic oscillations. From physical considerations, deterministic oscillations of very long periods are likely only a function of changing insolation resulting from the Milankovich effect on insolation, as the only causal factor described by a precise mathematical time model. Other factors are rather speculative and without a quantitative mathematical support. For time spans of much less than about 20,000 years, the long-term deterministic component will appear only as a trend, representing a portion of the almost-periodic astronomical component.

Trend Component. The trend components in the $\delta(O^{18})$ curves of the ice-core series covering time spans of 10,000 and 780 years are approximated by a polynomial equation

$$T_i = \alpha_0 + \alpha_1 i + \alpha_2 i^2 + \alpha_3 i^3 + \ldots , \qquad 6.11$$

in which T_i is the value of the deterministic trend component at interval i, and α_j are the polynomial regression coefficients, to be estimated from sample data.

The regression coefficients are estimated by the least squares procedure. The t-statistic is used to test the hypothesis whether the slope of a linear trend is significantly different from zero. If the hypothesis is accepted, the regression coefficients of the polynomial equation are computed and an analysis of variance based on the F-test at the 95 percent confidence level is applied to find the significant higher-order terms of the equation.

Deterministic Modeling. The statement was made earlier that Fourier analysis technique cannot be applied in this study to seek out deterministic regularities in the $\delta(O^{18})$ time series. The reasoning behind this statement is as follows. Chapter V states that long-term variations in insolation as a result of the Milankovich mechanism are almost-periodic movements which do not have commensurate frequencies. Basic assumption is also made that the deterministic component in long-term climatic changes as reflected in the $\delta(O^{18})$ time series is the result of long-term variations in solar radiation. Since the oscillatory pattern of the deterministic input to the system is almost-periodic it is reasonable to assume that the deterministic output component contained in the $\delta(O^{18})$ time series is also almost-periodic. Since the $\delta(O^{18})$ time series have very short records relative to the oscillatory characteristics and the time span under consideration, it does not seem feasible to develop from the present data a statistically meaningful model using Fourier series representation.

The models proposed in this study are in the form of the mathematical functions which are postulated by

considerations involving inductive reasoning. Although the functions are developed empirically, they are designed to satisfy the hypothesis and assumptions underlying the conceptual interpretation of the physical process. The aim is to specify simple yet realistic mathematical models which will generate objective and quantitative estimates of the physical states of the deterministic phenomena at any given point in time.

For the purpose of this study, an empirical mathematical model based on a simple mass-budget relationship is used to describe the deterministic component. It was considered that more complex models using differential equations to describe the process would not be warranted at this time in view of the accuracy of the time scale and the rather coarse time resolution represented by existing data as well as the limited amount of data that is available for use in parameter estimation. In any event, the simple algebraic model proposed in this study apparently provides satisfactory representation of the deterministic component for a practical demonstration to meet the objectives of this study without excessive mathematical involvement. Simplicity of the model should permit easier interpretation of the results. The development and form of the model are presented in detail in Chapter IX.

Similarly, an empirical mathematical model based on a conceptual interpretation of the sediment deposition phenomena on the deep-sea floor was developed to provide a time scale for the $\delta(O^{18})$ data from the sea-sediment core. Details of the model are presented in Chapter VIII.

Parameter Estimation. In this study, the structural configuration of the deterministic model is assumed to be represented by a set of mathematical equations with unknown parameters that must be estimated from the data.

The technique used for optimization of the parameter estimations is based on the gradient or steepest descent method. The general layout of the identifier is shown in Fig. 20. The parameter optimization study was carried out using a computer program prepared by Dr. G. Johnson, Associate Director of the Colorado State University Computer Center. First and second partial derivatives with respect to each parameter are determined numerically to define the direction vector. Interpolation is then used to determine where the minimum is located along the direction vector. The objective function in the present work is the minimization of the squares of deviations between the observed and calculated values. Many variations to the approach are described in the literature. For further details the reader may refer to Graupe (1972) and to the unpublished dissertation of Tuffour (1973), in which the mathematics of the steepest descent algorithm that is contained in the computer package used in the present study are summarized.

6.4 Dependent Stochastic Component

The stochastic process Y_i is obtained from the original X_i series by removing the deterministic component which appears either as a trend or an almost-periodic function in the $\delta(O^{18})$ data. The form of Eq. 6.1 is rewritten as follows

$$Y_i = X_i - D_i \quad , \tag{6.12}$$

in which Y_i is the stochastic component, X_i is the original time series, D_i is the deterministic component in the mean which appears either as a trend or an almost-periodic movement. The Y_i random series thus obtained from the $\delta(O^{18})$ data is assumed to be stationary in the mean and the variance with but one exception in this study.

The stationary stochastic series Y_i is reduced to a standardized series ε_i using the nonparametric approach based on sample estimates

$$\varepsilon_i = \frac{Y_i - \overline{Y}}{S(Y)} \quad , \tag{6.13}$$

in which $S(Y)$ is the standard deviation of the Y_i series, and $\overline{Y}$ the mean of Y_i. The stochastic process ε_i obtained from Eq. 6.13 usually shows a time dependent structure.

(1) Dependence Models of Stochastic Components

Stationary stochastic processes with a dependence structure can be modeled by linear autoregressive-moving average schemes. Only the autoregressive models will be used in this study since they provide satisfactory representation of the data and have physical significance for hydrologic and geophysical applications (Yevjevich, 1972a and b). The reader may refer to Box and Jenkins (1970), and Jenkins and Watts (1969) for a thorough mathematical treatment of the various types of linear stationary models.

(2) Autoregressive Model

The general m-th order autoregressive model is given by

$$\varepsilon_i = \sum_{j=1}^{m} \alpha_j \varepsilon_{i-j} + \xi_i \quad , \tag{6.14}$$

in which α_j are the autoregressive coefficients, m is the order of the autoregressive model, and ξ_i is the independent stochastic component. In terms of variance, since $\text{var}(\varepsilon_i) = \text{var}(\varepsilon_{i-1}) = \ldots = \text{var}(\varepsilon_{i-m})$, Eq. 6.14 can be expressed as

$$\text{var}(\varepsilon_i) = \sum_{k=1}^{m} \sum_{j=1}^{m} \alpha_k \alpha_j \rho_{|k-j|} \, \text{var}(\varepsilon_i) + \text{var}\, \xi_i \quad , \tag{6.15}$$

because $\text{var}(\varepsilon_i) = 1$, the variance of the independent stochastic component is

$$\text{var}(\xi_i) = 1 - \sum_{k=1}^{m} \sum_{j=1}^{m} \alpha_k \alpha_j \rho_{|k-j|} \, . \tag{6.16}$$

Since it is more convenient in data generation to use

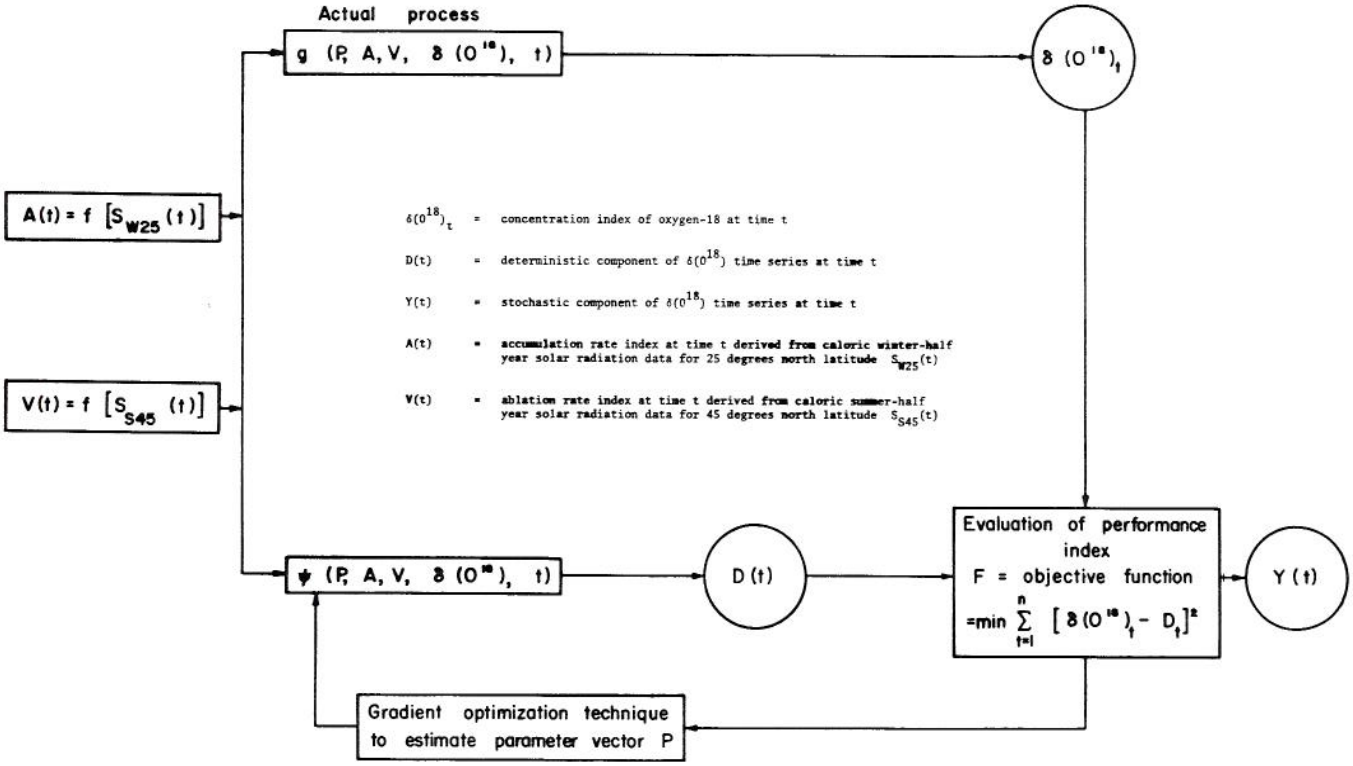

Fig. 20. General layout of the direct search technique of parameter estimation.

a random variable with unit variance, Eq. 6.14 can be modified to

$$\varepsilon_i = \sum_{j=1}^{m} \alpha_j \varepsilon_{i-j} + \left[1 - \sum_{k=1}^{m} \sum_{j=1}^{m} \alpha_k \alpha_j \rho_{|k-j|}\right]^{\frac{1}{2}} \xi_i \quad . \tag{6.17}$$

For most hydrologic time series the above model using either the first-, second- or third-order will result in a good fit within the limitations of data accuracies. Thus, the process ξ_i becomes a second-order stationary and standard (0, 1) random independent variable since ε_i has been standardized already as a random (0,1) variable with time dependent characteristics.

(3) Parameter Estimation

Estimates of the autoregressive parameters for any order m is obtained in terms of the autocorrelation coefficients r_k using the Yule-Walker equations (Box and Jenkins, 1970).

$$\begin{aligned} r_1 &= a_1 + a_2 r_2 + \ldots + a_m r_{m-1} \quad , \\ r_2 &= a_1 r_1 + a_2 + \ldots + a_m r_{m-2} \quad , \\ &\cdots \\ r_m &= a_1 r_{m-1} + a_2 r_{m-2} + \ldots + a_m \quad . \end{aligned} \tag{6.18}$$

Since the system of equations is linear in the a_j, it may be solved using multiple linear regression estimation techniques. Standard computer program packages are readily available for this purpose.

Estimates a_j of the population autoregression coefficients α_j as a function of the estimated autocorrelation coefficient r_k are summarized below for the models of the first three orders.

For the first-model where m = 1

$$a_1 = r_1 \quad . \tag{6.19}$$

For the second-order model where m = 2

$$a_1 = \frac{r_1 - r_1 r_2}{1 - r_1^2} \quad , \tag{6.20}$$

$$a_2 = \frac{r_2 - r_1^2}{1 - r_1^2} \quad . \tag{6.21}$$

For the third-order model where m = 3

$$a_1 = \frac{(1 - r_1^2)(r_1 - r_3) - (1 - r_2)(r_1 r_2 - r_3)}{(1 - r_2)(1 - 2r_1^2 + r_2)} \quad , \tag{6.22}$$

$$a_2 = \frac{(1 - r_2)(r_2 + r_2^2 - r_1^2 - r_1 r_3)}{(1 - r_2)(1 - 2r_1^2 + r_2)} \quad , \tag{6.23}$$

$$a_3 = \frac{(r_1 - r_3)(r_1^2 - r_2) - (1 - r_2)(r_1 r_2 - r_3)}{(1 - r_2)(1 - 2r_1^2 + r_2)} \qquad 6.24$$

in which r_k are estimates of the autocorrelation coefficients for lag k and a_j are estimates of the autoregressive coefficients.

(4) Selection of the Order of the Autoregressive Model

Several methods are used in this study to determine the appropriate orders of the autoregressive models for describing the time series under consideration. This involved the use of variance density spectra and correlograms.

The first approach uses the power or variance density spectrum of the ε_i series. A visual examination of the spectrum shows whether its shape is typical of a first-order or second-order autoregressive process.

The second approach assumes autoregressive models of various orders up to 10. The parameters of each order are estimated and the variances of the residuals between the observed ε_i series and the values ξ_i computed from the models, are plotted. The order of the model showing the lowest unbiased residual variance is selected for further analysis. Estimate of the residual variance is of the form

$$S_\xi^2(m) = \frac{1}{n - 2m - 1} \; A(a_1, a_2, \ldots, a_m) \; , \qquad 6.25$$

in which $S_\xi^2(m)$ is the residual variance of the m-th order autoregressive model, $\frac{1}{N - 2m - 1}$ takes into consideration the degrees of freedom and a_j are the estimated autoregression coefficients.

The third approach is essentially a follow-up of the second approach. Here, the residuals ξ_i of Eq. 6.17 obtained from the ε_i series for an m-th order autoregressive model are tested for independence using the autocorrelation technique. If the ξ_i series is shown to be an independent random series, then the m-th order autoregressive model is considered as an acceptable dependence model of the ε_i series. This is a whitening-series approach.

The third approach is a simplified method proposed by Yevjevich (1972b). The method uses the coefficient of determination R_j^2, j=1, 2, 3, ..., as the criterion for selection. The coefficient of determination indicates what portion of the total variation of ε_i is explained by the autoregressive part of the model, the remaining portion of the variance of ε_i being explained by the residual term $S \cdot \xi_i$, in which S is the standard deviation of Eq. 6.17 and ξ_i is the independent standard random variable. The coefficient of determination of the first three order autoregressive models are given by

$$R_1^2 = r_1^2 \; , \qquad 6.26$$

$$R_2^2 = \frac{r_1^2 + r_2^2 - 2r_1^2 r_2}{1 - r_1^2} \qquad 6.27$$

$$R_3^2 = \frac{r_1^2 + r_2^2 + r_3^2 + 2r_1^3 r_3 + 2r_1^2 r_2^2 + 2r_1 r_2^2 r_3 - 2r_1^2 r_2}{1 - 2r_1^2 - r_2^2 + 2r_1^2 r_2} - \frac{4r_1 r_2 r_3 + r_1^4 + r_2^4 + r_1^2 r_3^2}{1 - 2r_1^2 - r_2^2 + 2r_1^2 r_2} \qquad 6.28$$

The first-order model is selected if

$$R_2^2 - R_1^2 \leq 0.01 \quad \text{and} \quad R_3^2 - R_2^2 \leq 0.02 \; . \qquad 6.29$$

The second-order model is selected if

$$R_2^2 - R_1^2 > 0.01 \quad \text{and} \quad R_3^2 - R_2^2 \leq 0.01 \; . \qquad 6.30$$

The third-order model is selected if

$$R_2^2 - R_1^2 > 0.01 \quad \text{and} \quad R_3^2 - R_2^2 > 0.01 \; . \qquad 6.31$$

6.5 Independent Stochastic Component

The independent stochastic component ξ_i is obtained by removing the autoregressive structure from the dependent stochastic component ε_i. This is accomplished by Eq. 6.17 which can be rewritten as

$$\xi_i = \frac{\varepsilon_i - \sum_{j=1}^{m} \alpha_j \varepsilon_{i-j}}{\left[1 - \sum_{k=1}^{m} \sum_{j=1}^{m} \alpha_k \alpha_j \rho_{|k-j|}\right]^{1/2}} \; . \qquad 6.32$$

The ξ_i series is then accepted as a second order stationary independent process assuming that the autoregression coefficients are not periodic. Values of the ξ_i series are used to find a probability distribution function which will best fit the empirical frequency distribution. For this purpose, two symmetric distributions, the normal and the bilateral or double-branch exponential distribution function are used as well as one asymmetric distribution (the three parameter lognormal function).

(1) Normal Probability Function

Density Function. The probability density function of the normal distribution used is

$$f(\xi) = \frac{1}{\sigma\sqrt{2\pi}} \exp\left[-\frac{1}{2\sigma^2}(\xi - \mu)^2\right] \; , \qquad 6.33$$

in which μ is the expected value of ξ_i and σ its standard deviation.

Parameter Estimation. The maximum likelihood estimators of the parameters of the normal density function are

$$\hat{\mu} = \frac{1}{N} \sum_{i=1}^{N} \xi_i \qquad 6.34$$

$$\hat{\sigma} = [\frac{1}{N} \sum_{i=1}^{N} (\xi_i - \hat{\mu})]^{\frac{1}{2}} \quad , \qquad 6.35$$

with N the sample size.

(2) Bilateral or Double-Branch Exponential Probability Function

Density Function. The probability density function of the bilateral exponential distribution is

$$f(\xi) = \frac{1}{2\beta} \exp[-\frac{1}{\beta} |\xi-\mu|] \quad , \qquad 6.36$$

in which μ is the expected value of the random variable ξ_i, and $2\beta^2$ its variance.

Parameter Estimation. If a value of either μ or β is obtained from apriori knowledge of the process, then a maximum likelihood estimator of the remaining parameter can be derived analytically. If neither μ nor β is known, an empirical approach using numerical methods may be required to maximize the likelihood function for estimating the two parameters. For the purpose of this study, it is assumed that an apriori knowledge for μ known, with $\mu=0$, because ξ_i is an independent random series derived from ε_i which has been standardized as a (0, 1) series. Thus the maximum likelihood estimator of β is given by

$$\hat{\beta} = \frac{1}{N} \sum_{i=1}^{N} |\xi_i| \quad , \qquad 6.37$$

(3) Three-Parameter Log-Normal Probability Function

Density Function. The three-parameter log-normal probability density function is

$$f(\xi) = \frac{1}{\sqrt{2\pi}\, \sigma_n\, (\xi-\xi_o)} \exp\{-[\ln(\xi-\xi_o) - \mu_n]^2/2\sigma_n^2\} \qquad 6.38$$

in which μ_n is the mean of $\ln(\xi - \xi_o)$, σ_n is the standard deviation of $\ln(\xi - \xi_o)$, and ξ_o is the lower boundary or location parameter.

Parameter Estimation. The lower boundary ξ_o is estimated from the following equation by an iterative procedure in which the allowable error must be prescribed.

$$\sum_{i=1}^{N} \frac{1}{(\xi_i - \hat{\xi}_o)} \{ \frac{1}{N} \sum_{i=1}^{N} [\ln(\xi_i - \hat{\xi}_o)]^2 - [\frac{1}{N} \sum_{i=1}^{N} \ln(\xi_i - \hat{\xi}_o)]^2 - \frac{1}{N} \sum_{i=1}^{N} \ln(\xi_i - \hat{\xi}_o) \} + \sum_{i=1}^{N} \frac{\ln(\xi_i - \hat{\xi}_o)}{\xi_i - \hat{\xi}_o} = 0 \quad , \qquad 6.39$$

Once ξ_o is estimated, the other two parameters may be estimated from the following

$$\hat{\mu}_n = \frac{1}{N} \sum_{i=1}^{N} \ln(\xi_i - \hat{\xi}_o) \quad , \qquad 6.40$$

$$\hat{\sigma} = \{\frac{1}{N} \sum_{i=1}^{N} [\ln(\xi_i - \hat{\xi}_o) - \hat{\mu}_n]\}^{1/2} \quad . \qquad 6.41$$

(4) Criteria of Best Fit

The chi-square statistic is used exclusively in this study to test the goodness of fit of probability functions to empirical frequency distributions. In carrying out a test, the total range of sample observations is divided into k mutually exclusive class intervals, each having an observed frequency denoted by N_i and equal class probability denoted by p=1/k. The measure of the departures between the observed frequencies N_i and the expected probabilities Np (corresponding to the distribution function to be fitted) is defined as the chi-square statistic

$$\chi^2 = \sum_{i=1}^{k} \frac{(N_i - Np)}{Np} \quad . \qquad 6.42$$

This statistic is asymptotically chi-square distributed with k - 1 - D degrees of freedom, where D is the number of parameters already estimated from the observed data.

The chi-square test prescribes the critical value χ_o^2 for a given confidence level so that for $\chi^2 < \chi_o^2$ the null hypothesis of a good fit is accepted, and for $\chi^2 \geq \chi_o^2$ it is rejected.

CHAPTER VII
DATA DESCRIPTION

This chapter deals with the general characteristics of the data used in this study. Background information is presented earlier in Chapters III and IV.

7.1 Sea-Sediment Core Data

Extensive work by Emiliani (1966a, 1966b, 1972) has produced a number of $\delta(O^{18})$ curves for Pleistocene cores in the Caribbean. Four of the longest cores analysed by Emiliani are from the Miami P6304 core series taken in the Caribbean during November to December of 1963. The curves for the four cores are shown on Fig. 8. Shown on the same figure is the $\delta(O^{18})$ curve produced by van Donk (Broecher and van Donk, 1970) for Lamont core V12-122 which was also taken in the Caribbean. Oxygen-isotope analyses of selected species of pelagic foram shells were done at stratigraphic intervals of about 10 cm for all five cores. The ordinates of the cores expressed as $\delta(O^{18})$ are given in units of per mil deviation from the Chicago Standard PDB-1 with the lowest representing the warmest climate (cf. Chapter III). The abscissas represent stratigraphic positions below the sea floor and are given in units of centimeters of depth from the top of the core. In order to convert stratigraphic positions to an absolute time scale, some means of dating the various layers within the core is needed. This subject is the concern of the next chapter.

Emiliani (1966a, 1972) has examined all four cores of the P6304 series for microfaunal similarities of stratigraphic levels based on the first appearance, extinction, coiling direction, and occasional eclipse of certain pelagic species or subspecies. Such stratigraphic similarities are used as key horizons in correlation to provide a means of transfer of a time scale established by radiometric dating from one core to other cores. Also, by examining many cores using microfaunal cross-correlation techniques, it is possible to infer whether a core represents essentially a continuous and complete stratigraphic section.

According to Emiliani all four of the cores from the P6304 series show good microfaunal correlations and represent complete stratigraphic sections. Also, the cores, including the Lamont V12-122 core, show remarkedly consistent fluctuation patterns in the $\delta(O^{18})$ recorded which can be correlated visually as indicated by the dotted lines on Fig. 8.

Since all five cores were taken essentially from the same ocean area in the Caribbean sea and are highly correlated it was decided that analysis of one core from this suite of cores would be sufficient to meet the objective of this study. The locations of the cores in terms of latitude and longitude are given in Fig. 8.

The Miami P6304-9 core was selected over the others for the following reasons:

(a) P6304-9 is the longest of the five cores. With a length of 1428.5 centimeters, the core represents a possible time duration of about 500,000 years. This permits model testing by a split sample technique. The upper zone of the core corresponding to the time period from the present to about 300,000 years ago will be used for calibration purposes. Values from the lower zone of the core representing a time span of about 200,000 years, extending from about 300,000 years B.P. to 500,000 years B.P., will be used to test the adequacy of the model.

(b) The $\delta(O^{18})$ record of core P6304-9 appears superior in detail to that of other cores of Fig. 8. This may indicate less effect on the time resolution of the core from disturbances by ocean-bottom dwelling organisms. Thus, records of climatic oscillations during the Pleistocene epoch may have been better preserved in the $\delta(O^{18})$ curve of core P6304-9 than in the other cores.

7.2 Ice-Core Data

The Camp Century, Greenland ice core which spans a period of 126,000 years (Fig. 10) offers the most detailed and probably the most accurate representation of climatic history of the late Pleistocene yet produced to date. As explained in Chapter III, the 1390 meter long core was sampled at a great number of points to determine their ratios of O^{18} to O^{16}. The measurements are expressed as $\delta(O^{18})$ in units of per mil deviations from that of Standard Mean Ocean Water (SMOW). Since the ice core represents essentially a continuous sequence of annual layers of snow, and since values of $\delta(O^{18})$ in high-latitude snow depend mainly on the air temperature at the time of formation and deposition of the snow, a curve presenting a plot of $\delta(O^{18})$ values along the length of the core should therefore show a sequence of relative temperature changes through time. The highest $\delta(O^{18})$ values represent the warmest climate.

Time calibration of the $\delta(O^{18})$ curve from the Camp Century, Greenland ice core was carried out by Dansgaard et al. (1971) using a mathematical treatment based on Glen's Creep Law. The preliminary time scale obtained from the theoretical model was then subjected to power spectral analysis to detect persistent $\delta(O^{18})$ oscillations. The oscillations evident in the power spectrum were identified as those matching the 78, 190, 405, and 2400 cycles evident in C-14 analysis of tree-ring data. The results were then used to make a non-linear adjustment to the preliminary time scale to obtain a corrected time scale following the tree-ring chronology. This approach is considered reasonable since the $\delta(O^{18})$ series from the ice core and the tree-ring series calibrated by C-14 dating probably represent the same realization of the climatic process as it changes in time.

In the Dansgaard study the 78 and 180 year oscillations were treated as deterministic cycles; whereas in the work for this report, all oscillations of several decades and more are considered stochastic in nature with exception of oscillations induced by the Milankovich mechanism.

The time scale for the upper portion of the ice core representing the past 780 years back to about 1200 A. D. appears to agree with instrumental and historical records to an accuracy of ± 3 percent (Flint, 1971). The time scale for the past 10,000 years is considered to have an accuracy of ±10 percent although agreement within ± 1 percent were found when comparing stratigraphic features with those obtained from both C-14 dates and varves dates according to the Swedish varve chronology for the same periods (Dansgaard et al. 1971).

The ice-core data for this study were obtained from the published figures presented by Dansgaard et al. (1971). Figures representing about 126,000, 10,000, and 780 years of climatic history each with different time resolution are given. The figure which represents about 126,000 years of history gives average values of $\delta(O^{18})$ in 200 year increments. However, for the upper portion of the core, the values of $\delta(O^{18})$ are shown as averages for unequal increments of time. For the purpose of this report, the unequal increments for the 10,000 year $\delta(O^{18})$ series were reduced to equal increments representing 50 year averages. For the 780 year $\delta(O^{18})$ series, the unequal increments were reduced to equal increments representing 10 year averages.

7.3 Incoming Solar Radiation Data

The data for long-period variations in incoming solar radiation are based not on observations but on a mathematical model of the axial and orbital motions of the earth following the Milankovich theory. The computations by Vernekar (1972) contain revisions and improvements in some of the original mathematical formulas developed by Milankovich. The data are presented as Meteorological Monograph Number 34 by the American Meteorological Society.

The data are presented in the Monograph as deviations (langleys per day) of the solar radiation from their 1950 A.D. values for the caloric winter and summer half-years for both the northern and southern hemisphere. The radiation chronology is given in 1000 year intervals spanning a historical period of 2 million years and is extended for 119,000 years into the future. The data are used as the deterministic inputs for the climatic models proposed in this study.

CHAPTER VIII
RATES OF DEPOSITION OF DEEP-SEA SEDIMENTS

In order to treat the $\delta(O^{18})$ curves of core P6304-9 as a time series, the first requisite is to develop a time-length scale for the core. The approach used for this purpose is carried out in four steps. In the first step, data from various sources on radioactive dating and high sea levels are combined to establish a preliminary time scale marking the prominent peaks and troughs in the $\delta(O^{18})$ curve of the upper zone of the core. In the second step, conceptual interpretation of the sediment deposition phenomenon is developed and the assumptions for model building are made. In the third step, the mathematical model of the sedimentation rate is postulated which incorporates variables and parameters that can generate objective estimates of the deposition rate. In the fourth and final step, the preliminary time scale developed in the first step is used in an optimization routine to estimate values for the parameters of the mathematical model postulated in step 3. With this model, it is then possible to specify an absolute time scale for the entire core on the basis of a varying sedimentation rate.

8.1 Preliminary Time Scale

Core P6304-9, with a length of 1428.5 cm, has 144 $\delta(O^{18})$ data points measured at 10 cm intervals. In order to obtain a reasonable number of sample points for model calibration, it was decided to establish a preliminary time scale for the top 760 cm of the core which would provide 77 data points for parameter estimation. The 760 cm level was chosen for three reasons: (1) it marks a prominent peak in the $\delta(O^{18})$ curve; (2) it is located at about the mid-length of the core; and (3) the depth scale of this zone, representing a time span from 0 to about 280,000 B. P., can be correlated to radiometric dating with reasonable degree of confidence. Radiometric dating beyond 200,000 to 300,000 years are subject to a high degree of uncertainty with standard errors ranging up to several tens of thousands of years.

The glacial chronology for the late Pleistocene epoch extending back to about 70,000 years is well established through C-14 dating of various terrestrial deposits in many parts of the world such as the glacial deposits in the Ontario and Erie basins in North America (Goldthwait et al. 1965) and the pollen and varve deposits in Europe, South America, Asia, and Africa (Flint 1971). For example, according to Goldthwait et al., radiocarbon datings of geological deposits show glacial maxima to have occurred at 18,000, 40,000 and 60,000 years B.P. It has also been established that interstadials (intervals of minor retreat of the ice sheet) occurred at about 35,000, 50,000 and 70,000 years B.P. Furthermore, Broecker et al. (1968) have indicated on the basis of radiometric dating of deposits from coral reef terraces found in Barbados, that high sea levels have occurred at about 82,000, 105,000 and 125,000 B.P. Prominent periods in the advance and retreat of the ice sheet determined from such terrestrial evidences can be correlated directly with the prominent peaks and troughs that are evident in the $\delta(O^{18})$ curve from the P6304-9 core. Through this technique it was possible to establish a preliminary time-length scale for the upper zone of the core corresponding to 70,000 years of climate history.

For the period beyond 70,000 years, Rona and Emiliani (1969), and Broecker and Ku (1969), have carried out, independently, time-length measurements of several Caribbean cores, including core P6304-9, using the protactinium-ionium dating technique to provide absolute dates for several strategic stratigraphic levels extending back to about 400,000 years. Average sedimentation rates were used to determine ages between radiometrically dated levels. As mentioned in Chapter III, conflicting estimates were obtained by the two groups of investigators. Broecker and Ku produced a time scale about 25 percent longer than that of Rona and Emiliani. Since the Broecker and Ku estimates seem to be supported by independent estimates based on magnetic reversals and on the high sea-level estimates from absolute dating of coral reefs on the island of Barbados (Broecker and van Donk, 1970), the longer time scale was adopted in this study.

Broecker and van Donk (1970) reported an average sedimentation rate of 2.67 cm per 1000 years for the upper 340 cm of core P6304-9. This value is based on radiometric dating and corresponds to the longer time scale proposed by Broecker and Ku (1969). Using this rate for extrapolation, the age of the 760 cm level was determined to be about 285,000 years B.P.

On the basis of the age-depth relationship established for the 70,000 year period, average sedimentation rates were computed for non-glacial, glacial, and deglaciation intervals represented in the upper zone of the core. These average rates were then applied to similar intervals represented in the core zone down to the 760 cm level.

The results are shown on Fig. 21 where the $\delta(O^{18})$ values for the upper 760 cm core length are plotted against the preliminary time scale established as described. Superimposed on the same figure are the results from the sedimentation-rate model which is discussed in the following pages.

8.2 Concepts and Assumptions Relating to the Build-Up of Sea Sediments

Core sediments are mixtures of fine particles derived from the lands and from marine organisms formed in the ocean itself. The sediment of terrigenous origin are mainly lutite consisting of clay sized particles formed during the process of terrestrial erosion. Most lutite is carried into the ocean by rivers and a much smaller proportion is brought by wind. The sediment of oceanic origin consists chiefly of the shells of microscopic single-celled marine animal such as forams, and plants such as diatoms (Flint, 1971). The build-up of sea sediments through time is mainly determined by the rate of deposition of the terrigenous lutite since it composes by far the bulk of the sediment. The rate of deposition of lutite is in turn controlled by terrestrial events such as the advance and retreat of continental ice sheets which affect erosion and wind characteristics. The following concepts

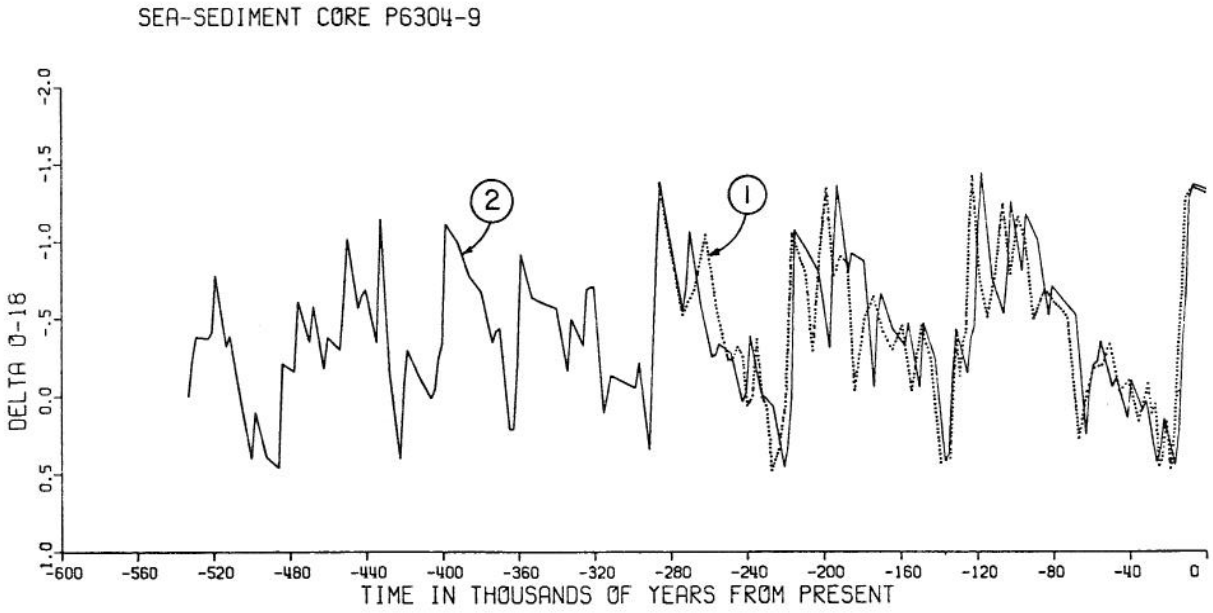

Fig. 21 A chronology for sea-sediment core P6304-9 based on: (1) correlations with radiometrically dated data from terrestrial sources; and (2) the model developed in this study for determining the rate of deposition of deep-sea sediments as a function of the Oxygen-18 data.

of the sediment deposition phenomenon are hypothesized in order to specify the mathematical form of the sedimentation model.

Assumptions Applicable During a Glacial Retreat Interval:

(1) Sedimentation rate will be higher when the ice sheet is large than when the ice sheet is small. The rationale here is that when the ice sheet is large, widespread melting will produce large runoff. The melt water throughout the zone of ablation will flush out the finer clay fractions (lutite) during or even before deposition by retreating ice sheet of the residual coarse sediments (Flint, 1971). The larger the ice sheet, the greater the amount of melt water and the larger will be the amount of fine sediments flushed from the glacial till for transporting into the Caribbean at the location of the sea-sediment coring program. On the other hand, when the ice sheet is small, melt water runoff from the ice sheet will also be small thus limiting the amount of outwash of lutite from the glacial debris. (2) A large rate of melt of the ice sheet will produce higher sedimentation rate than a small rate of melt of the ice sheet. It is obvious that, for the same size ice sheet, a higher melt rate will produce higher runoff and consequently higher sediment load than that produced by a lower melt rate.

Assumptions Applicable During a Glacial Advance Interval:

(1) Sedimentation rate will be considerably lower during a general glacial advance than during a general glacial retreat. During a glacial advance interval, melt water runoff will be minimal and large quantities of fine clay particles from the glacial debris will not be available for discharge into the rivers and streams. Most of the runoff into the Caribbean will be from rainfall occurring beyond the edge of the ice sheet and this rainfall will not produce the quantity of sediment load comparable to that from glacial melt during a general glacial retreat. (2) Sedimentation rate will be higher when the ice sheet is small than when the ice sheet is large. In a glacial advance stage, high precipitation will occur over large regions of the continent much of which will be in the form of snow. Melting of the snow during the summer will produce high runoff. When the ice sheet is small, the area contributing to snowmelt runoff will be greater than when the ice sheet is large and will thus contribute more runoff and consequently more sediment for transport into the Caribbean. (3) A high rate of accumulation of the ice sheet will be associated with a higher sediment rate than that for a small rate of ice accumulation. When the rate of ice accumulation is high, precipitation will also be high and thus producing high runoff and erosion. On the other hand, low rate of accumulation or advance of the ice sheet will be associated with low sediment rate as a consequence of low precipitation and low runoff.

8.3 A Model for the Deposition Rate of Sea Sediments

On the basis of the foregoing assumptions, it is clear that the deposition rate of sea sediments will have to be specified by a model which is a function of two variables: (1) the $\delta(O^{18})$ values, which reflect both temperatures and sizes of ice sheet; and (2) the rate of change of the $\delta(O^{18})$ values, which reflects rate of change of accumulation or ablation on the ice sheet, the rate of precipitation in the form of rain or snow over non-glaciated areas, and the rate of runoff which is intimately associated with the amount of sediments carried into the Caribbean sea where P6304-9 was cored.

Several forms of the model were postulated and the form which gives the best fit to the preliminary time scale was chosen. The model is given in the form of two mathematical functions. One function is applicable when the 10 cm increment of core under consideration represents a cooling or glacial advance phase of the process and the second function is applicable when

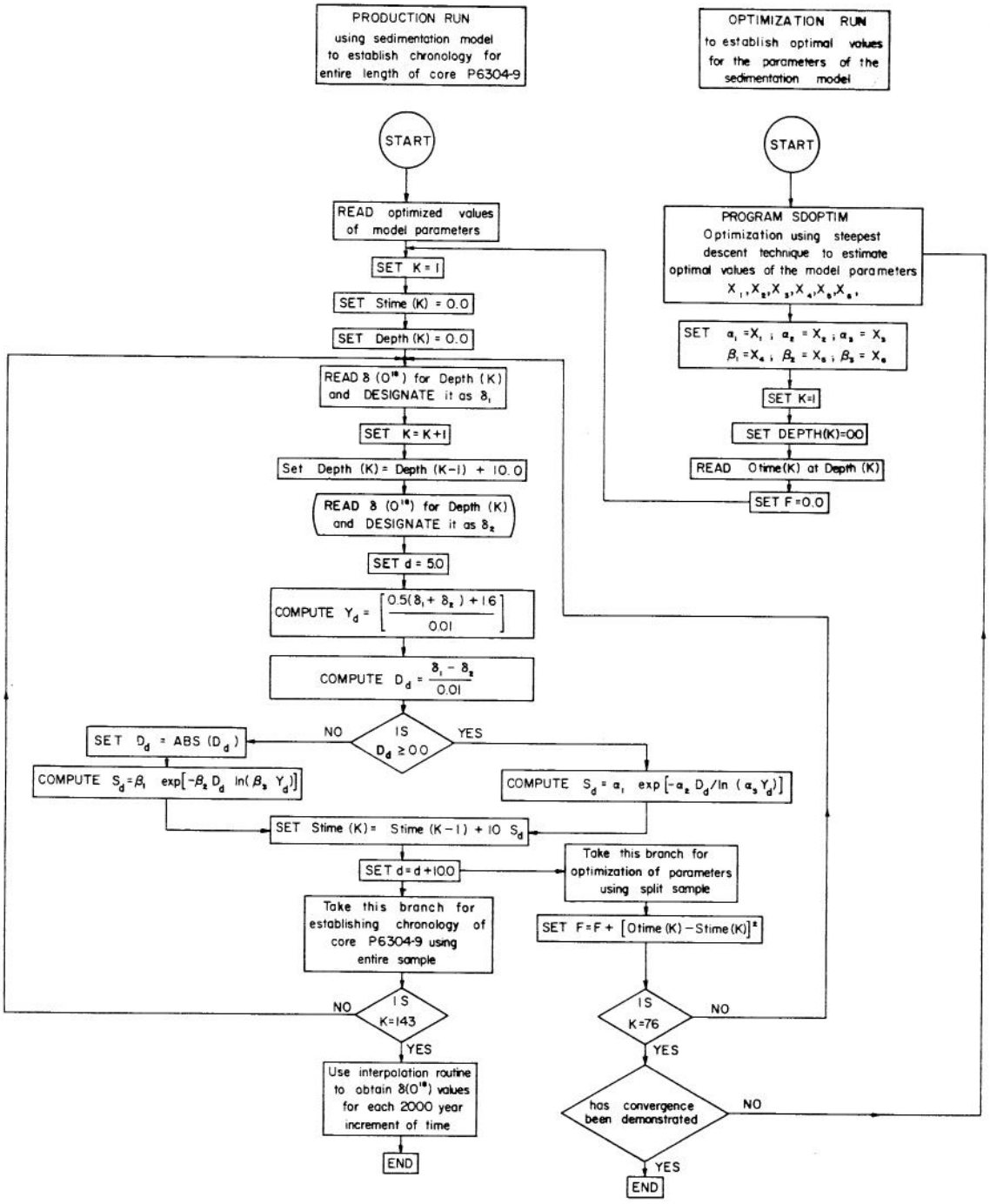

Fig. 22 Flow chart of the model for determining the deposition rate of deep-sea sediments as a function of the Oxygen-18 data.

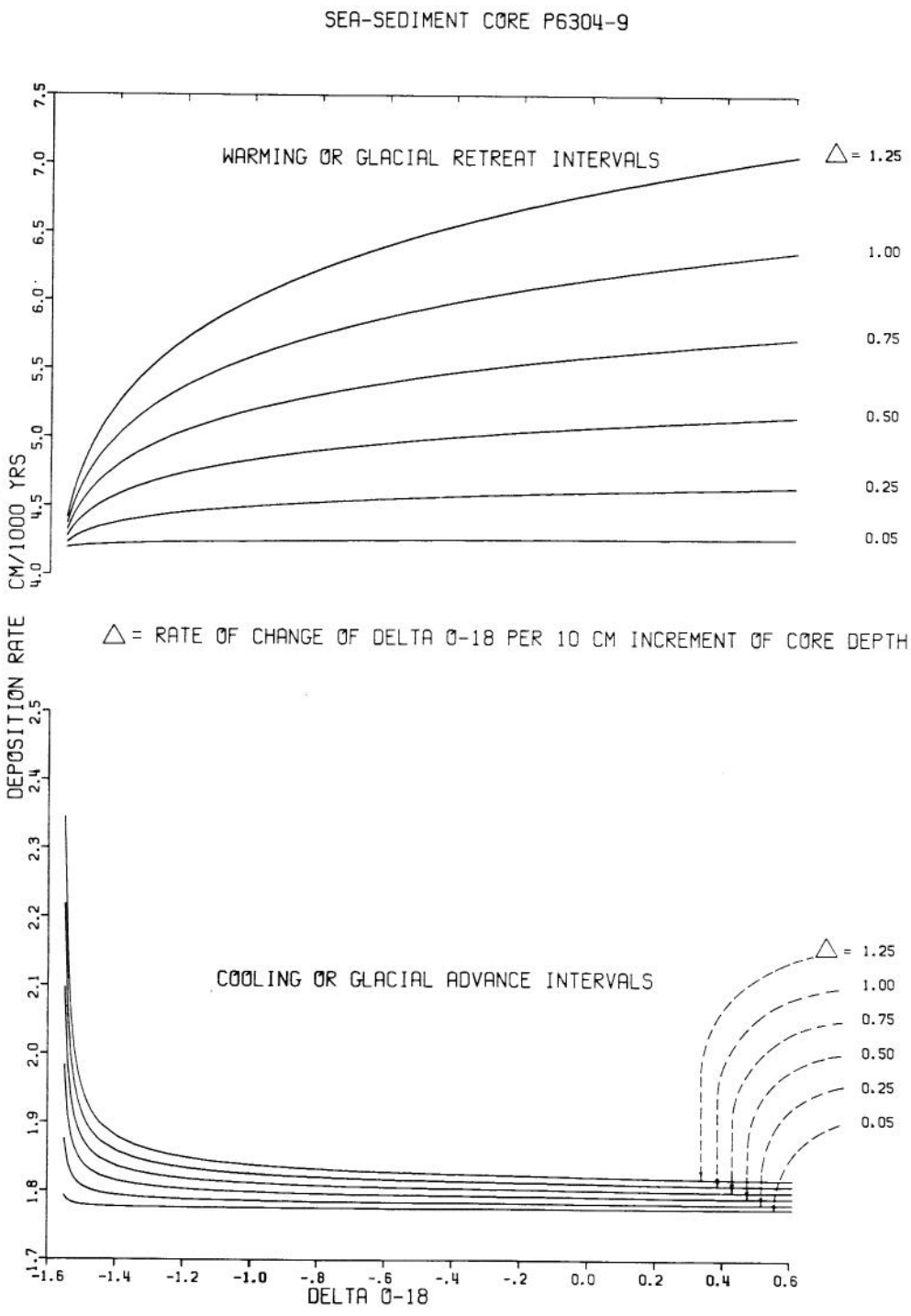

Fig. 23 Rates of deposition of sea sediments in core P6304-9 as a function of Oxygen-18 data and the rate of change of delta 0-18 per 10 cm increment of core depth.

the increment of core represents a warming or glacial retreat phase of the process. A cooling interval occurs when the $\delta(O^{18})$ value increases with time and a warming interval occurs when the $\delta(O^{18})$ value decreases with time. The two functions are

$$S_{d,c} = \alpha_1 \exp [-\alpha_2 D_d / \ln (\alpha_3 Y_d)] \qquad 8.1$$

$$S_{d,w} = \beta_1 \exp [-\beta_2 D_d \ln (\beta_3 Y_d)] \quad , \qquad 8.2$$

in which d is a subscript referring to the average depth of the 10 cm increment of core under consideration, $S_{d,c}$ is the reciprocal of the deposition rate during a cooling interval, $S_{d,w}$ is the reciprocal of the deposition rate during a warming interval, Y_d is the average value of $\delta(O^{18})$ given in transformed units for the 10 cm increment of core under consideration, D_d is the rate of change of $\delta(O^{18})$ given in transformed units per 10 cm of the core increment at depth d, and α_1, α_2, α_3, β_1, β_2, and β_3 are the model parameters to be estimated. Note that $S_{d,c}$ and $S_{d,w}$ are expressed in units of years/cm.

If $\delta_1 = \delta(O^{18})$ at the start of the 10 cm increment and $\delta_2 = \delta(O^{18})$ at the end of the 10 cm increment, then

$$Y_d = \left[\frac{0.5\ (\delta_1 + \delta_2) + 1.6}{0.01}\right] \quad , \qquad 8.3$$

and

$$D_d = \left|\frac{\delta_1 - \delta_2}{0.01}\right| \quad . \qquad 8.4$$

8.4 Parameter Estimation and Results

The flow chart of the deposition model is given in Fig. 22. The six parameters of the model were estimated using the optimization technique based on the steepest descent method as outlined in Chapter VI. In carrying out the optimization procedure, starting values of the six parameters are assumed, from which the computer program using the steepest descent technique generates new values for each parameter so as to minimize the objective function (the least square error). Numerous starting values for each parameter were tried. The results of the many trails showed approximately the same minimum value of F regardless of the starting values. Thus, the assumption is made that the estimates of the parameter vector showing the lowest value of F represents an optimal solution within the accuracy limits of data.

The estimated values of the parameters with three significant figures are: $\alpha_1 = .564$ $\alpha_2 = .000829$, $\alpha_3 = .291$, $\beta_1 = .239$, $\beta_2 = .000993$, and $\beta_3 = .309$.

Curves of deposition rate as a function of two variables, the average $\delta(O^{18})$ for a particular 10 cm increments of core depth and the rate of change of $\delta(O^{18})$ for the particular increment, are presented in Fig. 23.

The age-depth relationship for the entire length of the core as determined from the mathematical model is presented on Fig. 21 along with the preliminary data used in estimating the model parameters. Recall that the preliminary time-length scale was developed from average deposition rates determined between radiometrically dated points.

The results from the model show that deposition rates can range from 4 to 7 cm per 1000 years during a glacial retreat and from 1.5 to 2.5 cm per 1000years during a period of glacial advance. On the basis of the model, the maximum rate apparent in core P6304-9 is 6.1 cm per 1000 years and the minimum rate is 1.8 cm per 1000 years. These values are well within the range of deposition rates determined from C-14 dating and other means (Flint, 1971; Broecker et al. 1958). Estimates of the deposition rates can be greatly improved if the core can be sampled at much finer increments during intervals when the rate of change of the $\delta(O^{18})$ values is high.

CHAPTER IX
THE DETERMINISTIC COMPONENT OF LONG-TERM CLIMATIC CHANGES

The deterministic component found in the $\delta(O^{18})$ time series are manifested in two forms as mentioned in Chapter VI. For the very long time series covering a span of hundred thousand years or more, the oscillatory pattern of the deterministic component consist of an almost-periodic movement. For time span of less than 10,000 or 20,000 years with time resolution of a decade or more, the deterministic component appears only as a trend which can be described by a polynomial equation.

9.1 Almost-Periodic Deterministic Component

(1) Basic Concept

The deterministic component of the $\delta(O^{18})$ time series is considered as primarily a function of long-term changes in insolation. The secondary influences of atmospheric, oceanic, and terrestrial origin are considered responsible for the stochastic component. Since long-term changes in insolation is an almost-periodic process, it is logical to assume that the resulting deterministic component of the $\delta(O^{18})$ time series is a transformed almost-periodic process. This assumption is borne out by inspection of the $\delta(O^{18})$ curves shown on Fig. 8. It can be seen that the maxima and minima of $\delta(O^{18})$ values vary irregularly in amplitude and spacing through time.

In the classical approach to time series decomposition, the almost-periodic component is represented by a Fourier series with trigonometric functions containing noncommensurate frequencies. However, because of the shortness of the $\delta(O^{18})$ time series relative to the time span under consideration, it is not feasible to develop from the present data a statistically meaningful model using Fourier series representation. Scores of frequencies may be needed to adequately describe the almost-periodic component as a Fourier series. To identify these frequencies would require very long records for analysis. Deterministic modeling offers a viable alternative approach to the problem.

The deterministic model in this study is considered as a gray box with inputs in the form of long-term incoming solar radiation and outputs in the form of $\delta(O^{18})$ data. The gray box is viewed as a representation of the atmospheric-oceanic-terrestrial system which has the ability to convert deterministic input of solar radiation imposed on the system into $\delta(O^{18})$ output represented by a process composed of a deterministic component and a stochastic component. The input is derived from the Milankovich theory and is assumed to represent accurately the variations in incoming solar radiation at the top of the earth's atmosphere during the past two million years and over the next 120,000 years. The output, in the case of the sea-sediment core, is known for the past 532,000 years.

In the search for a suitable form of a functional relationship to describe the system it was decided that a model analogous to the mass-balance concept used in studies of the growth and retreat of glaciers could well serve the purpose. As discussed in Chapter III, the $\delta(O^{18})$ records may represent changes in ice volume just as well as changes in air temperature or sea surface temperature. Since all these factors reflect directly or indirectly long-term climatic changes, the question of the exact interpretation of the $\delta(O^{18})$ curves need not be of concern in this study. This is one of the basic assumptions listed in Chapter V.

The mass balance concept may be described by the following equation (Paterson, 1969):

$$B_n = B_{n-1} + \int_{t_1}^{t_m} (a+v)dt + \int_{t_m}^{t_2} (a+v)dt \quad , \qquad 9.1$$

in which a is the accumulation rate with positive values, v is the ablation rate with negative values, t_1 through t_m represents the winter season, t_m through t_2 the summer season, and B_n is the net balance over the n-th annual period which is positive unless the glacier has completely disappeared in which case it becomes zero.

Before entering a discussion on the mathematical form of the model and on the rationale behind the selection of the variables and parameters, it is necessary to be aware of the difference between the requirements of this study and those of deterministic modeling only, the objective is to develop a set of hypotheses about the system behavior so as to obtain a mathematical model which will produce a response identical to that of the real system for the same input. Such an objective is almost never achieved. However, the smaller the dissimilarity the better is the model for describing the real system. On the other hand, in this study, the problem is not connected with modeling the actual output of the system, but is concerned with modeling the deterministic component of the output using a deterministic set of inputs. The assumption is that the dissimilarity between the deterministic output component and the response of the real system for the same input is due to stochastic influences which can be described only in probablistic terms. Thus a large residual between the results from the model and the actual data is not viewed as an indication of a poor model but as an indication of a high degree of stochasticity in the system response. This is similar to harmonic analysis when time series are composed of periodic parameters and a stochastic component. It is recognized that a part of the residuals in this study is due to the inadequacy of the model, errors in the records, and other error sources which may include the solar radiation data as well.

(2) Mathematical Form of the Model

On the basis of the concepts and hypotheses formulated in Chapter V, many forms of functional relationships were postulated using the insolation data in various ways as indices to represent the input variables of the model. Since the various model forms were all empirically derived, only the final model is presented here.

The general form of the model, expressed in terms of the mass-balance analogy, is mathematically defined as

$$D(n) = D(n-1) + G(n) - R(n) - W(n) \qquad 9.2$$

in which D(n) is the deterministic component of the $\delta(O^{18})$ time series in the n-th interval of time and is analagous to the net mass-balance of the ice sheet, G(n) is the accumulation during the n-th time interval, R(n) is the ablation during the n-th time interval, and W(n) is a term representing accelerated ablation under conditions favorable to the complete destruction of an ice sheet of continental size. R(n) and W(n) are mutually exclusive. Capital letters are used hereon as symbols for variables, and lower case letters as symbols for parameters and coefficients. A flow chart of the model is presented in Fig. 24. The variables and parameters of the model are defined in the following sections.

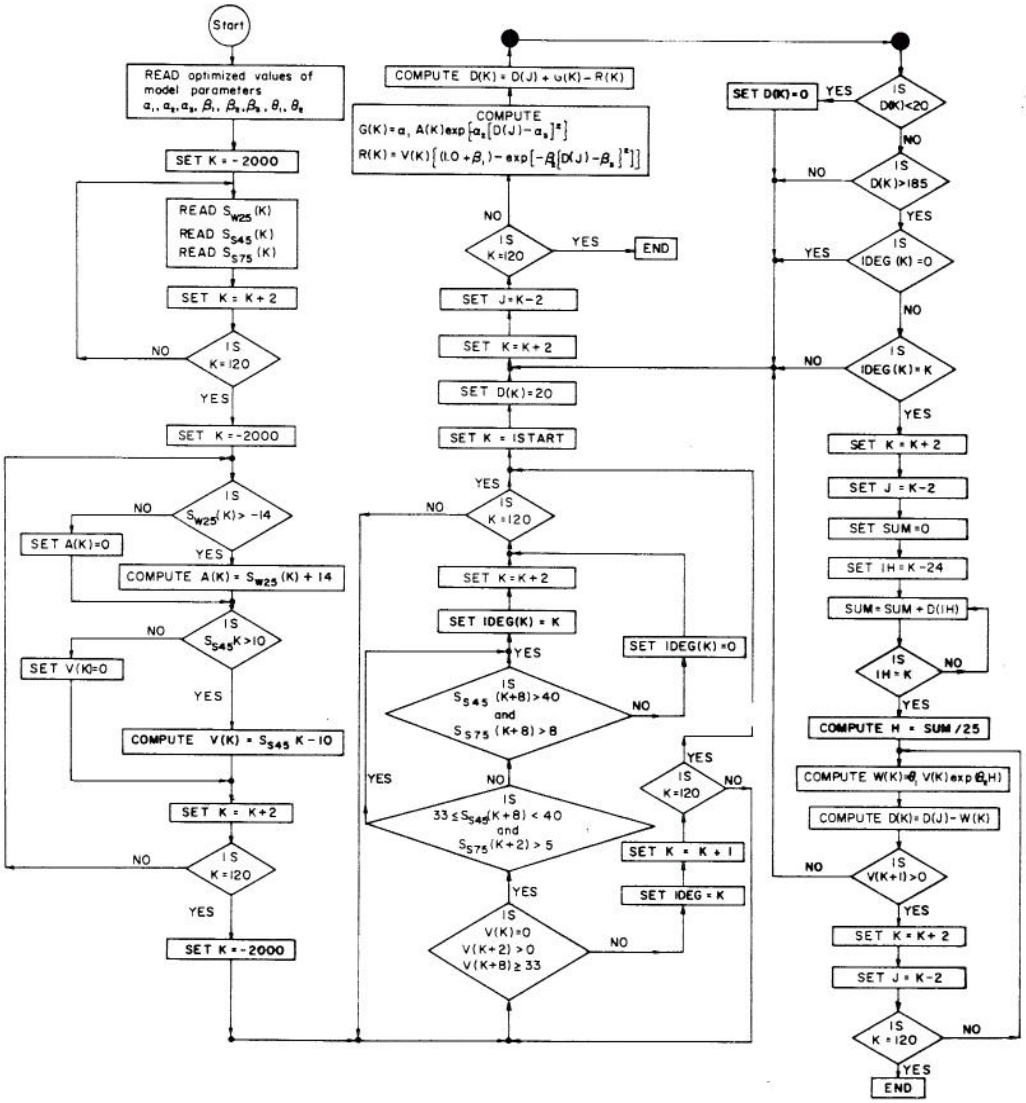

Fig. 24. Flow chart of the model for synthesizing the deterministic component of the almost-periodic Oxygen-18 time series with solar radiation data derived from the Milankovich astronomical theory as the only input.

In describing the model, it is convenient to separate the system in terms of two distinct parts: (1) the input variables which are functions of the solar radiation data; and (2) the gray-box response which is postulated as a set of empirical mathematical equations with coefficients or parameters representing a certain but unknown characteristic behavior that is deterministic in nature, going on in the system during the response process.

(3) Input Variables

Variable A(n). This is an index representing the equivalent of the accumulation rate during the n-th interval of time in the mass-balance equation. The accumulation rate is the rate of increase in the mass of the ice sheet and is mainly a function of the amount of winter snow precipitated over the ice sheet. Winter snow is affected by three principal factors: input of water vapor into the atmosphere which depends on the winter heat energy available for the evaporation from oceans and continents; transportation of the water vapor by winds from the oceans to above the ice sheets; and the extraction of the water vapor from atmosphere as snow over the ice sheet. By far the most important factor for modeling purposes is the winter heat energy which can be used as an index to model the net accumulation or growth rate.

The winter heat energy available from solar input can be indexed by the caloric winter-half year insolation data computed by Vernekar. Since the winter insolation data at all latitudes are highly correlated with each other, selection of an appropriate radiation time series to serve as the index variable A(n) poses no problem. However, the choice was made on the following basis. Consider an ice sheet over north-eastern Canada. It is easy to visualize winter precipitation being brought into the region in moist, maritime air mainly from low latitude sources in the Atlantic and Gulf of Mexico to nourish the ice sheet. Thus the selection of the radiation time series for 25°N latitude to derive the index variable A(n) is appropriate. To show that winter data from 25°N latitude can be representative of the whole northern hemisphere and not just the low latitudes, the correlation coefficient between winter radiation data at 25°N latitude and those at all other northern latitudes are computed. The correlation coefficient exceeds 0.98 in every case (Fig. 25).

The time series values of the index variables A(n) is obtained by truncating the winter solar radiation time series for latitude 25°N at the level of 629 langleys per day. The assumption is that as soon as the caloric winter-half year solar radiation at the latitude 25°N exceeds 629 langleys per day, the northern hemisphere will be entering a period of mild winters in which winter snow accumulation will usually exceed summer ice ablation. The truncation level was determined by trying several levels and selecting the one which produces oscillations in the deterministic component that most nearly matches the oscillations evident in the sea-sediment curve. Note that the insolation values presented by Vernekar are tabulated as deviations from its 1950 A.D. values. The 1950 A.D. value of the caloric winter-half solar radiation at latitude 25°N is 651 langleys per day. Thus, the truncation level of 629 langleys per day corresponds to the truncation level of -14 langleys per day when using tabulated values given by Vernekar (1972).

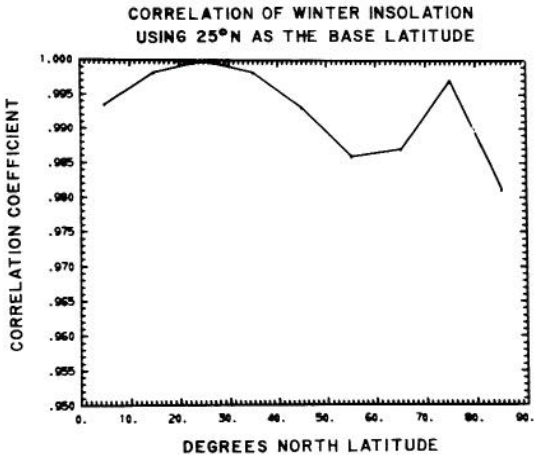

Fig. 25. Correlation of winter insolation at selected latitudes in the northern hemisphere using 25°N as the base latitude.

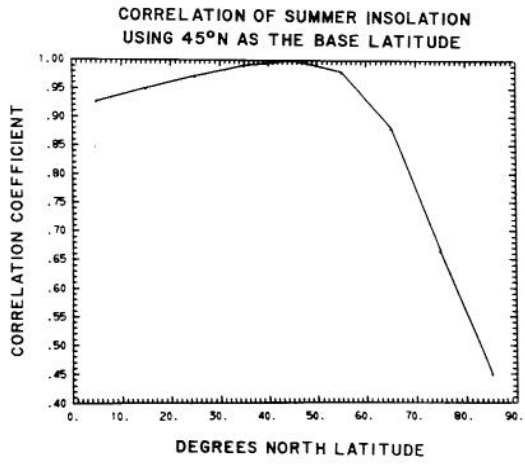

Fig. 26. Correlation of summer insolation at selected latitudes in the northern hemisphere using 45°N as the base latitude.

Values of A(n) are obtained by

$$A(n)=\begin{cases} S_{W25}(n) + 14 & \text{if } S_{W25}(n) > -14 \\ 0 & \text{if } S_{W25}(n) \leq -14 \end{cases} \qquad 9.3$$

A(n) is the index of the accumulation or growth rate during the n-th interval of time, $S_{W25}(n)$ is the deviation from 1950 A. D. value of the caloric winter-half year insolation at latitude 25°N, and -14 is the truncation level in langleys per day.

The value of A(n) as used in the model represents an index of the net accumulation rate. This net rate is assumed to apply over the entire year rather than just for the winter-half year. The rationale for this approach is based on the assumption that summer accumulation during a period of cool summers is balanced off by winter ablation during the concurrent period of mild winters. Thus, only the winter accumulation rates during such periods need be considered. Studies of models which separated winter accumulation rates and summer accumulation rates were made but the results were no better than this simplified approach.

Variable V(n). This is an index representing the equivalent of the ablation rate during the n-th interval of time in the mass-balance equation. The ablation or retreat rate is defined as the rate of decrease in the mass of ice sheet.

The problem, again, is to derive an appropriate index based on solar radiation data which can be incorporated in a model to best represent the effects of the various influences on the ablation rate. On the assumption that the albedo of the ice surface remains nearly constant, any increase in the ablation rate will be caused mainly by an increase in the incoming summer solar radiation over the ice sheet and by an influx of warm summer air and warm summer rain from the low latitudes. These influences usually occur concurrently during periods of high contrast between summer and winter radiation intensities.

After testing summer radiation series for several nothern latitudes, the radiation time series for 45°N latitude was selected as giving the best results. The correlation coefficient between summer radiation data at 45°N and those at all northern latitudes was computed (Fig. 26). The results show a correlation coefficient of well over 0.85 for all latitudes up to 65°N which certainly indicates that the series should be adequate to represent those contributory influences arising from the mid and low latitudes.

The time series values of the index variable V(n) was obtained by truncating the summer solar radiation time series for latitude 45°N at the level of 882 langleys per day. The assumption is that as soon as the caloric summer-half year solar radiation at latitude 45°N exceeds 882 langleys per day, the northern hemisphere will be entering a period of hot summers in which summer ablation will dominate with little or virtually no accumulation. The truncation level was determined in the same way as that for variable A(n). Note that the 1950 A.D. value of the caloric summer-half year solar radiation at latitude 45°N is 872 langleys per day. Thus, when using the tabulated values presented by Vernekar, which are expressed in deviation from the 1950 A.D. values, the truncation level to be used is 10 langleys per day rather than 882 langleys per day.

Values of V(n) are obtained from

$$V(n) = \begin{cases} S_{s45}(n) - 10 & \text{if } S_{s45}(n) > 10 \\ 0 & \text{if } S_{s45}(n) \leq 10 \end{cases} \qquad 9.4$$

where V(n) is the index of the ablation or retreat rate during the n-th interval of time, $S_{s45}(n)$ is the deviation from 1950 value of the caloric summer-half year insolation value at latitude 45°N, and 10 is the truncation level in langleys per day.

The V(n) as used in the model represents an index for determining the net ablation or retreat rate. This net rate is assumed to apply over the entire year rather than just the summer-half year. Periods of hot summers usually have cold winter. Ablation during cold winter periods is considered negligible because of cold anticyclonic conditions and low humidity. Consequently during periods of high contrast in radiation intensities between the summer and winter-half years, the winter period is assumed to have little or no effect on both the net ablation and net accumulation in the continental glacial system.

(4) The Gray-Box Approach

In keeping with the glacier mass-balance analogy, the gray-box approach that converts the almost-periodic input variables A(n) and V(n) into the deterministic output component D(n) can be described as having three facets: growth, retreat, and deglaciation. The concepts and hypotheses concerning the three facets are described in Chapter V.

In specifying the functional form of the mathematical equations for each facet of the model, it is necessary to build into the equation a feedback mechanism to take into account the tremendous influence of the ice sheet itself on the surrounding environment. For example, cold summer temperatures (or low summer radiation) would increase the size of the ice sheet, which would increase the albedo, which would further decrease the summer temperature.

This feedback effect is built into the model in two ways. The first way is by designing the functional equations so that they act as a filtering system. The filters assign different weights to the input variables A(n) and V(n) at different time intervals. The weights are dependent on the extent of the ice sheet at the time interval under consideration. The extent of the ice sheet is expressed as a function of D(n-1). The second way is by incorporating parameters into the functional equation in such a way that they can represent certain characteristic feedback behavior of the system during the response process.

All components of the gray-box model described in the next few paragraphs are defined for modeling of the sea-sediment core. Certain minor adjustments are necessary to adapt the model for use in analyzing the 126,000 year ice-core series.

Growth Component. The functional equation for the growth component is designed so that during the initial stage of the ice sheet, nourishment and growth are very slow. As the ice sheet increases in size, the A(n) values become more effective until the ice sheet reaches a critical size. Once it reaches the critical size, rapid calving will occur on reaching a sea coast, and developing stability will occur when the southern edge of the ice sheet reaches the line of accumulation. Thus the A(n) values again become less effective. The critical size is represented by the α_3 parameter in the functional equation. The functional equation for the growth component is

$$G(n) = \alpha_1 A(n) \exp[-\alpha_2\{D(n-1) - \alpha_3\}^2] , \qquad 9.5$$

where G(n) is the incremental growth or accumulation during the n-th time interval, A(n) is the index of the accumulation rate during the n-th time interval, D(n-1) is the deterministic component of the $\delta(O^{18})$ time series at the (n-1) time interval, α_1, and α_2 are scaling or weighting parameters, and α_3 is the parameter representing the critical size of the ice sheet with reference to the accumulation rate.

Retreat Component. The functional equation for the retreat component is designed to permit high ablation rates when the ice sheet is still small. As the ice sheet grows in size the ablation rate will decrease rapidly because of the increase in albedo. Once the ice sheet grows past a critical size, the ablation rate will again increase due to calving into the sea coast and to high melt rate at the southern edge of the ice sheet caused by high temperatures at the lower latitudes. The form of the functional equation is

$$R(n) = V(n) \{(1.0 + \beta_1) - \exp[-\beta_2\{D(n-1) - \beta_3\}^2]\} , \qquad 9.6$$

where R(n) is the incremental retreat or ablation during the n-th interval of time, V(n) is the index of the ablation rate during the n-th time interval, D(n-1) is the deterministic component of the $\delta(O^{18})$ time series during the (n-1) time interval, β_3 is the parameter representing the critical size of the ice sheet with references to the retreat rate.

Deglaciation Component. The functional equation of the deglaciation component is designed to permit complete destruction of ice sheet of a continental size once the following three sets of conditions are met:

(a) The ice sheet must reach a minimum size represented by D(n) = 185 in the transformed units used in sea-sediment core model or D*(n) = - 0.25 in the original $\delta(O^{18})$ units of per mil deviation from Chicago Standard PDB-1.

(b) The V(n) index series must be in a positive upturn such that at the start of the deglaciation interval V(n) = 0 , V(n+1) > 0, and V(n+4) $\geq$ 33. These conditions are set up to ensure that the rate of increase of the summer solar radiation is great enough to initiate the deglaciation.

(c) Oscillations of the summer-half year insolation during the deglaciation interval must be essentially in phase for all northern latitudes. The condition is specified by the following criteria based on the caloric summer-half year insolation at 45°N and at 75°N

$$[33.0 \leq S_{s45}(n+4) < 40.0] \text{ and } [S_{s75}(n+1) > 5.0],$$

or

$$[S_{s45}(n+4) > 40.0] \text{ and } [S_{s75}(n+4) > 5.0] , \qquad 9.7$$

where $S_{s45}(n+i)$ is the caloric summer half year insolation during the (n+i) time interval and is expressed as deviations from the 1950 A. D. values in langleys per day for 45°N latitude, and $S_{s75}(n+i)$ is the caloric summer-half year insolation given in deviations from the 1950 A.D. values in langleys per day for 75°N latitude.

The positions in time which have the potential (according to Eq. 9.7) for starting the deglaciation process are indicated on Figs. 28 and 29. The functional equation for the deglaciation component in the sea-sediment core model is

$$W(n) = \theta_1 V(n) \exp(\theta_2 H) , \qquad 9.8$$

in which W(n) is the incremental deglaciation amount during the n-th time interval, V(n) is index of ablation rate during the n-th time interval, and H is a heat storage index, given by

$$H = \frac{1}{25} \sum_{i=n-24}^{n} D(n) , \qquad 9.9$$

D(n) is the deterministic component of the $\delta(O^{18})$ time series during the n-th time interval, and θ_1 and θ_2 are scaling or weighting parameters.

It should be noted that in the modeling procedure an upper constraint is imposed on the value of D(n), (upper means the warm part of the curve). This constraint is necessary because of the coarse time unit (2000 years) used in the analysis. With such a coarse time interval, it is not possible to constrain the upper boundary through the model parameters alone. Without the upper constraint, an occasional unfortunate combination of values in the V(n) series can cause the negative exponential function term to "blow up" the model. In the ice-core analysis, where a 200 year time unit is used, it is possible to eliminate the upper boundary constraint by introducing an additional parameter into the model. This is done through the deglaciation facet. Thus for the deglaciation facet of the ice-core model the functional equation becomes:

$$W(n) = V(n) \{1.0 - [\exp\{-\theta_2[14D(n-1)-\theta_3]^2\}]\} \exp(\theta_1 H) , \qquad 9.10$$

where W(n) is the incremental amount during the n-th time interval, and V(n) is the index of the ablation rate during the n-th time interval, and H is a heat storage index with

$$H = \frac{1}{250} \sum_{i=n-249}^{n} D(n) \quad . \qquad 9.11$$

D(n) and D(n-1) are the deterministic component during the n-th and (n-1) time interval, respectively, θ_1 and θ_2 are scaling or weighting parameters, and θ_3 is the parameter representing the critical size of the ice sheet with reference to the deglaciation rate. The units of D(n) are expressed as per mil deviation from the Standard Mean Ocean Water (SMOW). The value of 14 associated with D(n-1) in the equation is a transformation coefficient.

Deterministic Component. With Eqs. 9.5, 9.6 and 9.8 specifying the growth, retreat, and deglaciation increments, respectively, during the n-th time interval and using the properties of additivity of the mass-balance approach, the general form of the model as given in Eq. 9.2 is thus completely defined

$$D(n) = D(n-1) + G(n) - R(n) - W(n),$$

in which D(n) is the deterministic component of the $\delta(O^{18})$ time series and is given in transformed units such that for the sea-sediment core

$$D^*(n) = 1.6 - 0.01\, D(n) \quad , \qquad 9.12$$

in which D*(n) is expressed in units of per mil deviation from the Chicago Standard PDB-1.

(5) Parameter Estimation

The eight parameters of the sea-sediment core model were estimated using a split sample of the P6304-9 time series. Estimates of the parameters values using the gradient optimization routine described in Chapter VI were made with data from the first half of the time series extending back to 286,000 B.P. The year 286,000 B.P. was chosen as the break-off point for the following reason. The model is so structured that computations must start at a point in time corresponding to the end of an interglacial or the beginning of a glacial period, otherwise nonsensical results will be obtained. According to the $\delta(O^{18})$ curve based on the preliminary time scale developed in this study, the year 286,000 B.P. represents the end of a short interglacial period at about the midpoint of the time span of the P6304-9 core. Accordingly, it was chosen as the starting point for calibration of the model (Fig. 27).

Extensive tests of the model in the final form were carried out. Numerous runs of the optimization routine were made using different starting values for each parameter. It was found that slight changes in the starting values did not produce significant changes in the objective function once the parameters values have been narrowed down to a reasonable range. A succession of runs was then made with each successive run producing a lower value of the objective function F until no further improvement was possible. Many iterations were made with different starting values for each parameter. The model was found to be reasonably stable in that each run converges to approximately the same value of F, although some variation in the values of the parameters did occur. However, the question of whether the final values selected for the parameters represent the global minimum for the objective function F or only a local minimum was not completely solved. The point is not critical for the present study, since the series is analyzed as a deterministic-stochastic process so that the adequacy of the model can be tested subsequently in the evaluation of the stochastic component.

Estimated values of parameters for the sea-sediment and ice-core models are:

Sea-Sediment Core Model

$\alpha_1 = 0.650$	$\beta_1 = .260$	$\theta_1 = 0.580$
$\alpha_2 = 0.0000366$	$\beta_2 = .000170$	$\theta_2 = 0.00744$
$\alpha_3 = 180.0$	$\beta_3 = 90.0$	

Ice-Core Model

$\alpha_1 = .02153$	$\beta_1 = .000005$	$\theta_1 = .015$
$\alpha_2 = .0002188$	$\beta_2 = .00000051$	$\theta_2 = .00000026$
$\alpha_3 = 518.0$	$\beta_3 = 380.0$	$\theta_3 = 303.0$

(6) Evaluation of the Model Output

Sea-sediment Core P6304-9. Values of A(n) and V(n) derived from the solar radiation data computed by Vernekar were used in conjunction with the optimized parameters to generate a deterministic component representing 2,000,000 years of climatic history and extending 118,000 years into the future. The results are shown on Figs. 28 and 29. Although the results may be considered as hypothetical at the present time, the oscillations in the curve for core P6304-9 in the time span from about 500,000 B.P. to the present, although only 286,000 years were used in the calibration. Further verification of the model will be possible as and when $\delta(O^{18})$ curves become available from longer cores which hopefully may cover the entire 2 million year time span. With longer records and better data, modification of the model and re-evaluation of the parameters will undoubtedly be necessary. Nevertheless, the results are encouraging as the first attempt at a mathematical description of the process. The model described above yields a stochastic component which is analyzed and described in the subsequent chapter.

The asymmetric sawtoothed oscillations mentioned in Chapter V appear prominently in the 2 million years of synthesized data for the deterministic component of the $\delta(O^{18})$ curve of the sea-sediment core. The pattern shows a slow glacial buildup, taking from about 70,000 to 200,000 years to reach a glacial maximum, followed by rapid deglaciation, requiring less than about 8,000 years to accomplish almost total destruction of a continental-size ice sheet. The results are in accord with the Weertman theory. Although the model cannot offer conclusive proof of the causes of the long-term climatic fluctuations during the Pleistocene epoch, it does show that long-term variations in solar radiation due to the Milankovich mechanism can provide controls of the right order of magnitude to explain

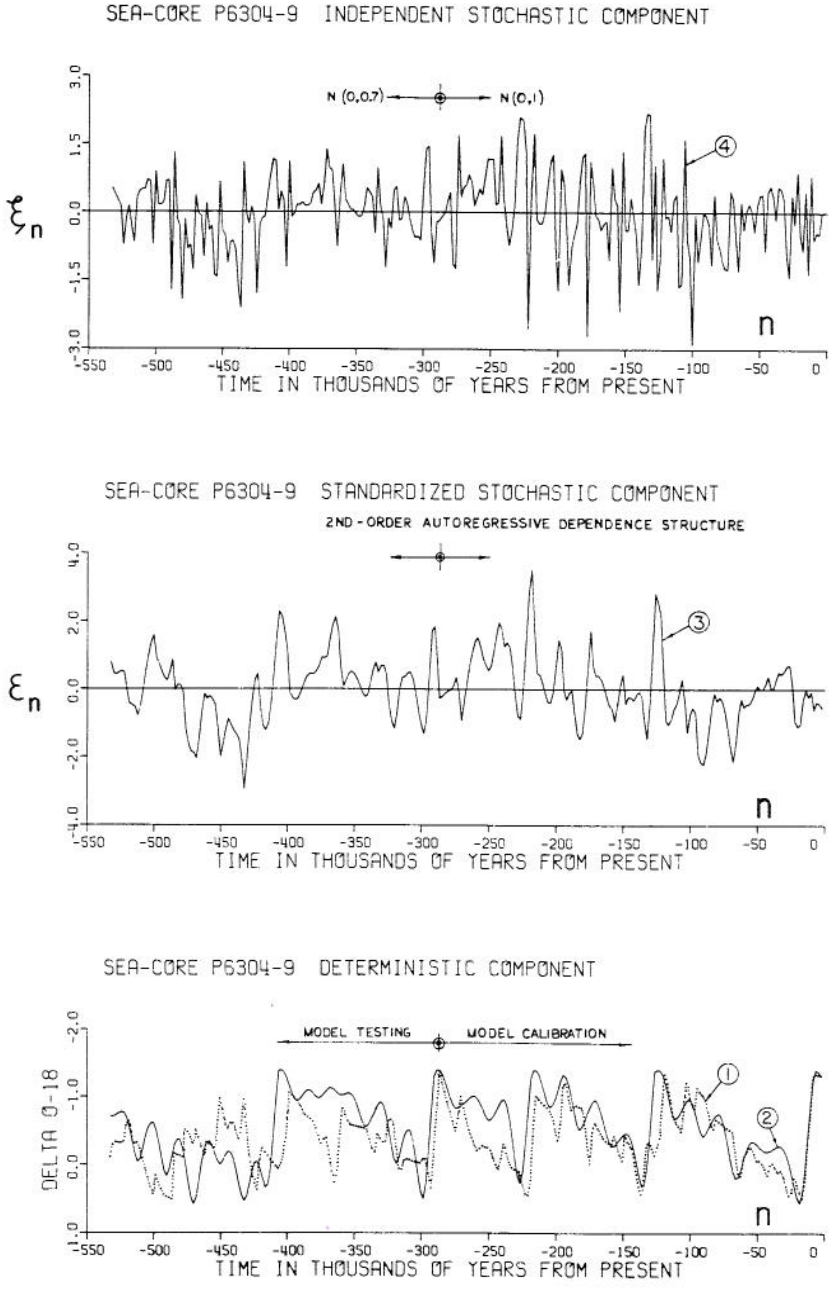

Fig. 27. Time series curves for sea-sediment core P6304-9 showing: (1) the Oxygen-18 values for the original series; (2) the deterministic component series; (3) the standardized stochastic component series; and (4) the independent stochastic component series. Note that half the sample was used in calibration of the model parameters and the other half used in testing the adequacy of the calibrated model (see text for description).

the primary sawtoothed pattern as well as the secondary oscillations apparent in the $\delta(O^{18})$ records.

Although the deterministic component should not normally be used as a separate series for predicting future events, it does provide a general indication of the pattern of events to come. It is interesting to note that although the model indicates a somewhat mildly cooling pattern over the next 100,000 years, an ice sheet of continental dimensions does not appear imminent, at least on the basis of this model.

Camp Century Greenland Ice Core (Ice-200 Series). The model was used to generate a deterministic component for the $\delta(O^{18})$ series from the Camp Century ice core. The results are shown on Fig. 30. In assessing the results, consideration should be given to the cautionary note made by Dansgaard et al. (1969) as to the proper interpretation of the $\delta(O^{18})$ record obtained from the ice core (cf. Chapter III).

9.2 Deterministic Trend Component

In the analyses of the ice-core data for the 10,000 year and 780 year series (Ice-50 and Ice - 10 series), the assumption is made that the oscillations apparent in the $\delta(O^{18})$ records are basically the result of stochastic variations. The deterministic components, at the time scale and time resolution obtained for these series, will show up only as trends.

(1) Ice-Core Series (10,000-Year Period Ice - 50 Series)

This series, with 50-year mean values, is fitted by a cubic trend. The cubic trend was selected over a quadratic trend (both of which are significant) because of the apriori knowledge (from the study of the 780-years series) that the most recent portion of the curve has a linearly rising trend. The quadratic trend shows a negative slope for the same period.

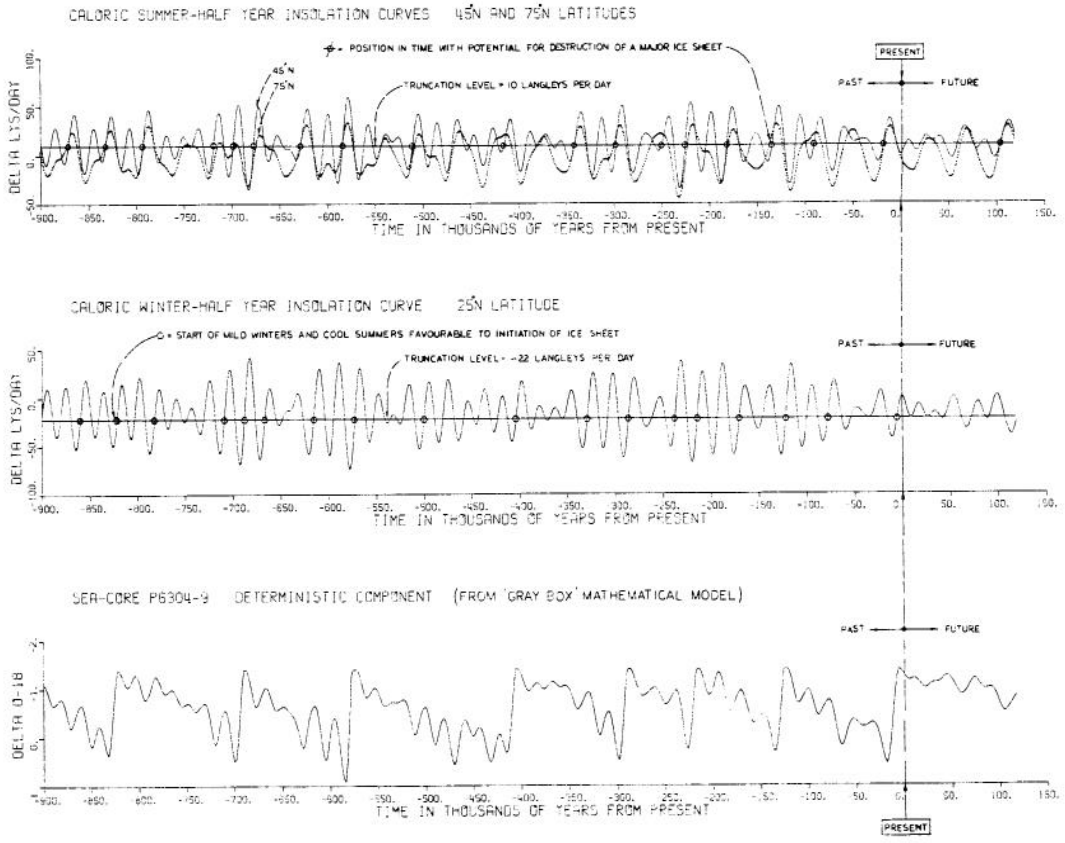

Fig. 28 Time series curve of the deterministic component of the Oxygen-18 data for deep-sea sediment core P6304-9 from 900,000 years B.P. to 118,000 years B.P. in 2000-year intervals. The incoming solar radiation data used as inputs to the model are also shown. Symbols are explained on the diagrams.

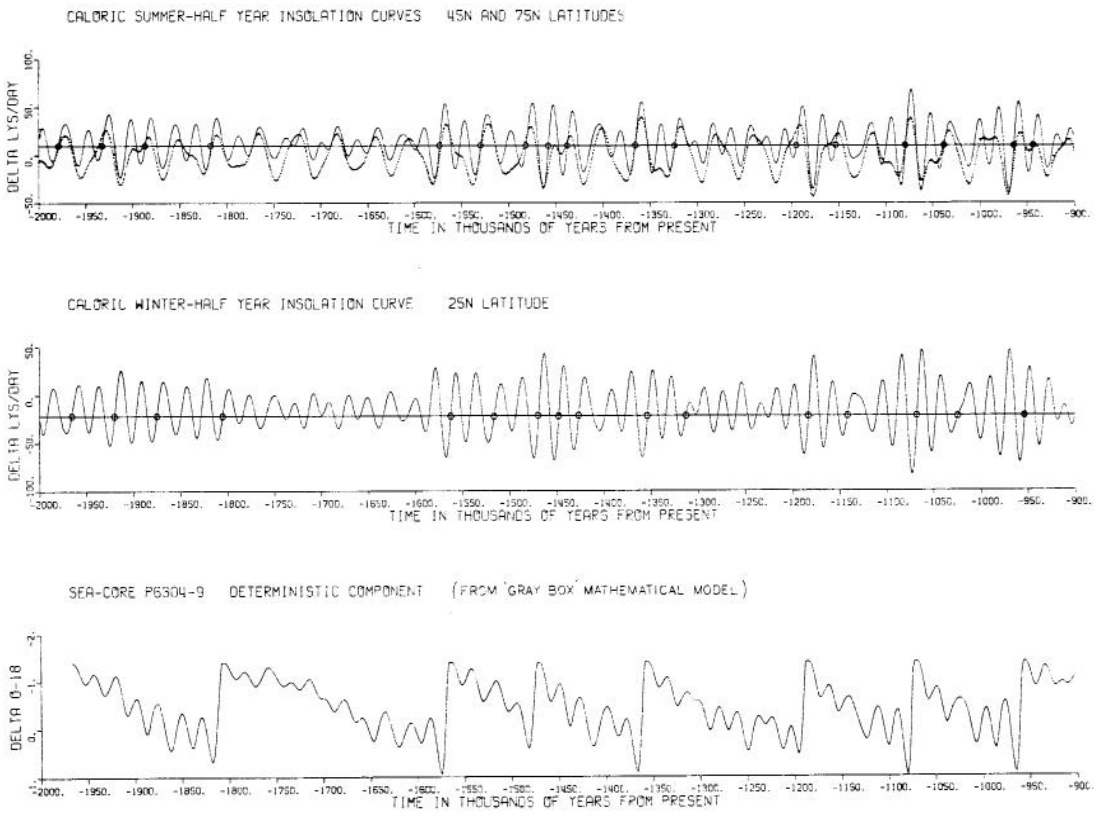

Fig. 29. Time series curve of the deterministic component of the Oxygen-18 data for deep-sea sediment core P6304-9 from 2,000,000 years B.P. to 900,000 years B.P. The incoming solar radiation data used as inputs to the model are also shown. Symbols are explained on Fig. 28.

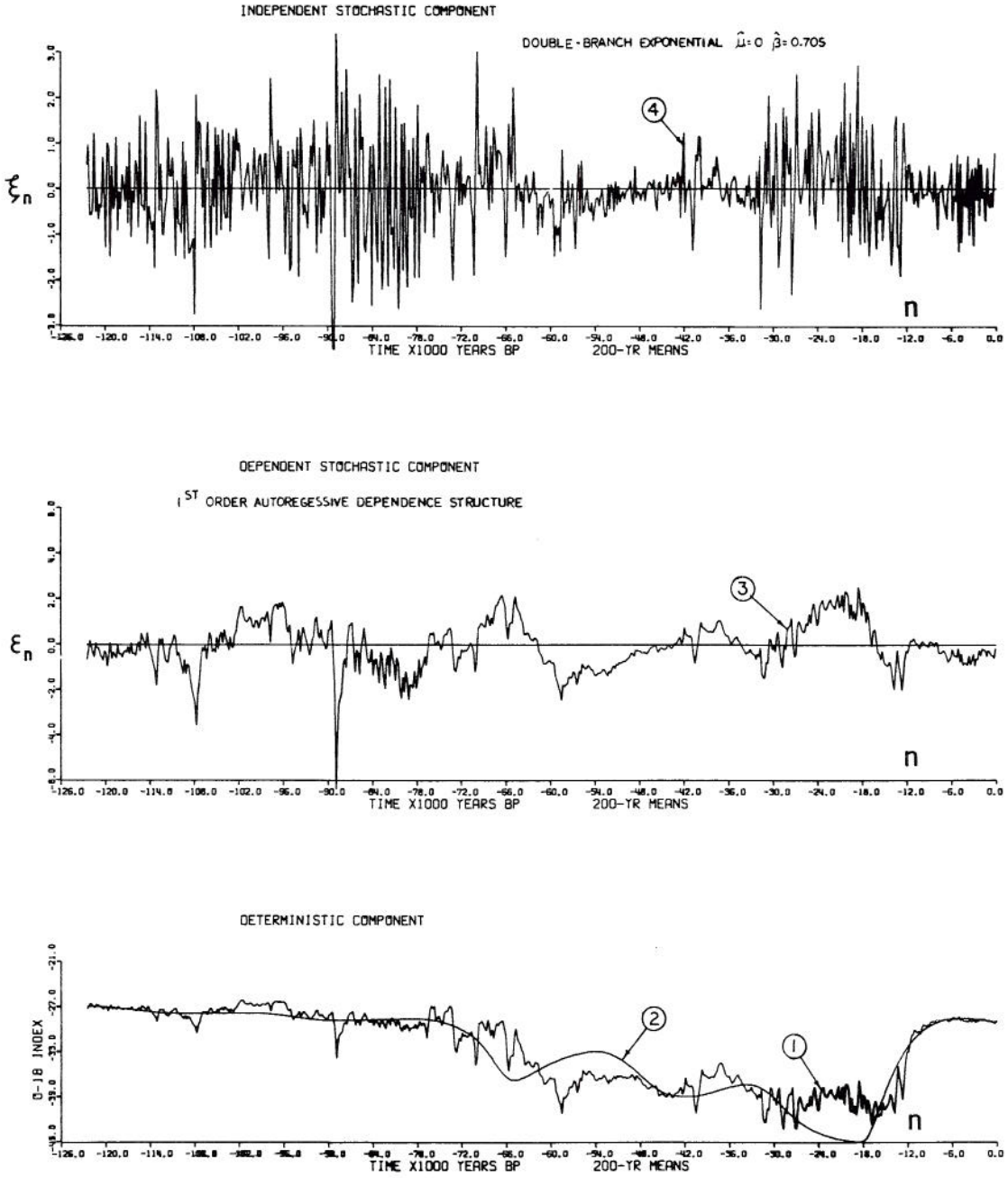

Fig. 30 Time series curves for the Ice-200 series showing: (1) the Oxygen-18 values for the original series; (2) the deterministic component series; (3) the standardized stochastic component series; and (4) the independent stochastic component series.

The equation of the cubic polynomial is

$$T(n) = -28.908 + 0.1255n + 0.0574n^2 + 0.00518n^3 \qquad 9.13$$

in which $T(n)$ is the trend value during the n-th time interval and is given in units of per mil deviation from Standard Mean Ocean Water (SMOW), and n is expressed in units of years x 10^{-3} measured from the present and is of negative value.

The residuals between the original $\delta(O^{18})$ series and the fitted cubic trend are analyzed as a stochastic series. Fig. 31 presents the results in graphical form.

(2) Ice-Core Series (780-Year Period Ice-10 Series)

The 780-year series with 10 year mean show a slightly rising linear trend which is almost signi-

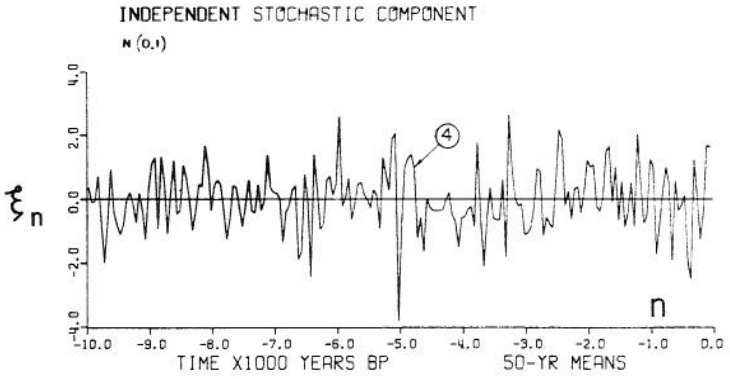

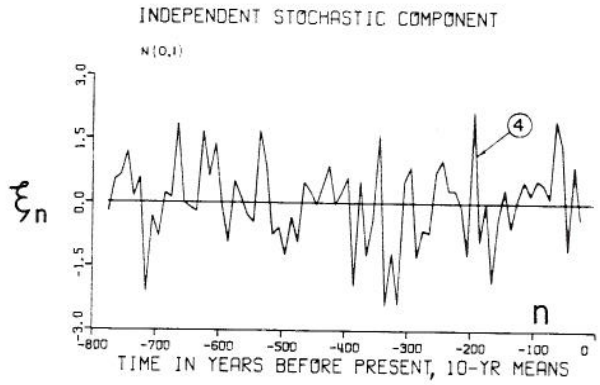

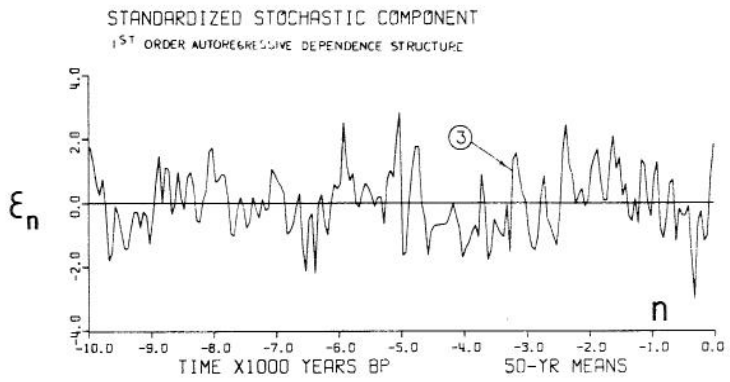

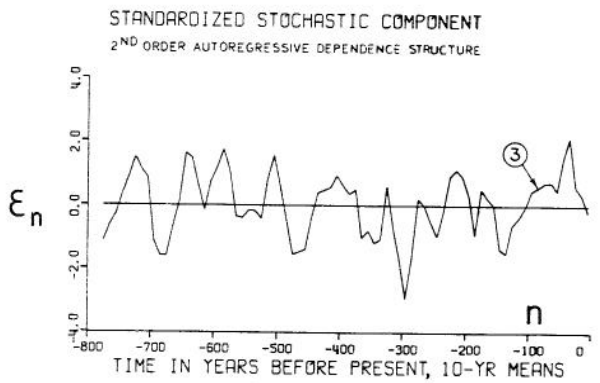

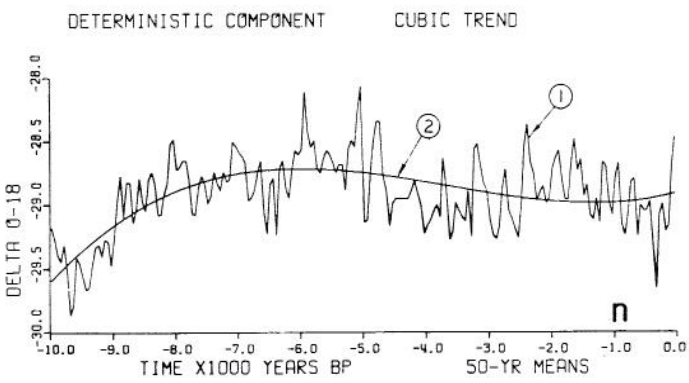

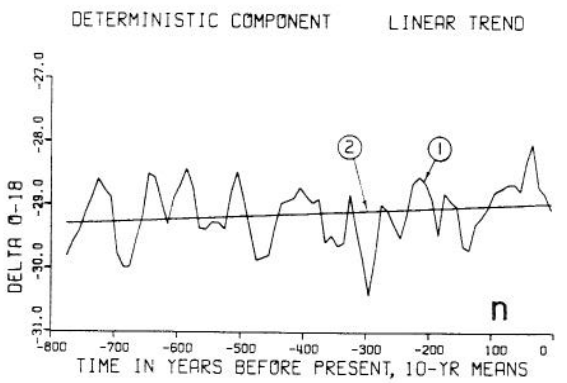

Fig. 31 Time series curves for the Ice-50 series showing: (1) the Oxygen-18 values for the original series; (2) the cubic polynomial trend series; (3) the standardized stochastic component series; and (4) the independent stochastic component series.

Fig. 32 Time series curves for the Ice-10 series showing: (1) the Oxygen-18 values for the original series; (2) the linear trend series; (3) the standardized stochastic component series; and (4) the independent stochastic component series.

ficant at the 95 percent level and definitely significant at the 90 percent level.

The equation of the linear trend is

$$T(n) = - 28.962 + 0.0436\ n, \qquad 9.14$$

in which $T(n)$ is the trend value during the n-th time interval and is expressed in units of per mil deviation from the Standard Mean Ocean Water (SMOW), and n is expressed in units of years x 10^{-2}, measured from the present and is of negative value.

The residuals between the original $\delta(O^{18})$ series and the fitted linear trend are analyzed as a stochastic series in the subsequent chapter. Fig. 32 presents the results in graphical form.

CHAPTER X
THE STOCHASTIC COMPONENT OF LONG-RANGE CLIMATIC CHANGES

This chapter is concerned with the analysis and identification of the structure of the stochastic components of the four $\delta(O^{18})$ time series analyzed previously.

10.1 Wide-Sense Stationarity and Standardization

The stochastic component for each series was obtained by subtracting either the deterministic component D(n) or the trend component T(n) from their respective $\delta(O^{18})$ time series. In many instances the stochastic component thus obtained exhibits approximately the property of wide-sense stationarity, that is, the expected mean of the series is a constant and its covariance is a function only of the lag. Of the four series examined, only the Ice-200 residual series appear to show that the variance is not constant with time as evident from Fig. 30.

To approximate wide-sense stationarity, the Ice-200 residual series was truncated into two parts; one part representing the interglacial conditions, and the second part representing the glacial conditions. The variances for each part were computed and the results were used to transform the series to approximating wide-sense stationarity and at the same time to standardize the series.

Given that

$$Y(n) = X(n) - D(n) \quad , \qquad 10.1$$

in which Y(n) is the residual series or stochastic component, X(n) is the original series, and D(n) is the deterministic component.

The transformation and standardization were made by

$$\varepsilon_n = \frac{Y_{n,p} - \overline{Y}}{S(Y_{n,p})} \quad , \qquad 10.1$$

in which $p = 1$ if Y_n belong to the interglacial part, $p = 2$ if Y_n belong to the glacial part, and $S(Y_{n,p})$ is the standard deviation of either the $Y_{n,1}$ series or the $Y_{n,2}$ series.

Similarly for the sea-sediment series, the Ice-50 series and the Ice-10 series were standardized using the simpler equation for a stationary series

$$\varepsilon_n = \frac{Y_n - \overline{Y}}{S(Y_n)} \quad . \qquad 10.2$$

The ε_n series for the sea-sediment, Ice-200, Ice-50, and Ice-10 processes are shown on Figs. 27, 30, 31, and 32.

10.2 Autoregressive Representation

Each of the ε_n series has a dependence structure, assumed to be approximated by a first, second, or third order autoregressive model. All four series were subjected to the tests outlined in Chapter VI.

(1) Spectral Analysis

Variance density spectra for each of the series were computed and the results are shown on Figs. 33 to 36, respectively. It can be seen that the Ice-200 series has the typical shape of a first-order Markov model. The Ice-50 series also exhibit a first-order shape but does not quite approach the classical form. The sea-sediment series and the Ice-10 series definitely show the typical shapes of a second-order Markov Model. All four spectra were computed using the Parzen window, although the Tukey, Bartlett and rectangular windows were also examined.

The window closing procedure used in estimating the four spectra is illustrated on Figs. 37 and 38. The Ice-200 series and Ice-10 series are shown as typical examples of the first-order and second-order Markov model, respectively. The bandwidth is decreased in three steps to show how the smoothing procedure affects the variance and the bias. It is evident that with decreasing bandwidth, the variance is increased while the bias is decreased and vice-versa.

An illustration of window carpentry is given on Figs. 39 to 42. Figures 39 and 41 show power spectra for the Ice-200 series and Figs. 40 and 42 for the Ice-10 series. In each figure are four curves each of which is smoothed by either the Parzen, Bartlett, Tukey or rectangular windows. Figures 39 and 40 show curves smoothed by the Parzen, Bartlett, Tukey and rectangular windows all using the same bandwidth corresponding to the best bandwidth selected for the Parzen window. The difference between the power spectra are quite evident. Figures 41 and 42 show curves that are smoothed by the same four windows but each using a bandwidth that is best suited to its own configuration. It can be seen that all four windows produced acceptable results indicating that the choice of windows is much less important in the analysis procedure than proper window closing.

(2) Residual Variance

Autoregressive models of all orders up to 10 were assumed for each of the ε_i series. The parameters of each order were estimated and the variance of the residuals between the ε_i series and the values computed for each autoregressive model are plotted. The plots are shown on Figs. 43 to 46. It can be seen that for the sea-sediment series, the second-order Markov model produced the minimum residual variance. For the Ice-200 series, the first-order Markov model is very close to the minimum residual variance so that any higher-order model would not produce significantly better results. For the Ice-10 series, the minimum residual variance is obtained by the second-order Markov model.

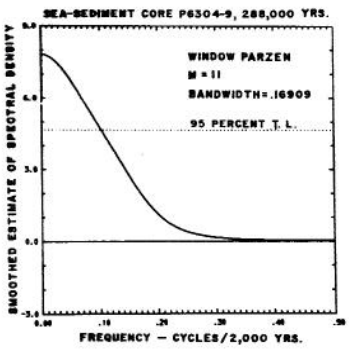

Figure 33. Smoothed variance density spectrum of the dependent stochastic components of the sea-sediment series. Data correspond to delta 0-18 values in 2000-year intervals from 286,000 years B.P. to the present.

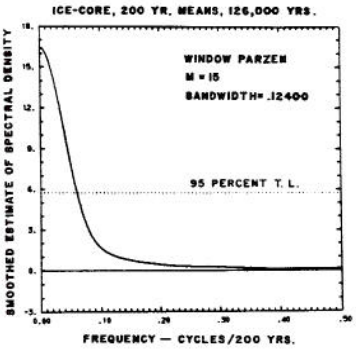

Figure 34. Smoothed variance density spectrum of the dependent stochastic component of the Ice-200 series. Data correspond to delta 0-18 values in 200-year averages from 126,000 years B.P. to the present.

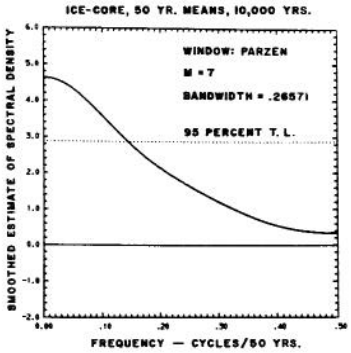

Figure 35. Smoothed variance density spectrum of the dependent stochastic component of the Ice-50 series. Data correspond to delta 0-18 values in 50-year averages from 10,000 years B.P. to the present.

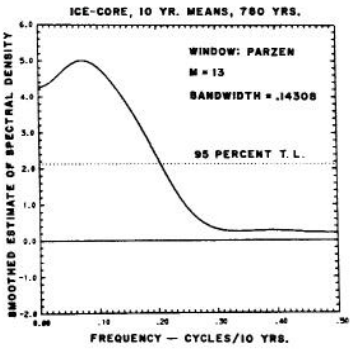

Figure 36. Smoothed variance density spectrum of the dependent stochastic component of the Ice-10 series. Data correspond to delta 0-18 values in 10-year averages from 780 years B.P. to the present.

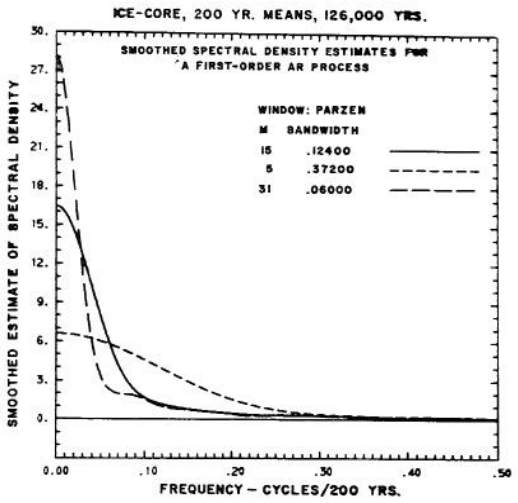

Figure 37. An example of the window closing technique for the Parzen window using a first-order ar process from the Ice-200 dependent random series.

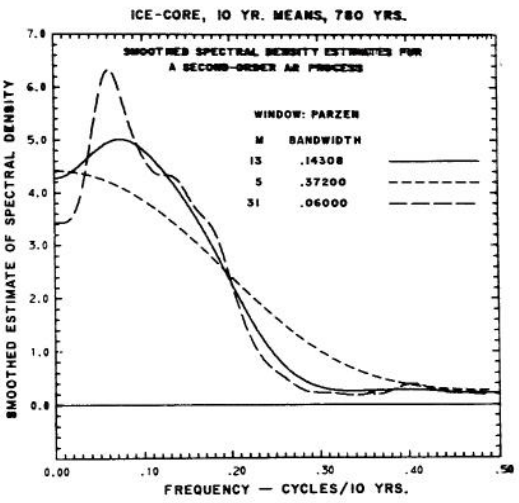

Figure 38. An example of the window closing technique for the Parzen window using a second-order ar process from the Ice-10 dependent random series.

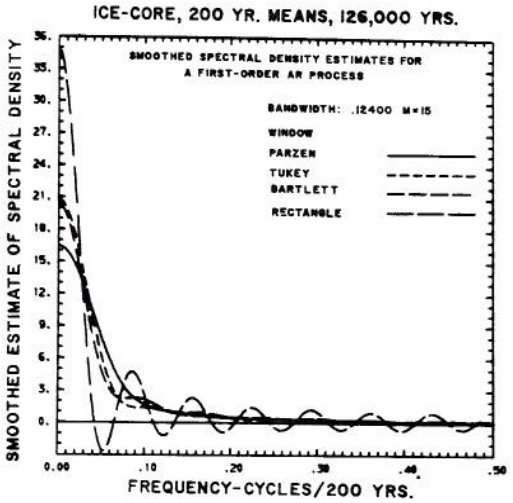

Figure 39. Comparison of the Parzen, Tukey, Bartlett, and rectangular windows for a constant bandwidth using a first-order ar process from the Ice-200 dependent random series. Bandwidth corresponds to that selected as best for the Parzen window.

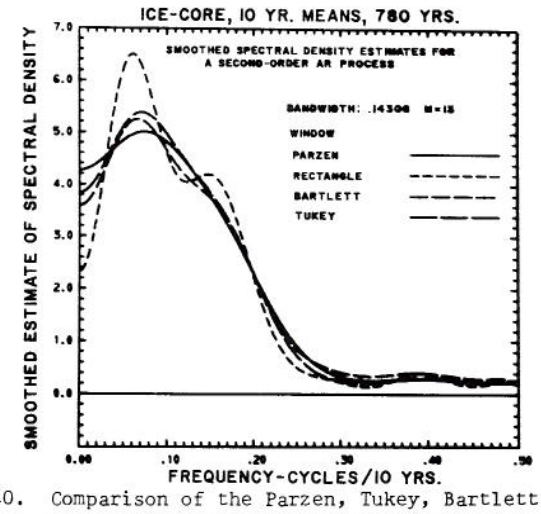

Figure 40. Comparison of the Parzen, Tukey, Bartlett, and rectangular windows for a constant bandwidth using a second-order ar process from the Ice-10 dependent random series. Bandwidth corresponds to that selected as best for the Parzen window.

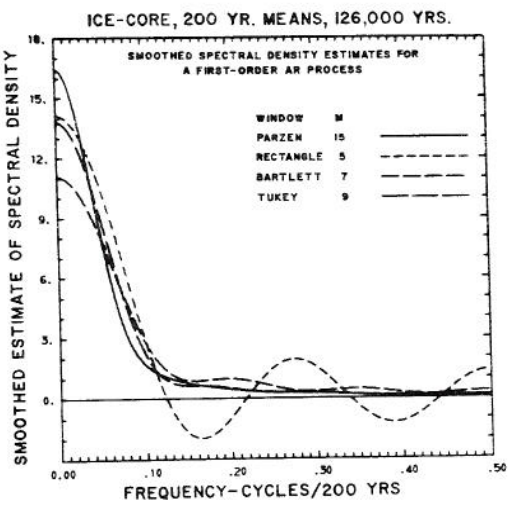

Fig. 41. An example of window carpentry using the Parzen, Tukey, Bartlett and rectangular window on a first-order ar process from the Ice-200 dependent random series. The bandwidth (maximum lag) corresponds to the best selected for each window.

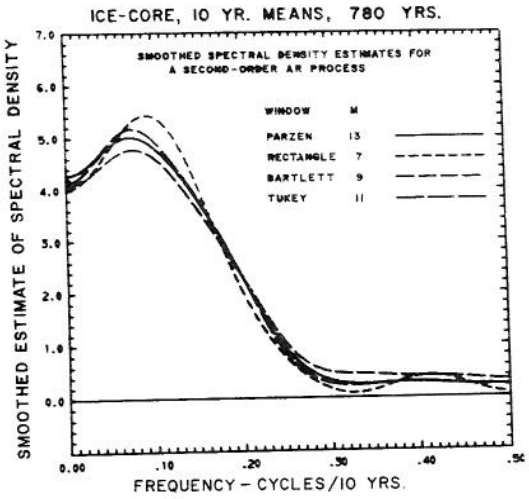

Fig. 42. An example of window carpentry using the Parzen, Tukey, Bartlett and rectangular window on a second-order ar process from the Ice-10 dependent random series. The bandwidth (maximum lag) corresponds to the best selected for each window.

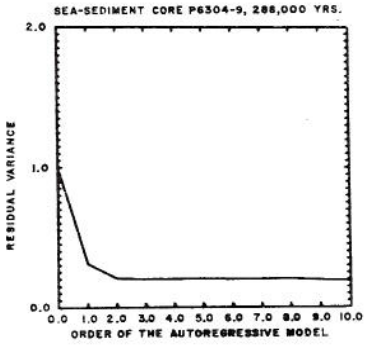

Figure 43. Residual variance for autoregressive models fitted to the sea-sediment core P6304-9 dependent random series.

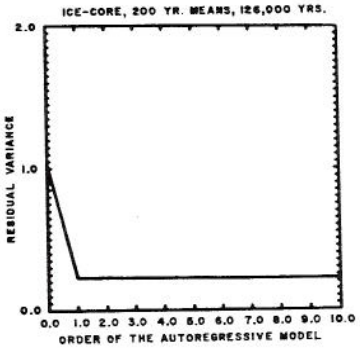

Figure 44. Residual variance for autoregressive models fitted to the Ice-200 dependent random series.

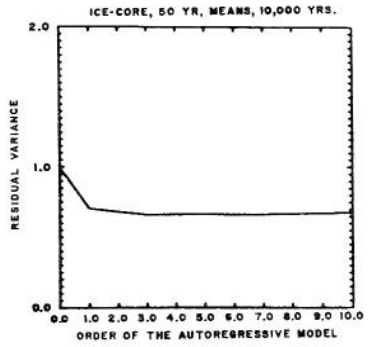

Figure 45. Residual variance for autoregressive models fitted to the Ice-50 dependent random series.

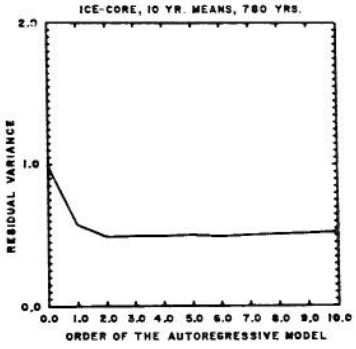

Figure 46. Residual variance for autoregressive models fitted to the Ice-10 dependent random series.

(3) Coefficient of Determination

The simplified approach proposed by Yevjevich of using the coefficient of determination as a criterion for selecting the appropriate order of the Markov process was tested. The equation and criteria for selection are given in Chapter VI.

Sea-sediment Series

$R_1^2 = .695$, $R_2^2 = .803$, $R_3^2 = .812$.

The second-order Markov model is selected according to Eq. 6.30 since $R_2^2 - R_1^2 = .008 < 0.01$

and $R_3^2 - R_2^2 = .009 \leq 0.01$

Ice-200 Series

$R_1^2 = .779$, $R_2^2 = .779$, $R_3^2 = .782$.

The first order Markov model is selected according to Eq. 6.29 since $R_2^2 - R_1^2 = 0 \leq 0.01$,

and $R_3^2 - R_2^2 = 0.003 \leq 0.01$.

Ice-50 Series

$R_1^2 = .308$, $R_2^2 = .338$, $R_3^2 = .364$.

The third-order Markov model is indicated according to Eq. 6.31 since $R_2^2 - R_1^2 = 0.02 > 0.01$,

and $R_3^2 - R_2^2 = 0.026 > 0.01$.

Ice-10 Series

$R_1^2 = .443$, $R_2^2 = .539$, $R_3^2 = .540$.

The second-order Markov model is selected according to Eq. 6.30 since $R_2^2 - R_1^2 = .096 > 0.01$,

and $R_3^2 - R_2^2 = .001 \leq 0.01$.

(4) Autocorrelation Analysis

Correlograms for each of the ε_n series were prepared and the results are shown on Figs. 47 to 50. The correlograms of the Ice-200 series and the Ice-50 series both show monotonic and slowly decreasing values of r_k, usually typical, of the first-order Markov model. The correlograms of the Ice-10 series and the sea-sediment series show values of r_k decreasing rapidly to zero within the first few lags and then oscillate with low amplitude about zero. This characteristic is fairly typical of the second-order Markov model.

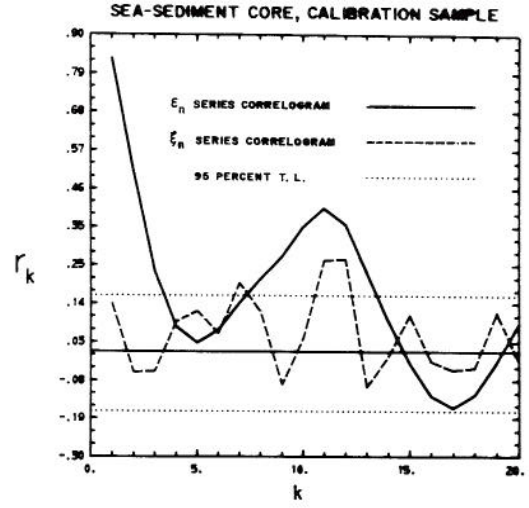

Fig. 47. Correlograms of the dependent random component and the independent random component of the sea-sediment core P6304-9 time series. Tolerance limits at the 95 percent level for N=142 are shown.

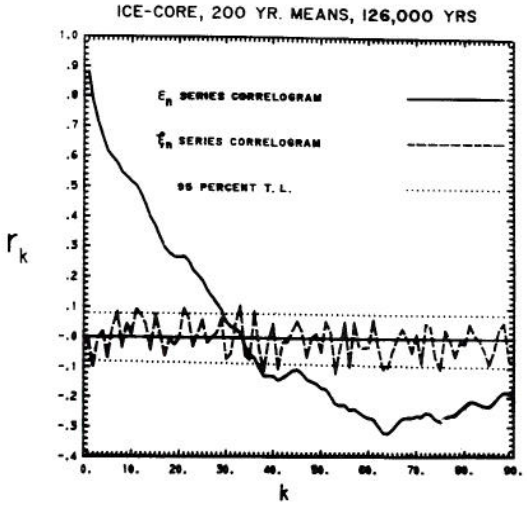

Fig. 48. Correlograms of the dependent random component and the independent random component of the Ice-200 series. Tolerance limits at the 95 percent level for N=612 are shown.

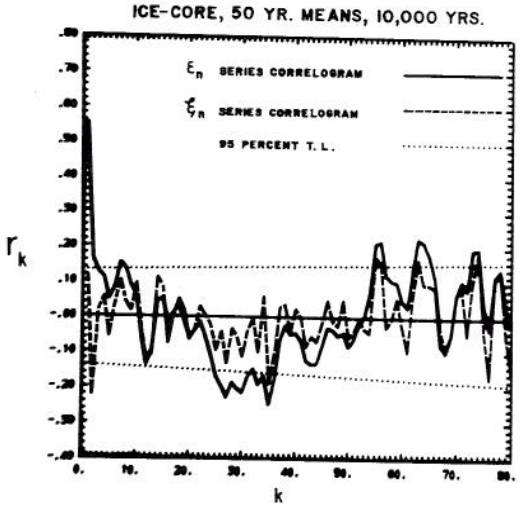

Fig. 49. Correlograms of the dependent random component and the independent random component of the Ice-50 series. Tolerance limits at the 95 percent level for N=199 are shown.

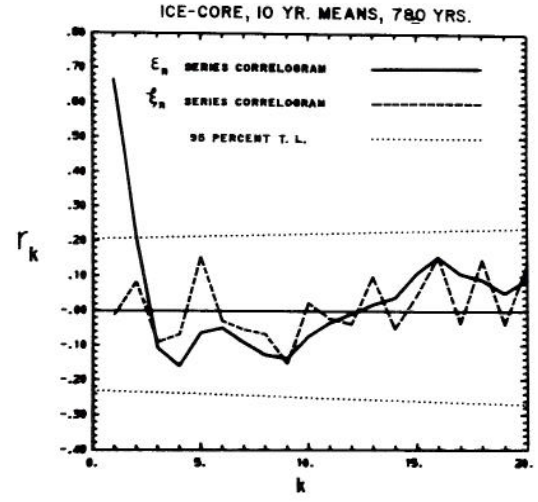

Fig. 50. Correlograms of the dependent random component and the independent random component of the Ice-10 series. Tolerance limits at the 95 percent level for N=76 are shown.

With the exception of the coefficient of determination test for the Ice-50 series, the results of all four diagnostic tests are in complete agreement with each other. Thus, the use of the first-order autoregressive model to approximate the dependence characteristics of the Ice-200 and Ice-50 series is acceptable. Also, the choice of the second-order auregressive model to approximate the dependence characteristics of the Ice-10 series and the sea-sediment series is acceptable by all the tests.

(5) The Dependence Model

The dependence models together with their parameters are listed below. The parameters were estimated using the Yule-Walker equations (Eq. 6.18). The dependent models are given in the form of Eq. 6.17 so that the independent stochastic component will have unit variance.

Sea-sediment series

$$\varepsilon_n = 1.317\ \varepsilon_{n-1} - 0.5855\ \varepsilon_{n-2} + 0.4543\ \xi_n, \qquad 10.4$$

Ice-200 series

$$\varepsilon_n = 0.8823\ \varepsilon_{n-1} + 0.4707\ \xi_n, \qquad 10.5$$

Ice-50 series

$$\varepsilon_n = 0.5458\ \varepsilon_{n-1} + 0.8379\ \xi_n, \qquad 10.6$$

Ice-10 series

$$\varepsilon_n = 0.9231\ \varepsilon_{n-1} - 0.3998\ \varepsilon_{n-2} + 0.6921\ \xi_n, \qquad 10.7$$

in which ε_n is the standardized dependent stochastic component during the n-th time interval, and ξ_n is the standardized independent stochastic component during the n-th time interval.

10.3 Independent Stochastic Component

The independent stochastic components ξ_n are obtained by removing the dependence structures from the standardized residual components using the autoregressive models determined in the previous section. The new series of ξ_n for the four processes are computed from Eq. 6.32 which is merely a rearrangement of the terms in Eq. 6.17.

The ξ_n of the process thus computed is a standard (0,1) random variable. The results are plotted in Figs. 27, 30, 31, and 32.

(1) Tests of Independence

Tests of whether the ξ_n series are random independent time process can be performed using either the correlogram or the variance density spectrum. In the correlogram analysis, the test is to show that the r_k values for all k's are not significantly different

from zero. In the spectral analysis, the test to show the variance density spectrum is not significantly different from a uniform density function. The correlogram approach was adopted in this study. A significance test for the open series was used based on the equation developed by Siddiqui (Yevjevich 1972b). The results are shown on Figs. 47 to 50. In each case, independence of the random variables was demonstrated, thus accepting the second-order stationarity of the processes investigated.

(2) Distribution of the Independent Stochastic Components

Determination of the best fitting probability function to the empirical frequency curve of ξ_t is one of the phases of the study. The generation of new samples of the original process by experimental statistical methods of time series decomposition is best accomplished using data for the independent stochastic component obtained as a theoretical probability distribution function rather than as the sample empirical frequency curve. The use of the empirical frequency curve in Monte Carlo generation would retain all biases of the original sample and would not permit the generation of values larger or smaller than those observed in the sample unless some arbitrary adjustments on the extremes are made. The fitting of a theoretical distribution function overcomes these objections.

In this study, the normal, lognormal-3, and the bilateral or double branch exponential probability density function are used for fitting the frequency distributions of the independent stochastic components, ξ_n. The best fit was chosen by the chi-square criterion. The mathematical background has been presented in Chapter VI.

The results show that the normal distribution with two parameters provided the best fit to the empirical frequency distribution for three of the ξ_n series. The independent stochastic component of the Ice-200 process was the only ξ_n series which departed from a normal distribution. The spiked nature of the empirical frequency distribution of this series can be modeled either by the Pareto distribution or other forms of the Pearson Type VI distribution or the double-branch gamma distribution. For the purpose of this report, the bilateral or double exponential distribution which is a special form of the double-branch gamma distribution is used. The choice is based on the fact that the empirical density function indicates a symmetrical distribution about zero. Thus the series can be modeled by the double exponential distribution function using only one parameter; assuming an apriori knowledge that the expected value is zero.

The parameters obtained for each case are given as

Series	Distribution Type	Parameters A	B
Core P6304-9	Normal	0.0	1.0
Ice-200	Double-branch exp.	0.0	0.705
Ice-50	Normal	0.0	0.992
Ice-10	Normal	0.0	0.996

The empirical density functions, the fitted distribution density functions and their corresponding empirical cumulative distributions and fitted cumulative distributions are shown on Figs. 51 to 58.

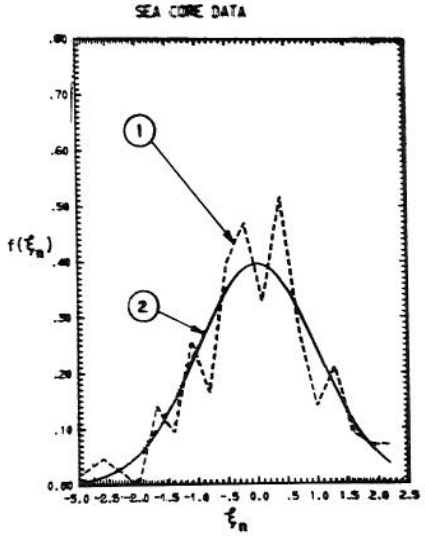

Fig. 51. Empirical (1) and fitted (2) normal density distribution functions of the independent stochastic component of the sea-sediment core P6304-9 series.

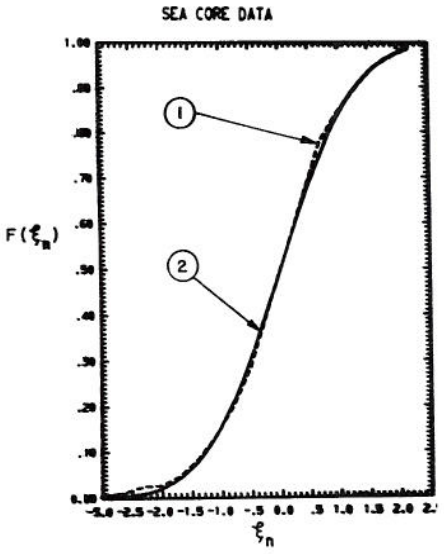

Fig. 52. Empirical (1) and fitted (2) normal cumulative distribution functions of the independent stochastic components of the sea-sediment core P6304-9 series.

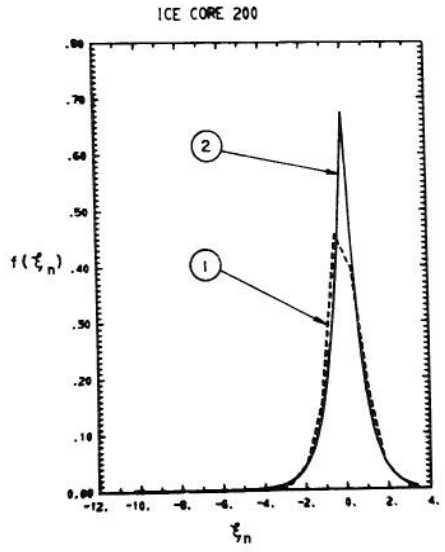

Fig. 53. Empirical (1) and fitted (2) double-branch exponential density distribution functions of the independent stochastic component of the Ice-200 series.

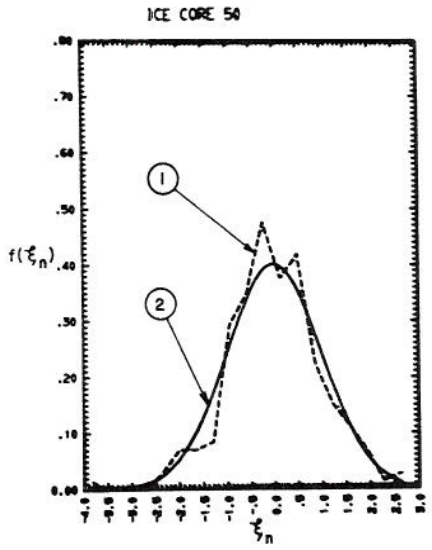

Fig. 55. Empirical (1) and fitted (2) normal density distribution functions of the independent stochastic component of the Ice-50 series.

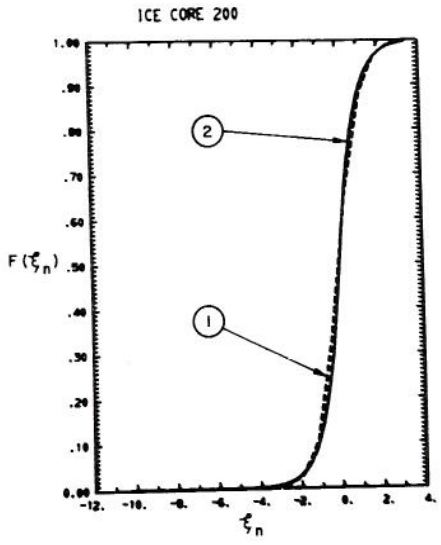

Fig. 54. Empirical (1) and fitted (2) double-branch exponential cumulative distribution functions of the independent stochastic component of the Ice-200 series.

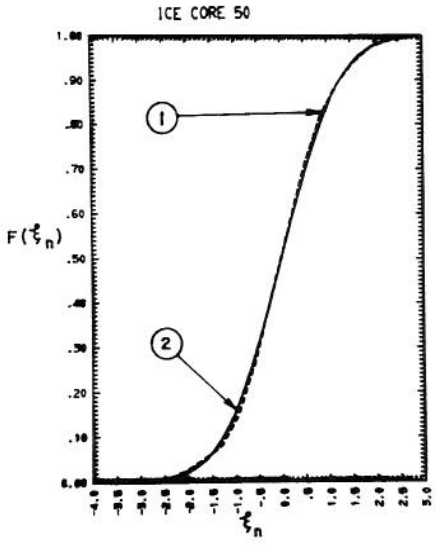

Fig. 56. Empirical (1) and fitted (2) normal cumulative distribution functions of the independent stochastic component of the Ice-50 series.

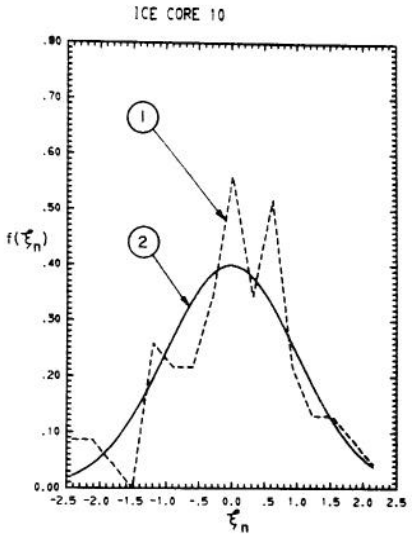

Fig. 57. Empirical (1) and fitted (2) normal density distribution functions of the independent stochastic component of the Ice-10 series.

(3) Model Verification with the Split Sample

Recall that all analyses carried out on the sea-sediment core so far have been based on the core data for the period from 286,000 years B.P. to the present. From this set of data, the model of the deterministic component was developed, the autoregressive model of the dependent stochastic component was defined, the frequency curves of independent stochastic components were determined, and the parameters for each of the component models were estimated.

A verification test of the component models is performed on the split sample taken from the lower half of the core which covers the period from 532,000 years B.P. to 286,000 years B.P. The models and their optimized parameters are used in the test in such a way so as to generate values for all three components of the time series for the period in question. The resulting time series are shown as part of Fig. 27. The correlograms are given in Fig. 59. The empirical density and cumulative distribution curves, and the fitted theoretical density and cumulative distribution functions are shown on Figs. 60 and 61.

Adequacy of the models is confirmed when (1) the independent stochastic component series for the period in question can be demonstrated by statistical test to be an independent series, and (2) the series can be well fitted by normal density function using the parameter values derived from the earlier calibration.

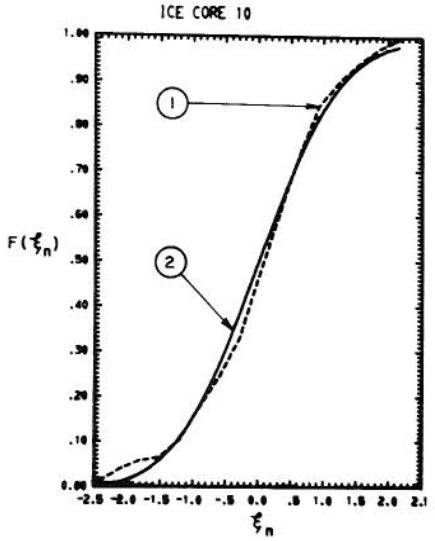

Fig. 58. Empirical (1) and fitted (2) normal cumulative distribution functions of the independent stochastic component of the Ice-10 series.

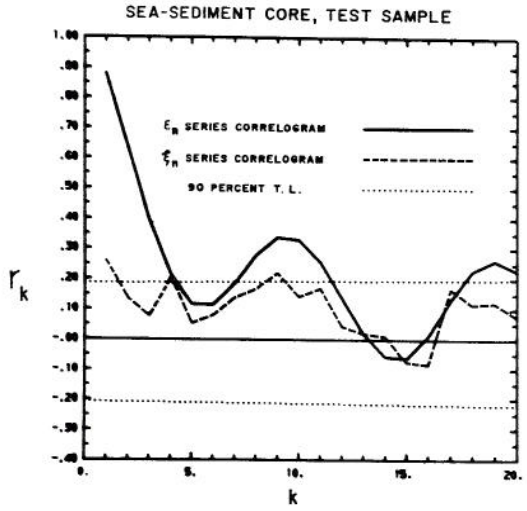

Fig. 59. Correlograms of the dependent and independent random components of the split sample used in model testing from the sea-sediment P6304-9 series. Tolerance limits at the 90 percent level for N=122 are shown.

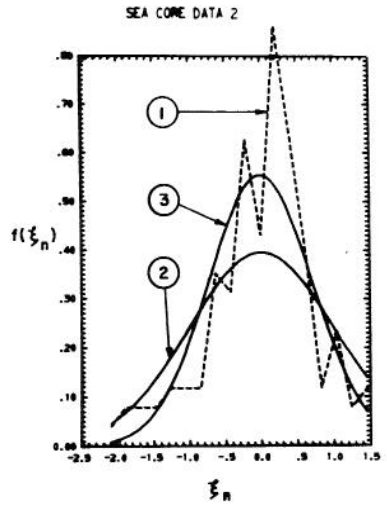

Fig. 60. Empirical (1) and the fitted (2) and (3) normal density distribution functions of the independent stochastic component of the second part of split sample used in model testing from the sea-sediment P6304-9 series (see text for explanation)

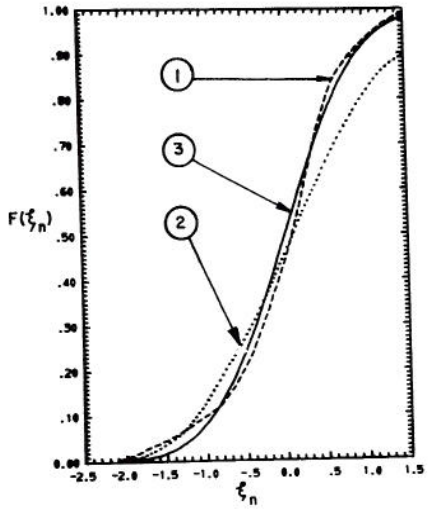

Fig. 61. Empirical (1) and the fitted (2) and (3) normal cumulative distribution functions of the independent stochastic component of the second half of split sample used in model testing from the sea-sediment P6304-9 series.

The test indicates a small dependence remaining in the ξ_n series. The fit of the normal density function using the standardized N(0,1) form is not good, nevertheless, only a slight change to N(0,0.7) is needed to obtain a good fitting model. The N(0,0.7) model is shown as an overlay on Figs. 60 and 61. The results of the test are considered sufficiently good to indicate general suitability of the models taking into account the relatively small size of the sample and the limitations in the accuracy and reliability of both the $\delta(O^{18})$ data and the chronology derived for a period so remote in time.

(4) Explained Variances

The contribution of deterministic and stochastic components to the original series may be expressed in terms of the explained variance.

From Eq. 6.1 the original series is given as

$$X_n = D_n + Y_n \quad . \qquad 6.1$$

Assuming independence between D_n and Y_n, the variance of X_n becomes

$$\text{Var } (X_n) = \text{Var } (D_n) + \text{Var } (Y_n) \quad . \qquad 10.8$$

The explained variance S_e^2 is defined as the variance of the component under consideration relative to the total variance of the original series. Thus the explained variance in terms of the deterministic component, the stochastic component, and the original series is

$$S_e^2 (D_n) = 1.0 - \frac{\text{Var } (Y_n)}{\text{Var } (X_n)} \quad . \qquad 10.9$$

A minor problem was encountered in applying the above equations in this study. For the case of the Ice-200 series, the variance of the deterministic component is greater than the variance of the original series. No constraints on the boundary conditions were imposed in modeling of the Ice-200 series. This resulted in having generated values for the deterministic component greater, in some instances than the extreme values of the original series caused a larger variance in the generated series.

Because of this problem it was decided to report only the ratio between the variance of the stochastic component and the variance of the original series. This should provide some measure of the degree of stochasticity in the process. A high ratio would indicate high stochasticity.

The following ratios expressed in percent were determined for the four series.

Series	Variance Ratio
Sea-sediment	59%
Ice-200	23%
Ice-50	61%
Ice-10	95%

As expected, a high degree of stochasticity is evident in all four series. In the case of the Ice-10 series, the process is almost entirely stochastic except for the slight upward linear trend that was detected at the 90 percent significance level. Results from the three ice-core series show that climatic variations at the smaller time scale have great stochasticity.

CHAPTER XI
SUMMARY, CONCLUSIONS, AND RECOMMENDATIONS

11.1 Summary

A mathematical procedure for quantitative evaluation of long-term climatic changes as a deterministic-stochastic process has been developed. The approach demonstrated in this study, relied on two basic hypotheses: (1) that long-term climatic changes are reflected in the fluctuations of $\delta(O^{18})$ content measured in carbonate shells from deep-sea sediment cores and in the ice core from the Greenland ice sheet; and (2) that long-period variation in the distribution of incoming solar radiation at the top of the earth's atmosphere as derived from the Milankovich theory of orbital and axial motions of the earth is the basic deterministic process affecting the long-term climatic changes. The background information necessary for a general appreciation of the nature of the oxygen isotope data and the probable cause and effect of the Milankovich mechanism are outlined.

Using radiometrically dated data from various sources, a preliminary chronology for a deep-sea sediment core was developed from which a sediment deposition rate model was conceived. This model was used to establish an absolute time scale for the entire depth of the sea-sediment core. The $\delta(O^{18})$ record for the core was then considered as a geological time series measuring climatic changes. On the basis of the sediment deposition rate model, the time series was found to span a period of 532,000 years. Values of $\delta(O^{18})$ representing averages over each 2000 year increment were derived for the sea-sediment series.

The $\delta(O^{18})$ records for the Greenland ice core have already been time calibrated by others and their results were accepted for use in this study. Three time series from the ice core were analyzed. The first series covers a time span of 126,000 years with $\delta(O^{18})$ values averaged over each 200 year increment. The second series covers a time span of 10,000 years with value averaged over each 50 year increment. The third series covers a time span of 780 years with values averaged over each 10 year increment.

An empirical gray-box response model was developed to describe the deterministic components of those $\delta(O^{18})$ time series which span a period of more than 100,000 years. The gray-box responses consist of a set of functional mathematical expressions. These equations are viewed as a representation of the atmospheric-oceanic-terrestrial system with the ability to convert deterministic almost-periodic solar radiation inputs, derived from the Milankovich theory, into outputs of $\delta(O^{18})$ time series consisting of a deterministic almost-periodic component and a stochastic component. For those $\delta(O^{18})$ time series which span a period of 10,000 years and less, the deterministic component was considered as a trend. The trend was approximated in the study by a mathematical expression in the form of a polynomial equation.

The stochastic component was obtained by subtracting the deterministic component from the original $\delta(O^{18})$ time series. The structure of the stochastic component for each series was evaluated. The results show that time dependence in the stochastic process was well approximated by either the first- or second-order autoregressive linear models. The removal of the time dependence in the stochastic process led to a second-order stationary and independent stochastic process.

Of the four series studied, only one series has an independent stochastic component which could not be well approximated by a normal probability distribution function. The one exception was found to have an empirical frequency distribution which was well fitted by the bilateral or double-branch exponential probability distribution function.

11.2 Conclusions

The problems of long-term climatic changes are amenable to analyses and syntheses by the deterministic-stochastic approach on the assumption that a deterministic almost-periodic input into the system generates an output which defines a deterministic pattern of change in the long-term climate. Thus the stochastic component can be isolated from the observed time series for structural analysis.

On the basis of the models developed herein, it has been shown that long-term climatic changes as reflected in the $\delta(O^{18})$ records have a high degree of stochasticity generated by the earth's environment.

The technique recognizes the inherent variability of the earth's environments and the presence of measurement noise. The separation of these two factors in the stochastic component is not possible at the present time without a better understanding of the meaning and nature of the $\delta(O^{18})$ records.

The procedures, functional mathematical relationships, and stochastic models discussed and developed herein appear to hold considerable promise as a tool not only for predictive purposes but also for reconstructing a detailed history of climatic changes encompassing a time span of nearly two million years. It must be remembered, however, that an empirical gray-box approach has been used in this study. This does not necessarily detract from its value since the study represents the first attempt at producing mathematical models designed expressly for evaluating long-term climatic changes as a deterministic-stochastic process on the time scales considered in this study.

As more data are accumulated to permit a better understanding of the $\delta(O^{18})$ process in sea cores and ice cores, a more theoretical approach using more advanced mathematical techniques will undoubtedly refine, improve, or change the methodology proposed in this study. Nevertheless, it should be emphasized that development of hypotheses and the acts of examining and accepting or rejecting the hypotheses are basic steps in the scientific approach used.

Although the almost-periodic component should not be used as a separate series for predicting the future outcome, it does provide a general indication of the pattern of events to come. It is interesting to note

that while the study shows a cooling pattern over the next hundred thousand years, with perhaps large advances in mountain glaciers, an ice sheet of continental dimensions does not appear to be forthcoming during this period on the basis of the deterministic part of the model. The stochastic part of the model will introduce uncertainty into the system which can make this trend deviate either toward a cooler or warmer climate, departing more or less from the indicated pattern. The stochastic component for the period can be added by using the Monte Carlo generation techniques in generating samples of the stochastic models and using parameters estimated in this study, and adding the stochastic component to the projected deterministic patterns.

11.3 Recommendations for Future Research

The models and analysis techniques have been applied only in a demonstration on one particular sea-sediment core with $\delta(O^{18})$ records. A systematic study by the same or refined theoretical methods on a suite of cores carefully chosen from different ocean areas of the world could be made. This of course would require $\delta(O^{18})$ data for the selected cores. Such data are as yet available only for a very few cores of sizable length. In any program of measurements of $\delta(O^{18})$ content, isotope analysis at a much smaller depth increment than 10 cm would be desirable particularly during intervals where there are rapid rates of change in the Oxygen-18 values.

Of particular significance to the hydrologic discipline is the real possibility that, in the near future, air temperatures, and snow or ice accumulation rates, can be derived from ice-core data with a time resolution of a year or less covering a time span of several hundreds and perhaps thousands of years. Such data are obtained even now, but they cover a time span extending back for only 200 years or less.

In any case, as more and better data with much finer time resolution are developed from both ice and sea-sediment cores, it is conceivable that such data can be applied in correlation studies to establish very long time series (from the hydrologic viewpoint) for defining the characteristics of future or past annual floods, droughts, and water yields in many parts of the world. If the techniques applicable to high latitude ice sheets can be adapted to temperate zone glaciers, it will open up attractive opportunities for deriving long-term temperature and precipitation records for the mountainous regions where historical records are sadly lacking. The derived records can then be applied through correlation and modeling methods to other temperature zone areas where the availability of such data will be of great hydrologic importance and value.

REFERENCES

Alyea, F.N., 1972, Numerical simulation of an ice age paleoclimate, Atmospheric Science Paper No. 193, Colorado State University, 120 pages.

Andrews, J.T., 1970, A geomorphological study of post-glacial uplift with particular reference to Arctic Canada. Institute of British Geographers, Kensington Gore, 156 pages.

Barry, R.G., 1966, Meteorological aspects of the glacial history of Labrador-Ungava with special reference to atmospheric vapour transport: Geographical Bulletin, Ottawa, Vol. 8, p. 319-340.

Beard, L.R., 1965, Use of interrelated records to simulate streamflow, Journal of the Hydraulics division, ASCE, Vol. 91, No. HY5, p. 13-22.

Beard, L.R., Simulation of daily streamflow, in Proceedings of the International Hydrology Symposium, Sept. 6-8, 1967, Fort Collins, Colorado, Vol. 1, p. 624-632.

Bertin, L., 1972, The New Larousse Encylopedia of the Earth: Crown Publishers, Inc., New York, 424 pages.

Box, E.P.G. and G.M. Jenkins, 1971, Time series analysis forecasting, and control: Holden-Day, San Francisco, 553 pages.

Broecker, W.S., 1965, Isotope geochemistry and the Pleistocene climatic record, in Quaternary of the United States (ed. Wright, Jr. and Frey): Princeton University Press, Princeton, New Jersey, p. 737-754.

Broecker, W.S., 1968, In defense of the astronomical theory of glaciation, in Causes of climatic change: Meteorological Monographs, Vol. 8, No. 30, p. 139-141.

Broecker, W.S., K.K. Turekian and B.C. Heezen, 1958, The relation of deep sea sedimentation rates to variations in climate: American Journal of Science, Vol. 256, p. 503-517.

Broecker, W.S., and T.L. Ku, 1969, Caribbean cores P6304-8 and P6304-9: New analyses of absolute chronology: Science, Vol. 166, p. 404-406.

Broecker, W.S., D.L. Thurber, J. Goddard, T.L. Ku, R.K. Matthews, and K.J. Mesolella, 1968, Milankovich hypothesis supported by precise dating of coral reefs and deep-sea sediments: Science, Vol. 159, p. 297-300.

Broecker, W.S., and J. van Donk, 1970, Insolation changes, ice volumes, and the 0-18 record in deep-sea cores: Reviews of Geophysics and Space Physics, Vol. 8, p. 169-198.

Brooks, C.E.P., 1949, Climate Through the Ages: McGraw-Hill Book Company, Inc., New York, 395 pages.

Bryson, R.A., W.M. Wendland, J.D. Ives, and J.T. Andrews, 1969, Radio-carbon isochrones on the disintegration of the Laurentide ice sheet: Arctic and Alpine Research, Vol. 1, No. 1, p. 1-14.

Cornwall, I., 1970, Ice Ages, Their nature and effects: Humanities Press Inc., New York, N.Y., 180 pages.

Cox, A., 1968, Polar watering, continental drift, and the onset of Quaternary glaciation, in Causes of climatic change: Meteorological Monographs, Vol. 8, No. 30, p. 112-125.

Cox, A. and R.R. Doell, 1968, Paleomagnetism and Quaternary correlation, in Means of Correlation of Quaternary Successions (ed. Morrison and Wright, Jr.): University of Utah Press, Salt Lake City, p. 253-266.

Craig, H., 1961, Standard for reporting concentrations of deuterium and Oxygen-18 in natural waters: Science, Vol. 133, p. 1833.

Daly, R.A., 1963, The changing world of the Ice age: Hafner Publishing Company, New York, 271 pages.

Dansgaard, W., 1964, Stable isotopes in precipitation: Tellus, Vol. 16, p. 436-468.

Dansgaard, W., S.J. Johnsen, J. Moller, and C.C. Langway, Jr., 1969, One thousand centuries of climatic record from Camp Century on the Greenland ice sheet: Science, vol. 166, p. 377-381.

Dansgaard, W., S.J. Johnsen, H.B. Clausen and C.C. Langway, Jr., 1971, Climatic record revealed by the Camp Century ice core: in the Late Cenozoic Glacial Ages (ed. Turekian, Yale University Press, p. 37-56.

Denton, G.H., R.L. Armstrong, and M. Stuiver, 1971, The late Cenozoic glacial history of Antarctica, in Late Cenozoic Glacial Ages (ed. Turekian): Yale University Press, p. 267-306.

Emiliani, C., 1955, Pleistocene Temperatures: The Journal of Geology, Vol. 63, P. 538-578.

Emiliani, C., 1958, Paleotemperature analysis of core 280 and Pleistocene correlations: The Journal of Geology, Vol. 66, p. 264-275.

Emiliani, C., 1961, Cenozoic climatic changes as indicated by the stratigraphy and chronology of deep-sea cores of globigerina ooze facies: Annals New York Academy of Sciences, Vol. 95, p. 521-535.

Emiliani, C., 1966a, Paleotemperature analysis of Caribbean cores P6304-8 and P6304-9 and a generalized temperature curve for the past 425,000 years: The Journal of Geology, Vol. 74, No. 2, p. 109-123.

Emiliani, C., 1966b, Isotopic Paleotemperatures: Science, Vol. 154, p. 851-856.

Emiliani, C., 1972, Quaternary paleotemperatures and the duration of the high-temperature intervals: Science, Vol. 178, p. 398-400.

Emiliani, C., and J. Geiss, 1957, On glaciations and their causes: Geologischen Rundschau, Vol. 46, p. 576-601.

Emiliani, C. and E. Rona, 1969, Caribbean cores P6304-8 and P6304-9: New analysis of absolute chronology. A reply: Science, Vol. 166, p. 1551-1552.

Epstein, S., R. Buchsbaum, H. Lowestam, and H.C. Urey, 1951, Carbonate-water isotopic temperature scale: Geological Society of America Bulletin, Vol. 62, p. 417-425.

Epstein, S., R. Buchsbaum, H. Lowestam, and H.C. Urey, 1953, Revised carbonate-water isotopic temperature scale: Geological Society of America Bulletin, Vol. 62, p. 417-425.

Ericson, D.B., M. Ewing, and G. Wollin, 1964, The Pleistocene epoch in deep-sea sediments: Science, Vol. 146, p. 723-732.

Ericson, D.B., and G. Wollin, 1968, Pleistocene climates and chronology in deep-sea sediments: Science, Vol. 162, p. 1227-1234.

Eriksson, E., 1968, Air-ocean-icecap interactions in relation to climatic fluctuations and glaciation cycles, in Causes of climatic change: Meteorological Monographs, Vol. 8, No. 30, p. 68-92.

Fairbridge, R.W., 1961, Convergence of evidence on climatic change and ice ages: Annals New York Academy of Sciences, Vol. 95, p. 542-579.

Fairbridge, R.W., 1963, The importance of limestone and its Ca/Mg content to paleoclimatology, in Problems in paleoclimatology (edited by Nairn): Interscience Publishers, New York, 705 pages.

Flint, R.F., 1971, Glacial and Quaternary Geology: John Wiley and Sons, Inc., New York, 892 pages.

Fritts, H.C., 1965, Dendrochronology, in The Quaternary of the United States (ed. Wright, Jr., and Frey): Princeton University Press, New Jersey, p. 871-880.

Gleissberg, W., 1944, A table of secular variations of the solar cycle, Terr. Magn. Stru. Telectr., Vol. 49, 243 pages.

Goldthwait,R.P., A. Dreimanis, J.L. Forsyth, P. F. Karrown, and G.W. White, 1965, Pleistocene deposits of the Erie lobe, in Quaternary of the United States (eds. Wright, Jr., and Frey): Princeton University Press, Princeton, New Jersey, pages 85-98.

Gow, A.J., 1968, Deep core studies of the accumulation and densification of snow at Byrd station and Little America V, Antarctica: Research Report 197, U.S. Army Cold Regions Research and Engineering Laboratory, Hanover, New Hampshire, 45 pages.

Graupe, D., 1972, Identification of systems: Van Nostrand Reinhold Company, New York, 276 pages.

Hamilton, W., 1968, Cenozoic climatic change and its cause, in Causes of climatic change: Meteorological Monographs, Vol. 8, No. 30, p. 128 - 133.

Hollin, J.T., 1962, On the glacial history of Antarctica: Journal of Glaciology, Vol. 4, p. 173-195.

Imbrie, J., and N.G. Kipp, 1971, A new micropaleontological method for quantitative paleoclimatology: application to a late Pleistocene Caribbean core, in Late Cenozoic Glacial Ages (ed. Turekian): Yale University Press, p. 71-182.

Jenkins, G.M. and D.G. Watts, 1969, Spectral Analysis and its Applications: Holden-Day, San Francisco, 525 pages.

Kutzbach, J.E., R.A. Bryson, and W.C. Shen, 1968, An evaluation of the thermal Rossby number in the Pleistocene, in Causes of climatic change: Meteorological Monographs, Vol. 8, No. 30, p. 134-138.

Langway, Jr., C.C., 1967, Stratigraphic analyses of a deep-ice core from Greenland: Research Report 77, U.S. Army Cold Regions Research and Engineering Laboratory, Hanover, New Hampshire, 130 pages.

Langway, Jr., C.C., and B.L. Hansen, 1970, Drilling through the ice cap: Probing climate for a thousand centuries: Bulletin of the Atomic Scientists, December 1970, p. 62-66.

Matthews, W.H., W.W. Kellog, G.D. Robinson, Eds., 1971, Inadvertent Climate Modification, report of the study of man's impact on climate (SMIC): M.I.T. Press, Cambridge, Mass., 308 pages.

Mellor, M., 1964, Snow and ice on the earth's surface: U.S. Army Cold Regions Research and Engineering Laboratory, Hanover, New Hampshire, 163 pages.

Milankovitch, M., 1941, Canon of insolation and the ice-age problem, translated from German by the Israel Program for Scientific Translations, Jerusalem, 1969: U.S. Department of Commerce, Springfield, Va., 484 pages.

Mitchell, Jr., J.M., 1965, Theoretical paleoclimatology, in The Quaternary of the United States (eds. Wright, Jr., and Frey): Princeton University Press, Princeton, New Jersey, 922 pages.

Mitchell, Jr., J.M., 1968, Concluding remarks, in Causes of climatic change: Meteorological Monographs, Vol. 8, No. 30, p. 155-159.

Moran, J.M., and R.A. Bryson, 1969, The contribution of Laurentide ice wastage to the eustatic rise of sea level: 10,000 to 6,000 B.P.: Arctic and Alpine Research, Vol. 1, No. 2., p. 97-104.

Morrison, R.B., 1968, Means of time-stratigraphic division and long-distance correlation of Quaternary successions, in Means of Correlation of Quaternary succesions (ed. Morrison and Wright, Jr.): University of Utah Press, Salt Lake City, p. 1-114.

Nairn, A.E.M., 1963, Problems in paleoclimatology, Proceedings of the NATO paleoclimates conference held at the University of Newcastle upon Tyne, January 7-12, 1963: Interscience Publishers, New York, 705 pages.

Nye, 1959, The motion of ice sheets and glaciers: Journal of Glaciology, Vol. 3, p. 493-507.

Paterson, W.S.B., 1969, The Physics of glaciers: Pergamon Press, Toronto, Canada, 250 pages.

Quimpo, R.G., 1967, Stochastic model of daily river flow sequences, Hydrology Paper, No. 18: Colorado State University, Fort Collins, Colorado, 30 pages.

Roesner, L.A., and V.M. Yevjevich, 1966, Mathematical models for time series of monthly precipitation and monthly runoff, Hydrology Paper No. 15: Colorado State University, Fort Collins, Colorado, 50 pages.

Salas La-Cruz, J.D., and V.M. Yevjevich, 1972, Stochastic structure of water use time series, Hydrology Paper No. 52: Colorado State University, Fort Collins, Colorado, 71 pages.

Schove, D.J., 1955, The sunspot cycle, 649 B.C. to A.D. 2000, F. Geophys. Res., Vol. 60, 127 pages.

Sellers, W.D., 1965, Physical climatology, The University of Chicago Press, Chicago, Ill., 272 pages.

Shackleton, N., 1967, Oxygen isotope analyses and Pleistocene temperature re-assessed: Nature, Vol. 215, p. 15-17.

Shapely, H., 1960, Climatic Change: Harvard University Press, Cambridge, 318 pages.

Suess, H., 1970, The three causes of the secular carbon-14 fluctuations, their amplitudes and time constants, in I, U, Olsson, ed., Twelfth Nobel Symp., Radiocarbon variations and absolute chronology, Uppsala, 1969, Almquist and Wiksell, Stockholm, and Wiley, New York.

Sutcliffe, R.C., 1967, Weather and climate: W.W. Norton and Company, Inc., New York, 206 pages.

Tanner, V., 1944, Outline of the geography, life and customs of Newfoundland-Labrador (the eastern part of the Labrador peninsula): Acta Geographica Fennise, Vol. 8, No. 1, 909 pages.

Thomas, H.A., and M.B. Fiering 1962, Mathematical synthesis of stream-flow sequences for the analysis of river basins by simulation, in Design of water resource systems: Harvard University Press, Cambridge, Massachusetts, p. 459-493.

Tuffour, S., 1973, Optimal parameter identification of non-linear time-variant hydrologic system models: Ph.D. Dissertation, Colorado State University, Fort Collins, Colorado, 160 pages.

van den Heuvel, E.P.J., 1966, On the precession as a cause of Pleistocene variations of the Atlantic Ocean water temperatures: Geophysical Journal, Vol. 11, p. 323-336.

van Woerkom, A.J.J., 1960, The astronomical theory of climate changes in Climatic Change (ed. Shapely) Harvard University Press, Cambridge, p. 147-157.

Vernekar, A.D., 1972, Long-period global variations of incoming solar radiation: Meteorological Monographs, Vol. 12, No. 34, 21 pages.

Weertman, J., 1964, Rate of growth or shrinkage of non-equilibrium ice sheets: Research Report 145, U.S. Army Cold Region Research and Engineering Laboratory, Hanover, New Hampshire, 16 pages.

Wollin, G., D.B. Ericson, and M. Ewing, 1971, Late Pleistocene climates recorded in Atlantic and Pacific deep-sea sediments, in late Cenozoic glacial ages (ed. Turekian): Yale University Press, p. 199-214.

Yevjevich, V.M., 1964, Fluctuation of wet and dry years, Part II, Analysis by serial correlation, Hydrology Paper No. 4: Colorado State University, Fort Collins, Colorado, 50 pages.

Yevjevich, V.M., 1972a, Stochastic processes in hydrology: Water Resources Publication, Fort Collins, Colorado, 276 pages.

Yevjevich, V.M., 1972b, Structural analysis of hydrologic time series, Hydrology Paper No. 56: Colorado State University, Fort Collins, Colorado, 59 pages.

Zeuner, F.E., 1970, Dating the past, an introduction to chronology: Hafner Publishing Co., Darien, Conn., 516 pages.

APPENDIX

The variation in ΔQ (ly day^{-1}) as a function of latitude and time. The upper half of each part of the figure shows the variations for the northern caloric winter and southern caloric summer. The lower half shows the variations for the northern caloric summer and southern caloric winter. The abscissa shows the time in thousands of years before (-) and after (+) 1950 A.D. (taken from Vernekar, 1972).

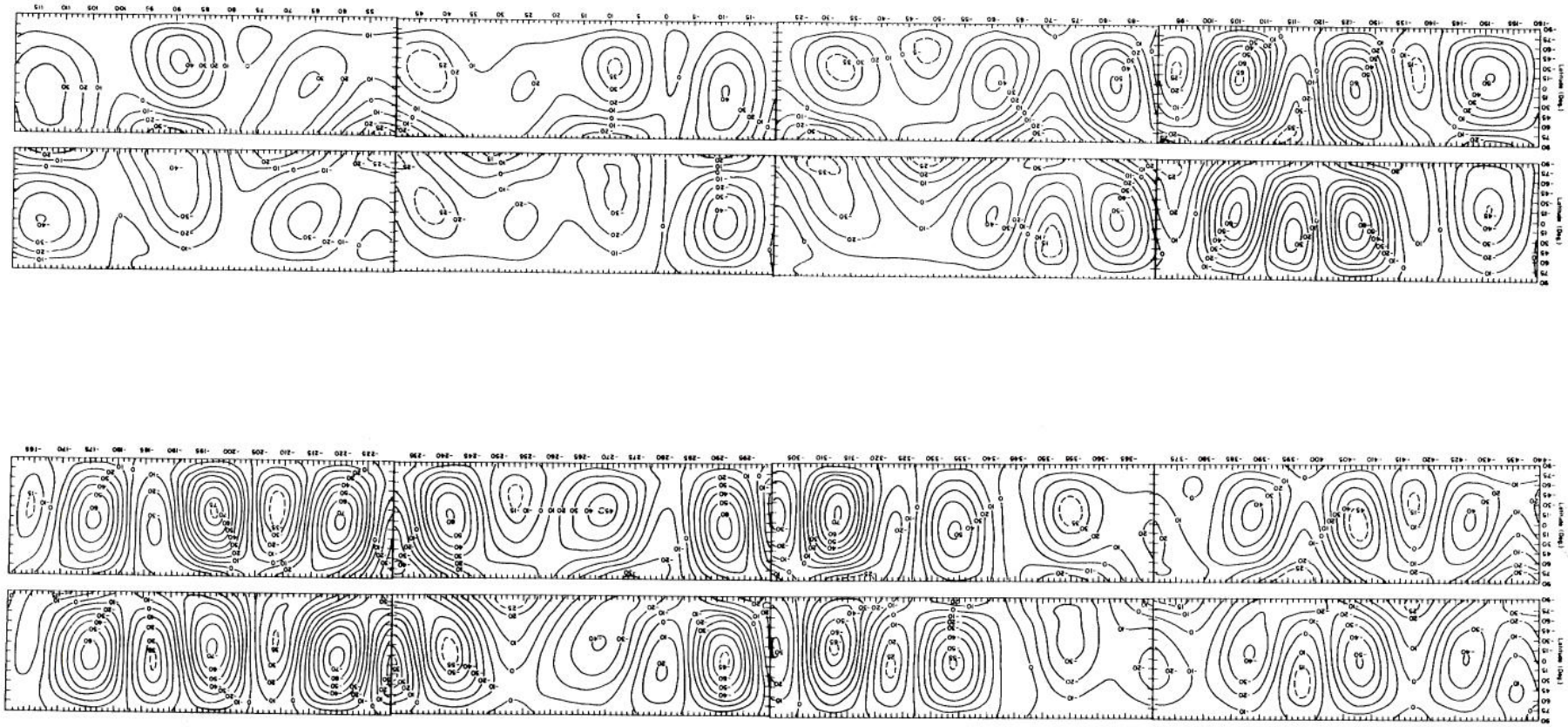

(a) The variation in Δ Q (ly day^{-1}) as a function of latitude and time for the period from - 440,000 B.P. to 119,000 A.P. The upper half of each part of the figure shows the variations for the northern caloric winter and southern caloric summer. The lower half shows the variations for the northern caloric summer and southern caloric winter. The abscissa shows the time in thousands of years before (-) and after (+) 1950 A.D.

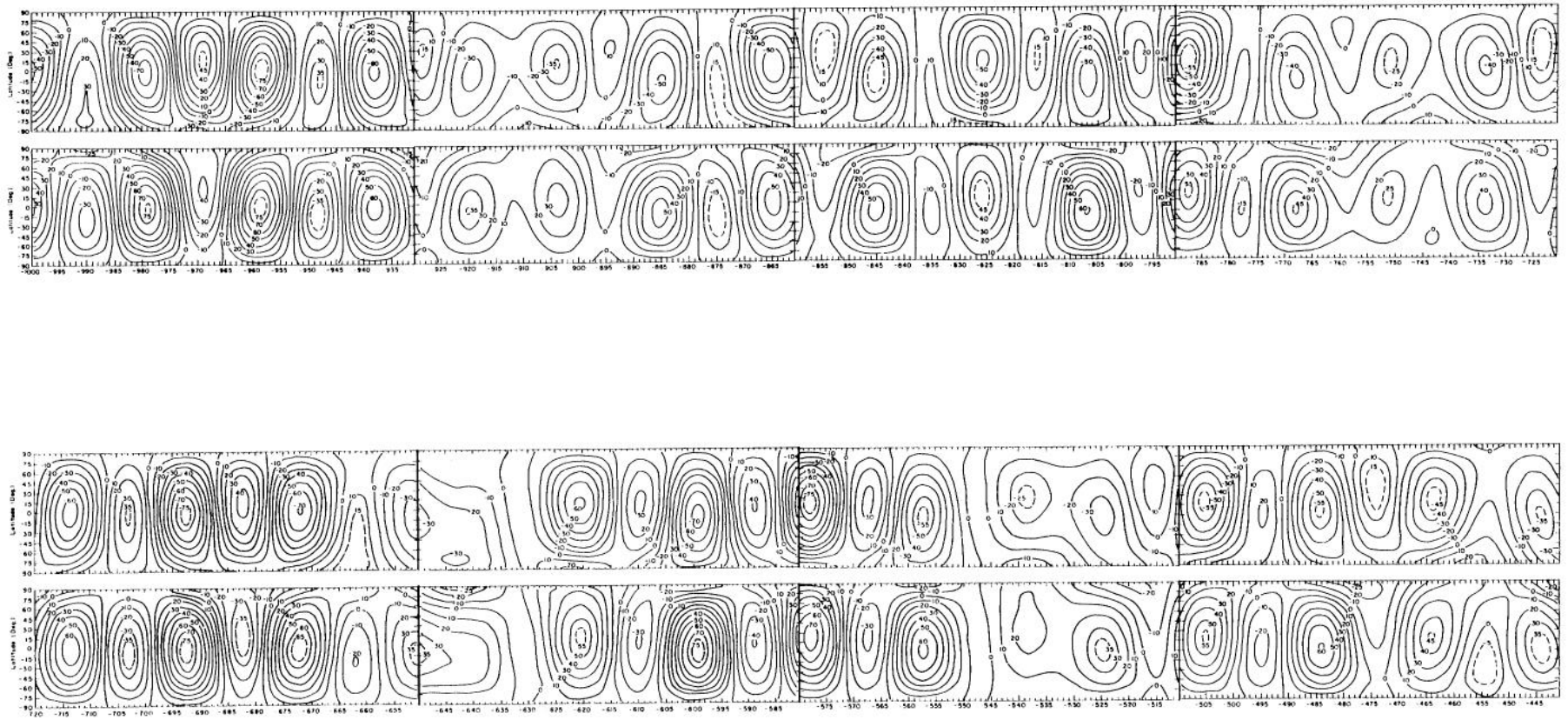

(b) The variation in ΔQ (ly day $^{-1}$) as a function of latitude and time for the period from -1,000,000 B.P. to -440,000 B.P. The upper half of each part of the figure shows the variations for the northern caloric winter and southern caloric summer. The lower half shows the variations for the northern caloric summer and southern caloric winter. The abscissa shows the time in thousands of years before (-) and after (+) 1950 A.D.

KEY WORDS: Climatic change, climatic processes, time series, deterministic-stochastic processes, hydrologic persistence, mathematical modeling.

ABSTRACT: A mathematical procedure for quantitative evaluation of long-term climatic changes as an almost-periodic, stochastic process is described. The procedure relies on two hypotheses: (1) that long-term climatic changes are reflected in Oxygen-18 content series as measured in carbonate shells from deep-sea sediment cores, and as measured in the ice core from the Greenland ice sheet, and (2) that the long-term almost-periodic variation in the distribution of solar radiation entering the earth's atmosphere, as derived from the Milankovich theory of orbital and axial motions of the earth, is the basic deterministic process affecting the long-term climatic changes. Information on the oxygen-isotope core data is given, and the behavior of the astronomical mechanism is outlined. Models of deterministic component in the process

---

KEY WORDS: Climatic change, climatic processes, time series, deterministic-stochastic processes, hydrologic persistence, mathematical modeling.

ABSTRACT: A mathematical procedure for quantitative evaluation of long-term climatic changes as an almost-periodic, stochastic process is described. The procedure relies on two hypotheses: (1) that long-term climatic changes are reflected in Oxygen-18 content series as measured in carbonate shells from deep-sea sediment cores, and as measured in the ice core from the Greenland ice sheet, and (2) that the long-term almost-periodic variation in the distribution of solar radiation entering the earth's atmosphere, as derived from the Milankovich theory of orbital and axial motions of the earth, is the basic deterministic process affecting the long-term climatic changes. Information on the oxygen-isotope core data is given, and the behavior of the astronomical mechanism is outlined. Models of deterministic component in the process

---

KEY WORDS: Climatic change, climatic processes, time series, deterministic-stochastic processes, hydrologic persistence, mathematical modeling.

ABSTRACT: A mathematical procedure for quantitative evaluation of long-term climatic changes as an almost-periodic, stochastic process is described. The procedure relies on two hypotheses: (1) that long-term climatic changes are reflected in Oxygen-18 content series as measured in carbonate shells from deep-sea sediment cores, and as measured in the ice core from the Greenland ice sheet, and (2) that the long-term almost-periodic variation in the distribution of solar radiation entering the earth's atmosphere, as derived from the Milankovich theory of orbital and axial motions of the earth, is the basic deterministic process affecting the long-term climatic changes. Information on the oxygen-isotope core data is given, and the behavior of the astronomical mechanism is outlined. Models of deterministic component in the process

---

KEY WORDS: Climatic change, climatic processes, time series, deterministic-stochastic processes, hydrologic persistence, mathematical modeling.

ABSTRACT: A mathematical procedure for quantitative evaluation of long-term climatic changes as an almost-periodic, stochastic process is described. The procedure relies on two hypotheses: (1) that long-term climatic changes are reflected in Oxygen-18 content series as measured in carbonate shells from deep-sea sediment cores, and as measured in the ice core from the Greenland ice sheet, and (2) that the long-term almost-periodic variation in the distribution of solar radiation entering the earth's atmosphere, as derived from the Milankovich theory of orbital and axial motions of the earth, is the basic deterministic process affecting the long-term climatic changes. Information on the oxygen-isotope core data is given, and the behavior of the astronomical mechanism is outlined. Models of deterministic component in the process

are determined by a gray-box approach. The atmospheric-oceanic-terrestrial system, in response to the deterministic solar radiation as computed by the Milankovich theory, converts this input into an output as the deterministic component of the long-term climatic changes. Dependence in stochastic components is approximated by Markov models. Independent stochastic components are found to be approximately normally distributed. Although the deterministic component should not be used separately for predicting the future climate, it does, however, provide a general indication of expected changes. A mild cooling pattern over the next 100,000 years is indicated, perhaps with some large advances in mountain glaciers. No ice sheet of continental dimensions is apparent for that period.

HYDROLOGY PAPER No. 65 - ALMOST-PERIODIC, STOCHASTIC
PROCESS OF LONG-TERM CLIMATIC CHANGES
by
W.Q. Chin and V. Yevjevich
Colorado State University

are determined by a gray-box approach. The atmospheric-oceanic-terrestrial system, in response to the deterministic solar radiation as computed by the Milankovich theory, converts this input into an output as the deterministic component of the long-term climatic changes. Dependence in stochastic components is approximated by Markov models. Independent stochastic components are found to be approximately normally distributed. Although the deterministic component should not be used separately for predicting the future climate, it does, however, provide a general indication of expected changes. A mild cooling pattern over the next 100,000 years is indicated, perhaps with some large advances in mountain glaciers. No ice sheet of continental dimensions is apparent for that period.

HYDROLOGY PAPER No. 65 - ALMOST-PERIODIC, STOCHASTIC
PROCESS OF LONG-TERM CLIMATIC CHANGES
by
W.Q. Chin and V. Yevjevich
Colorado State University

are determined by a gray-box approach. The atmospheric-oceanic-terrestrial system, in response to the deterministic solar radiation as computed by the Milankovich theory, converts this input into an output as the deterministic component of the long-term climatic changes. Dependence in stochastic components is approximated by Markov models. Independent stochastic components are found to be approximately normally distributed. Although the deterministic component should not be used separately for predicting the future climate, it does, however, provide a general indication of expected changes. A mild cooling pattern over the next 100,000 years is indicated, perhaps with some large advances in mountain glaciers. No ice sheet of continental dimensions is apparent for that period.

HYDROLOGY PAPER No. 65 - ALMOST-PERIODIC, STOCHASTIC
PROCESS OF LONG-TERM CLIMATIC CHANGES
by
W.Q. Chin and V. Yevjevich
Colorado State University

are determined by a gray-box approach. The atmospheric-oceanic-terrestrial system, in response to the deterministic solar radiation as computed by the Milankovich theory, converts this input into an output as the deterministic component of the long-term climatic changes. Dependence in stochastic components is approximated by Markov models. Independent stochastic components are found to be approximately normally distributed. Although the deterministic component should not be used separately for predicting the future climate, it does, however, provide a general indication of expected changes. A mild cooling pattern over the next 100,000 years is indicated, perhaps with some large advances in mountain glaciers. No ice sheet of continental dimensions is apparent for that period.

HYDROLOGY PAPER No. 65 - ALMOST-PERIODIC, STOCHASTIC
PROCESS OF LONG-TERM CLIMATIC CHANGES
by
W.Q. Chin and V. Yevjevich
Colorado State University